Investigation of the Composition of Woodsmoke and Methods for Apportioning Woodsmoke to Air Pollution in Launceston

Timothy Bain Jordan

BAppSc (Hons)

Submitted in fulfilment of the requirements

for the degree of

Doctor of Philosophy

University of Tasmania

April 2005

This thesis contains no material which has been accepted for a degree or diploma by the University or any other institution, except by way of background information and duly acknowledged in the thesis. To the best of the candidate's knowledge and belief, no material previously published or written by another person is included in the text of the thesis except where due acknowledgment is made.

This thesis may be made available for loan and limited copying in accordance with the *Copyright Act 1968*.

_____

Timothy Jordan

14 April 2005

Statement of Authorship

The following people contributed to the publication of the work undertaken as part of this thesis:

1. *Effect of airflow setting on the organic composition of woodheater emissions.*
   Timothy B. Jordan, Andrew J. Seen

   Submitted to *Environmental Science and Technology*, 8 August 2004.
   Accepted for publication 4 March, 2005.

- Andrew Seen assisted with guidance and general supervision in all aspects of producing the manuscripts.
- John Gras provided feedback on the manuscript prior to submission.

I agree with the above stated "proportion of work undertaken" for each of the above submitted peer-reviewed manuscripts contributing to this thesis:

_____

Dr. Andrew Seen (Supervisor)
14 April 2005

Abstract

Launceston, a city with a population of approximately 80,000 located in the north of Tasmania, Australia, regularly experiences high levels of air pollution during winter. Ambient PM_{10} (particulate matter with an aerodynamic diameter smaller than 10 μm) levels exceed the Australian 24-hour guideline of 50 $\mu g/m^3$ around 20-40 times during the May to September period each year. This is generally attributed to residential woodburning, with approximately one third of households using woodheaters or open fireplaces. This thesis reports on investigations into characterising and quantifying the contribution of woodsmoke to wintertime air pollution in Launceston.

An historical record of air quality in Launceston was reconstructed using polycyclic aromatic hydrocarbons (PAHs) as surrogates for air pollution in a dated sediment core taken from the upper Tamar Estuary. The overall depth profile showed that levels of PAHs began increasing at the end of the 19th century and have been relatively steady since the 1930s. Pyrogenic source ratios similar to woodburning were found in both atmospheric and sedimentary samples, although quantification of the woodburning contribution was not possible using PAHs alone. Factors affecting atmospheric sampling of PAHs were investigated, including the impact of sampling rate, the vapour-particle phase distribution on various components of the sampling system and degradation caused by different filter media.

Because of the inability of PAHs to differentiate between fossil fuel and wood combustion there was a need to identify alternative tracers for wood combustion. A

dilution tunnel was used to collect emissions from woodheaters operated with different airflow settings, and around 100 organic compounds were quantified. Although the majority of compounds were not detected in ambient air samples, levoglucosan was found to be not degraded in the atmospheric samples and was identified as a consistent tracer for woodsmoke. Levoglucosan concentrations in ambient PM_{10} indicated that woodheaters contributed about 80% of wintertime air pollution in Launceston.

To validate the use of levoglucosan as a tracer for woodsmoke, the contribution of "biomass" and "fossil fuel" sources of carbon to Launceston ambient aerosols was determined by measuring the carbon-14 content using accelerator mass spectrometry. Fossil sources had a relatively low and constant input irrespective of the particulate loading, consistent with transport-related emissions. Conversely, the biomass input, most likely from woodsmoke, was found to increase linearly with particulate loading, and contributed around 97-99% of the total organic carbon fraction of Launceston wintertime PM_{10}. A modified combustion method was developed for samples collected on borosilicate filter media.

Acknowledgments

It would not have been possible for me to undertake this research without help from a multitude of people.

First and foremost, my eternal appreciation goes to my supervisor, Andrew Seen, for making all this possible. His mentoring of my academic pursuits will never be forgotten.

Geraldine Jacobsen for her help and supervision of the ^{14}C work. Thanks also to the other AMS staff for looking after me; Alan Williams, Quan Hua, Henk van der Gaast, Ugo Zoppi, and Shaun, Simon, Holly and Rachel, and to Dave Stathers for preparing combustion tubes and tolerating my constant harassment. A huge thanks must also go to AINSE for financial support for travel to ANSTO and AMS analyses through PGRA 11/02, and for ^{210}Pb dating through grant 01/126. In particular, Dennis Mather and Ben Thompson for all their support and understanding. I am also grateful to Nic and his flatmates for letting me doss on their couch on weekends while I was in Sydney.

John Gras at CSIRO Atmospheric Research for co-supervising the ^{14}C work at ANSTO, and for providing comments and feedback regarding the woodheater emissions results.

Mike Power and Michael Groth at DPIWE Environment Division for tracking down and supplying PM_{10} samples and also for allowing access to TSP sampler at Ti-Tree Bend.

Noel Davies at the CSL, University of Tasmania, for undertaking GC-MS analyses.

The Briton Family, Chris Bullard (Architects Workshop), and staff at the Ti-Tree Bend Waste Water Treatment Plant for allowing access to their properties for air sampling. Matthew French and Bonnie Atkinson for their assistance with collection of the sediment cores.

Significant financial support was given by the following organisations: University of Tasmania for funds for the dilution tunnel, associated equipment and analyses through the Internal Research Grant Scheme; Launceston City Council for general funding, and who also provided the woodheaters for testing through the "buyback" scheme; the Student Association (University of Tasmania, Launceston) provided funds towards my travel to San Diego to present at the Air and Waste Management Association annual conference, June 2003.

Thanks to the School of Chemistry for giving me the opportunity to undertake further study, and to the "others" in Launceston; Don, Trevor, Murray, Barlcay, Kym, Daniel, Bronwyn, Nathan, and Bonnie for the support, laughs and good times.

A tremendous thank you to all my family and friends for supporting and tolerating me throughout the whole process. I could not have done it without your understanding.

Finally, a hug for my late father, Bain, who unfortunately cannot be here to witness the final product.

A big thank you to you all.

Table of Contents

List of Figures

List of Tables

Glossary

AMS	Accelerator mass spectrometry
ANSTO	Australian Nuclear Science and Technology Organisation, Sydney
ANTARES	Australian National Tandem Accelerator for Applied Research, the AMS facility at ANSTO
Anth	Anthracene
AS/NZS	Australian Standard / New Zealand Standard
BaA	Benzo(a)anthracene
BaP	Benzo(a)pyrene
BTEX	Group of volatile organic compounds comprising benzene, toluene, ethylbenzene, and xylenes
CMB	Chemical mass balance
CSIRO	Commonwealth Scientific and Industrial Research Organisation
DBahA	Dibenz(a,h)anthracene
$\delta^{13}C$	Delta-carbon-13, isotopic measurement unit relative to standard reference material
DCM	Dichloromethane (CH_2Cl_2)
DPIWE	Department of Primary Industries, Water and Environment, Tasmanian State Government
EC	Elemental carbon
EF	Emission factor, mass of component or compound per kg dry wood burned
f_C	Fraction contemporary, radiocarbon unit relative to current atmospheric ^{14}C levels
Flu	Fluorene
FluA	Fluoranthene
f_M	Fraction modern, radiocarbon unit relative to ^{14}C content of reference material
GC-MS	Gas chromatography coupled to mass spectrometry detection
GFF	Glass-fibre filter
HPLC	High performance liquid chromatography
HV	High-volume PM_{10} sample(r)
LOI	Loss-on-ignition, mass lost after thermal treatment at 375^{o}C for 24 hours
Mass Fraction	Mass of compound per gram of particulate matter
m/z	mass per charge ratio (mass spectrometry)
Nap	Naphthalene
NEPM	National Environmental Protection Measure
NIST	US National Institute of Standards and Technology
NPI	National Pollution Inventory
OC	Organic carbon
ORBO tube	Glass tube containing XAD-2 adsorbent, marketed by Supelco
PAH	Polycyclic aromatic hydrocarbon
PEF	Particle emission factor, mass of particles emitted per kg dry wood burned
Phen	Phenanthrene
PM	Particulate matter
$PM_{2.5}$	Particulate matter with an aerodynamic diameter smaller than 2.5 μm
PM_{10}	Particulate matter with an aerodynamic diameter smaller than 10 μm
pMC	Percent modern carbon, radiocarbon unit relative to ^{14}C content of reference material, equal to 100 x f_M
PTFE	Polytetrafluoroethylene
Pyr	Pyrene
SIM	Selected-ion-monitoring (mass spectrometry)
SRM	Standard Reference Material
TEOM	Tapered element oscillating microbalance
TIC	Total-ion-current (mass spectrometry)
TMS	trimethylsilyl, derivative used to enhance GC analysis of highly polar compounds
TSP	Total-suspended-particles, encompasses all airborne particle-size fractions
USEPA	United States Environmental Protection Agency
VOC	Volatile organic compound

Chapter 1

Introduction

Chapter 1

Introduction

1.1 Air Pollution Regulations in Australia

Airborne particles with an aerodynamic diameter of less then 10 μm (PM_{10}) have been the subject of intensive monitoring around the world as they are able to penetrate deep into the lungs. It has been shown that an increase in ambient PM_{10} levels increases total mortality rates [1, 2], which has led to many regulatory bodies implementing ambient PM_{10} standards. The Australian Federal Government has introduced regulations through a National Environmental Protection Measure (NEPM) limiting 24-hour ambient PM_{10} levels in excess of 50 $\mu g/m^3$ to no more than 5 exceedences per year [3], and has been recently updated to include $PM_{2.5}$ (particles with a diameter less than 2.5 μm, and thought to have a greater health impact than PM_{10}). The chemical components of PM_{10} and other gaseous species can cause additional health problems, and a NEPM regarding these "air toxics" is also available . The NEPM outlines the species to be monitored, maximum allowable concentrations (Table 1.1), the methods of analysis, and requirements for reporting. A national reporting scheme for industry, the National Pollution Inventory (NPI), compiles information on emissions from various regulatory bodies and contains information on a variety of pollutants and their sources [4].

Table 1.1 Air quality standards and goals of the National Environment Protection Measure.

Pollutant	Averaging Period	Maximum Concentration	Maximum allowable exceedences by 2008
Carbon monoxide (CO)	8 hours	9.0 ppm	1 day / year
Nitrogen dioxide (NO_2)	1 hour	0.12 ppm	1 day / year
	1 year	0.03 ppm	none
Sulfur dioxide (SO_2)	1 hour	0.20 ppm	1 day / year
	1 day	0.08 ppm	1 day / year
	1 year	0.02 ppm	none
Ozone (O_3)	1 hour	0.10 ppm	1 day / year
	4 hours	0.08 ppm	1 day / year
Lead (Pb)	1 year	0.50 $\mu g/m^3$	none
Particles (PM_{10})	1 day	50 $\mu g/m^3$	5 days / year
Particles ($PM_{2.5}$)	1 day	25 $\mu g/m^3$	advisory reporting
	1 year	8 $\mu g/m^3$	standard only

Source: [3]

1.2 Air Pollution in Launceston, Tasmania

1.2.1 Study Location

The City of Launceston has a population of approximately 80,000, and is situated at the southern end of the Tamar Valley in the central north of Tasmania (Figure 1.1). Founded in 1805, Launceston is Australia's third oldest city. The city centre and northern suburbs are situated within a three-sided "bowl" created by the surrounding low-lying hills (200-500 metres high).

The Tamar Estuary runs from the confluence of the North Esk and South Esk Rivers, to Bass Strait, approximately 65 km to the north. The total area of the catchment is around 10,000 km^2 [5], or around 20% of Tasmania's land area. Land use within the catchment is dominated by agricultural and forestry operations, and a

number of historical mining activities are located over 100 km upstream of the city. The immediate area surrounding the upper estuary is urban and suburban, and has been the site of a number of industries, ranging from gasification of coal, timber yards, smelters and foundries, railway workshops, small shipyards and treated sewage outlets. The main channel of the upper reaches of the estuary (Home Reach) has been steadily silting up over the past century and has been dredged regularly over the past 20 to 30 years. A hydroelectric power station has been in operation since 1955, and diverts water from the South Esk River through to Ti-Tree Bend, about 2 km downstream from where the estuary meets the South Esk River.

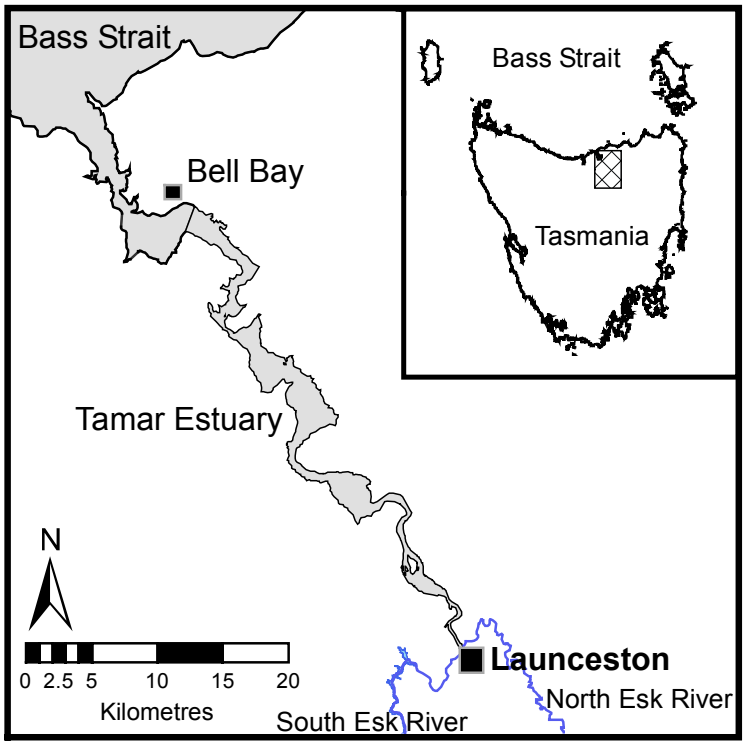

Figure 1.1 Study area; Launceston and the Tamar Estuary.
Adapted from Tasmap, Hobart.

1.2.2 Description of the Problem

Although Launceston has a relatively small population, it suffers from high levels of atmospheric pollution during the winter months (May – September, Figure 1.2). Levels of PM_{10} have been recorded in Launceston which exceed those found in Sydney, a city of nearly 4 million people. Launceston does not, however, have the photochemical smog problems usually associated with large amounts of fossil fuel use in larger cities. In the past decade, 24-hour average PM_{10} levels have exceeded the 50 $\mu g/m^3$ NEPM guideline around 15-40 times per year (Figure 1.3).

Figure 1.2 Launceston blanketed by fog and smog trapped under a temperature inversion.

Residents of Launceston have traditionally relied on woodburning as a heating source, as plentiful supplies of firewood are easily accessible close to the city. This reliance on woodburning has continued to this day, with around 46% of households (13,400) using woodheaters or open fireplaces in 2000, consuming a total of 66,300 tonnes of firewood per year [6]. There has been a steady decline in the number of households using woodheating over the past 5 years, reducing to about 26% of households (~8000) in 2004 [7].

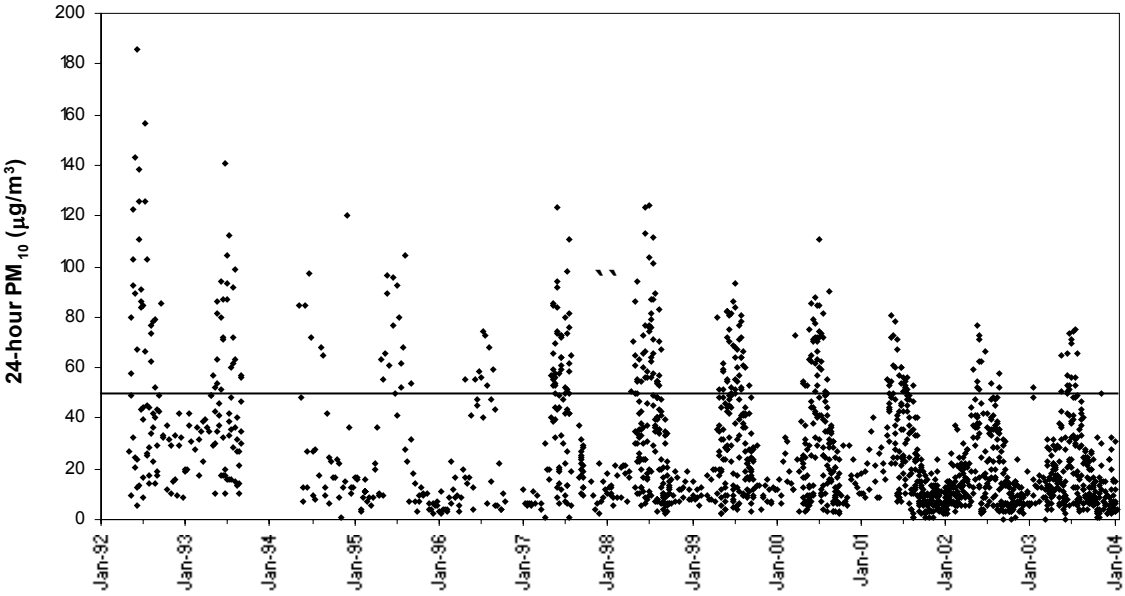

Figure 1.3 Ambient PM_{10} levels in Launceston.
24-hour average, measured by the Department of Primary Industries, Water and Environment (DPIWE, see Chapter 1.2.4). Line indicates NEPM guideline of 50 $\mu g/m^3$.

A further confounding factor contributing to high pollution levels during winter is the frequent temperature inversions formed in the Tamar Valley. Inversions are formed when the land surface undergoes thermal loss during the night, cooling the overlying air. This cooler, denser air is trapped under the warmer air above, restricting vertical mixing. Cold nights with little to no wind and clear skies are ideal conditions for the formation of inversion layers. The inversion height increases as the air temperature rises during the morning, and the inversion layer usually dissipates by midday [8].

It has been estimated from emission inventories undertaken by the NPI that around 560 tonnes of PM_{10} are released into the Launceston atmosphere annually, with the main contributors being woodburning (60%), road dust (25%) and vehicles (7%),

(Table 1.2) [4]. Up to 5.5 tonnes per day is estimated to be emitted by woodburning appliances alone during the winter months [9]. It is also estimated that around 12 tonnes of carcinogenic polycyclic aromatic hydrocarbons (PAHs) are emitted per year, with 91% arising from domestic woodburning and 7.6% from motor vehicles. Australia wide, the total amount of PAHs estimated to have been emitted to the atmosphere rose from 16 to 57 tonnes per year between 2001-02 and 2003-04, while PM_{10} levels decreased 5% over the same period [10].

Table 1.2 Estimated annual source contributions of PM_{10} and PAHs to the Launceston atmosphere (kg/year).

Source	PM_{10}	PAHs
Woodburning	340,000	11,000
Road dust	140,000	-
Vehicles	41,000	910
Other sources	35,500	128

Adapted from NPI [4].

1.2.3 Previous Studies

Due to the high level of visible air pollution during winter, Launceston has been the subject of a number of ambient air studies. The most extensive was by a Working Group comprised of scientists, health professionals and government representatives during 1991-1993 [8]. The study involved sampling of ozone, lead, PAHs and PM_{10} at five sites around the city over a two year period, and also monitored possible health impacts. The small population base of Launceston precluded any definitive conclusions being made from the epidemiological study, although a slight increase in total respiratory related hospital admissions was evident during winter. From the

chemical analysis of the high-volume PM_{10} samples, it was concluded that the majority of the PM_{10} and PAHs were produced from the combustion of wood for heating purposes, despite a correlation between airborne lead (presumably from vehicle exhaust) and PM_{10} levels. Winter levels of benzo(a)pyrene (BaP), a particularly carcinogenic PAH, ranged from 1-3 ng/m^3 with a maximum of 34 ng/m^3. This is the highest BaP concentration ever recorded in Australia [11], and clearly exceeds the "investigation level" for BaP which has been set at an annual average of 0.3 ng/m^3 as part of the draft air toxics NEPM [3]. Meteorological measurements also conducted as part of the Working Group study found temperature inversions between 140-240 metres above ground level over two nights. Katabatic winds and a gentle south-east valley wind flow transported the pollution firstly to low-lying areas and then slowly towards the north.

Launceston was included in a pilot study undertaken by the CSIRO (Commonwealth Scientific and Industrial Research Organisation) and ANSTO (Australian Nuclear Science and Technology Organisation) during 1996-97 [12]. This study measured the chemical and physical properties of airborne particles from six cities around Australia during the winter months, while comparing different sampling and measurement methods employed by government agencies around the country. Instrumentation used included a low-volume $PM_{2.5}$ sampler, two different medium-volume samplers (PM_{10}, $PM_{2.5}$), continuous samplers (TEOM, nephelometer) and particle sizing samplers (including a 12-stage cascade impactor and ultrafine particle counter). Post-sampling analysis included determination of gravimetric mass, elemental carbon, elemental analysis by proton-induced-x-ray-emission, and soluble ions by ion-chromatography. Results of this study were also reported in part by

Keywood *et al.* [13]. Comparison of the physical and chemical properties of ambient PM_{10} with those of woodsmoke allowed the researchers to conclude that wood burning was the dominate source of PM_{10} in Launceston. For example, the mass size distribution of woodsmoke particles is unimodal with a peak between 0.1-1 μm [14], and PM_{10} was found to make up 90% of the total-suspended-particle (TSP) mass. The similarity of this size distribution with that for non-sea salt potassium (nssK, a tracer for woodsmoke) was used to indicate that wood burning was the major source of PM_{10} in Launceston (Figure 1.4). This was backed up by the high organic matter content of the PM_{10} (~70% of total mass), another feature characteristic of woodsmoke [15].

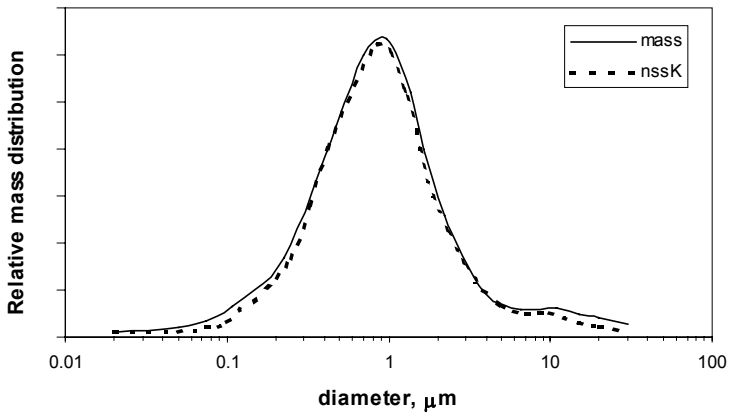

Figure 1.4 Mass distributions for total aerosol mass and non-sea-salt-potassium (nssK) in Launceston ambient air.
Adapted from Keywood *et al.* [13].

Gras *et al.* used aerosol light scattering and meteorological models to derive source functions to describe observed diurnal light scattering trends, and estimated that each woodheater in the city emitted between 11-28 g $PM_{2.5}$ per hour during the evening [16]. Mixing heights (inversion heights) were calculated to be around 150-200 m during the night, rising to over 500 m by mid-afternoon, similar to those

measured by the Working Group [8]. The diurnal cycle showed highest particulate mass during the night, with smaller peaks at 8:00am and 5:00pm coinciding with woodheater startup during the morning and evening (Figure 1.5).

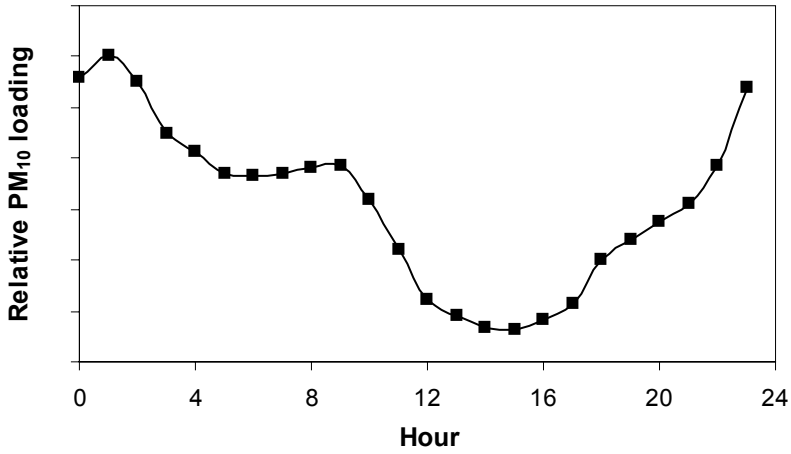

Figure 1.5 Relative diurnal variation of ambient PM in Launceston during winter.

Measured using dry-aerosol scattering coefficient during periods of low wind speed, adapted from Gras *et al.* [16].

Dispersion modelling of woodsmoke emissions from within the Launceston airshed was undertaken by Michael Power as part of his PhD project at the University of Tasmania [9]. A dispersion model was run over 33 hours, starting from a hypothetical zero pollution "episode". Within a few hours of woodheaters first being used, localised PM_{10} concentrations within Launceston's city centre had reached 30-50 $\mu g/m^3$ (Figure 1.6). A large woodsmoke plume had extended almost the entire length of the valley after 4 hours, mostly confined to the western side. Drainage from areas to the west (Deloraine, Westbury, Hagley) into the Tamar Valley north of Launceston occurred from the early evening and continued late into the night, although their contribution was relatively small. Early morning (4:00-9:00) katabatic winds from mountains to the east resulted in some of the plume

being transported in a southerly direction back towards Launceston. Maximum PM_{10} concentrations in the order of 150-220 $\mu g/m^3$ were predicted between 17:00 and 23:00, at which time levels began steadily decreasing. Sources from outside the city were found to contribute only 1.2 $\mu g/m^3$ (~4%) of PM_{10} in Launceston, and it was estimated that a 72% decrease in the number of woodheaters was required to meet the requirements of the ambient air NEPM (Table 1.1).

A recent study commissioned by Environment Australia found that woodheaters were a significant source of selected volatile organic compounds in Launceston during winter [17]. Personal exposure, and indoor and outdoor concentrations of benzene, toluene, ethylbenzenes and xylene (BTEX) were measured using passive samplers. Surprisingly, indoor concentrations of BTEX (and PM_{10}) were not influenced by the presence or absence of a woodheater in the house, indicating that indoor exposure to these pollutants originates primarily from outdoors.

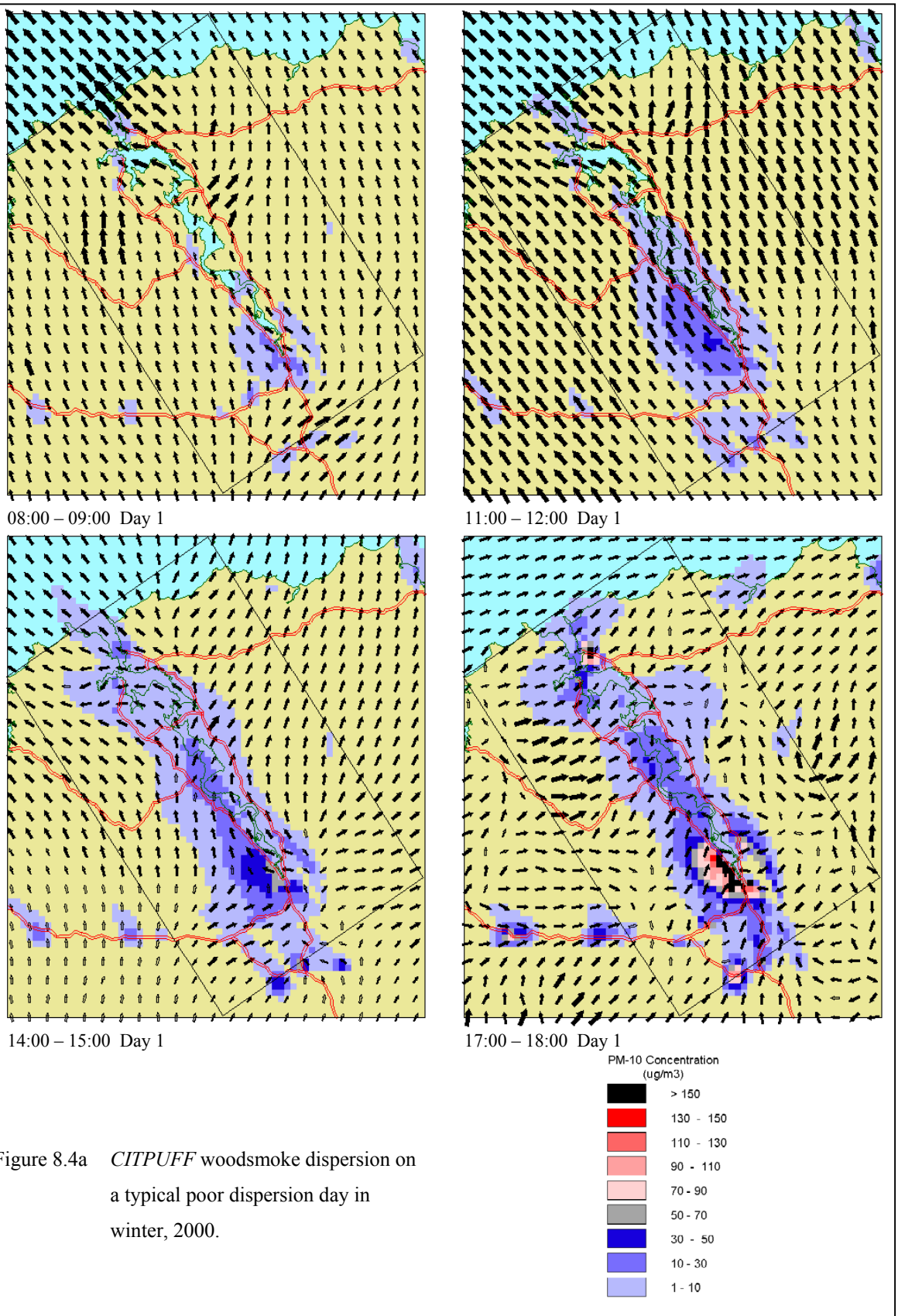

Figure 8.4a *CITPUFF* woodsmoke dispersion on a typical poor dispersion day in winter, 2000.

Figure 1.6 Dispersion modelling of woodsmoke in the Tamar Valley. Arrows indicate the wind field strength, and the colours show the predicted concentration of the smoke plume. Reproduced with permission from Power [9].

1.2.4 What is Being Done to Fix the Problem

In an effort to reduce wintertime pollution in Launceston, the Federal Government funded a "buyback" program worth two million dollars [18]. In addition to a grant of up to $500 to replace existing woodheaters with cleaner forms of heating (newer woodheater model, electric or gas), the program involved education campaigns conducted through the local media, and visits to households with persistently "smokey" chimneys. When this program concluded in early 2004 it had removed over 2000 heaters, and around 95% of these were replaced with electric heaters [7]. It was estimated that around 8000 heaters remained in use in the airshed. A comprehensive scoping study undertaken for the buyback scheme on behalf of Environment Australia identified the need to reduce PM_{10} levels in Launceston by around 60% to bring it into line with the 50 $\mu g/m^3$ guideline set down in the NEPM [6]. Thus there is a continual need to monitor the contribution of woodheaters to ambient air pollution in Launceston to assess the effectiveness of the buyback program.

An on-going monitoring program run by the Department of Primary Industries, Water and Environment (DPIWE, Tasmanian State Government) has measured 24-hour PM_{10} levels at the Ti-Tree Bend site using high-volume samplers (Figure 1.7). Data was initially collected every sixth day from 1992, expanded to every day during the winter months (May – September) in 1997, and expanded again to every day of the year in 2001 (see Figure 1.3). Continuous (1-hour average) levels have been measured since 2002 using a tapered element oscillating microbalance (TEOM) and Dust-Track particle counter.

Figure 1.7 Air sampling units operated by DPIWE at Ti-Tree Bend.
L-R: high-volume total-suspended-particulates (TSP), 2 x high-volume PM_{10}, TEOM (low-volume PM_{10}) housed in an air-conditioned container.

The Australian Bureau of Meteorology issues forecasts of predicted PM_{10} levels in Launceston through the local media. The model was derived from historical PM_{10} measurements by DPIWE through multiple linear regression of a number of meteorological observations and predictions, including temperature, dew point, surface wind speed, south-to-north component of surface wind, total cloud amount, mean sea level pressure and the date [19]. Although the model only explained approximately half of the observed variance, of the 126 forecasts made during 2003, 75% predicted the correct pollution category (i.e. "good" $\leq$40 $\mu g/m^3$, "moderate" 41-50 $\mu g/m^3$, "bad" >50 $\mu g/m^3$), and 16% were one category out.

1.3 Overview of Source Apportionment Techniques

Determining sources of pollutants is of primary importance for governments, environmental agencies and regulatory bodies, especially when levels may have health impacts. While in some cases there may be one obvious source of pollution, such as bushfires, mining activities, or fossil fuel fired power stations, the majority of urban regions experience pollution emanating from a multitude of sources. In these cases, mathematical models must be used in order to unravel the contributing sources. To this end, two opposite but complementary methods are commonly used; source- and receptor- based models.

1.3.1 Source-Based Models

Emission inventories are a simple source-based method for calculating source contributions to an airshed. An estimate of the total emissions from a source category is calculated by multiplying the average emission factor from that source by the number of units in operation. This is then repeated for each source category. Inventory based studies require accurate emissions data from as many point- and area- sources as possible. The Australian Department of Environment and Heritage manages the National Pollution Inventory (NPI), a database of pollutant emissions from many regions around Australia [4].

Source-based models, also called dispersion models, calculate the impact of source j (S_j) at a site (termed the "receptor") using the emission rate from the source (E_j) and a dispersion factor (D_j, Equation 1.1) [20, 21]. A dispersion factor is calculated for

each source using detailed meteorological data such as air temperature, wind speed, and wind direction gathered within an airshed during the period under investigation.

$$S_j = D_j E_j \quad (1.1)$$

Dispersion models are good at determining contributions from specific point sources, such as coal fired power stations [22]. They are also useful in modelling past- and possible future- scenarios arising from the release of radioactive material from nuclear power plants or storage facilities [23].

Factors incorporated in dispersion models include transport, dispersion, deposition, and chemical and physical transformations [21]. Many different dispersion models are available (for example, the USEPA provide access to numerous models, with many provided for specific applications such as O_3 and CO_2 [24]), and the selection of the appropriate model depends on the application and on the level of sophistication required.

A study by Barna *et al.* into air pollution in Christchurch, New Zealand, is a good example in the use of dispersion modelling in an urban environment [25]. Christchurch is another city which experiences high wintertime pollution caused by residential woodheating, where 24-hour PM_{10} levels up to 300 $\mu g/m^3$ have been recorded. This study used detailed emission inventories, residential surveys and meteorological data as input to the CALMET and CALPUFF meteorological and dispersion modelling software, respectively. Predicted PM_{10} levels generally followed the observed diurnal patterns at the four monitoring sites. Various

pollution abatement strategies were also investigated, with a decrease in PM_{10} levels between 31-52% predicted if wood fires and/or coal fires were banned from use.

1.3.2 Receptor-Based Models

Receptor models, often called chemical mass balance (CMB) models, are in essence the opposite of dispersion models. The basis of this technique is to determine source contributions using data gathered at the receptor and knowledge of the composition of emissions from potential sources, assuming conservation of mass during transport. Thus, the chemical composition at the receptor is modelled as the linear sum of each compound emitted from each source multiplied by the sources' respective contributing factor. Hence, the concentration of compound *i*, per gram of particulate matter in ambient air, C_i, is given as:

$$C_i = \sum_j f_j a_{ij} \tag{1.2}$$

where a_{ij} is the concentration of compound *i* emitted per gram of particulate matter emitted from source *j*, and f_j is the fractional contribution of source *j* at the receptor. Overviews of receptor models have been presented by Cooper and Watson [26], Henry *et al.* [20], Watson [27], and Gordon [28].

All CMB models require a number of assumptions to be made, with many of them not strictly met in practice. The degree to which they are met will influence the uncertainty of the calculated source contributions. The six basic assumptions are [29]:

1: the composition of the source emissions remain constant over the period of ambient and source sampling.
2: chemical species do not react with each other, and add linearly at the receptor.
3: all contributing sources have been identified and had their emissions characterised.
4: the source profiles are linearly independent of each other.
5: the number of sources is less than the number of measured species.
6: measurement uncertainties are random, uncorrelated, and normally distributed.

Assumptions 1 and 2 will probably never be true in practice, as emissions will rarely be constant over a given (sampling) time period, and chemical transformations (i.e. reactions, degradation, deposition) are almost guaranteed to occur for most chemical species during transport from the source to the receptor. Artificial aging of source profiles and degradation factors can be incorporated into the model in an attempt to counter these problems. Whenever there are diffuse sources such as automobiles and residential woodheaters, assumption 3 will not be strictly true, as it would be impossible to include every single emitting source. In these cases it is possible (even essential) to group similar sources into a generalised source "category" (e.g. car exhaust, diesel exhaust, wood burning). The composite profiles are generally created by averaging the emission profiles across a sampled population. These composites can also help reduce or remove collinearity problems associated with assumption 4, where sources that have similar chemical profiles cannot be

sufficiently resolved. As CMB models use multiple linear regression techniques, the number of measured species (*i*) must be greater than or equal to the number of sources (*j*) otherwise the set of linear equations (Equation 1.2) will be indeterminate (assumption 5). As many of the fundamental assumptions of receptor modelling are generally not met, the output from receptor models, and dispersion models [21], should only be treated as estimates.

Watson *et al.* state that "source and ambient measurements must be paired in time to establish reasonable estimates of source/receptor relationships" [29]. Thus it is important that they are also paired spatially, because emissions from many sources are known to vary between regions. For example, emissions from combustion sources such as automobiles and wood combustion vary depending on the fuel. Source profiles may be either taken from the literature, or can be determined as part of the overall study. Source profiles used in CMB models are comprised of the mass fraction of each chemical species, normalised to either total particle mass or the total volatile compound concentration, for particle- and vapour- phase studies, respectively. Reviews of the principles for creating profiles from combustion sources are given by Mitra *et al.* [30], and Zhang and Morowska [31].

A software package for undertaking CMB calculations is freely available from the USEPA, namely CMB8 [32]. This program uses the effective variance weighted method, where species with higher precision have greater influence on the calculations. A detailed discussion on the theory and use of CMB8 has been prepared to complement the software user's manual [29]. An outline of the eight steps necessary to ensure the model produces meaningful data are presented, along

with many previous studies from the literature. Chow, Watson and others have also compiled extensive reviews of previous source apportionment studies [33, 34].

The simplest form of a receptor model uses just a single "tracer" species for each source. For example, retene is produced exclusively by combustion of softwoods [35], and syringol from hardwoods [36], and so these compounds may be used to discriminate between these two source categories. However, using many more chemical species allows differentiation between a much larger number of sources, and also potentially increases the accuracy of the CMB.

1.3.3 Radiocarbon as a Tracer for Air Pollution

Tracer species are not limited to chemical compounds, and the isotopic composition (carbon-14) of species can also be used to trace for biomass combustion emissions. Trees and other biomass contain essentially "modern" levels of ^{14}C, whereas fossil fuels are so old (millions of years) that all the radioactive ^{14}C has decayed ($t_{1/2}$ = 5730 years). As emissions from combustion sources contain the same isotopic ratio as the fuel, the relative contributions of biomass burning and fossil fuel combustion can be established by measuring the ^{14}C content of ambient particulate matter [37, 38]. Despite the technique only being able to discriminate between two broad source categories, it is a powerful tool able to complement or verify other source apportionment methods [39]. It is not a common technique, however, due mainly to the high cost of analysis; the carbon content of atmospheric samples tends to be too small to allow analysis by traditional β-decay counting, and thus samples must be

analysed by the more sensitive (and expensive) technique of accelerator mass spectrometry (AMS).

1.4 Outline of Thesis

This thesis will describe the three sections of work undertaken during my PhD candidature to assess methods to characterise and quantify the contribution of woodsmoke to Launceston wintertime air pollution.

An attempt will be made to reconstruct historical levels and sources of air pollution in Launceston using polycyclic aromatic hydrocarbons (PAHs) measured in a dated sediment core collected from the upper Tamar Estuary. Various factors influencing the sampling of PAHs in ambient air will also be investigated.

The organic composition of emissions from woodheaters operated with different airflow settings will be evaluated. These profiles will then be compared to ambient air samples, and an estimate made of the woodheater contribution to wintertime air pollution in Launceston.

The third method employed to determine the contribution of woodsmoke to Launceston air pollution utilised the ^{14}C isotopic variability in emissions from "biomass" and "fossil fuel" combustion sources. Results will be compared to those obtained using woodsmoke tracer compounds. This is only the second time that radiocarbon has been used as a means of source apportionment in Australia, and the first to use accelerator mass spectrometry.

1.5 References

1. Dockery, D.W.; Pope, C.A.; Xu, X.; Spengler, J.D.; Ware, J.H.; Fay, M.E.; Ferris, B.G.; Speizer, F.E. An association between air pollution and mortality in six U.S. cities, *New Eng. J Med* **1993**, 329(24), 1753-1759.
2. Morgan, G.; Corbett, S.; Wlodarczyk, J.; Lewis, P. Air pollution and daily mortality in Sydney, Australia, 1989 through 1993, *Am. J. Pub. Health* **1998**, 88(5), 759-764.
3. National Environmental Protection Council, National environment protection measure (ambient air quality), http://www.ephc.gov.au/.
4. Department of Environment and Heritage, National Pollution Inventory, http://www.npi.gov.au/.
5. Pirzl, H.; Coughanowr, C. State of the Tamar Estuary: a review of environmental quality data to 1997, Supervising Scientist Report 128, Supervising Scientist, Canberra, **1997**.
6. Atech Group Woodheater emissions management program for the Tamar Valley - Scoping study, Environment Australia, Canberra, http://www.ea.gov.au/atmosphere/airquality/woodsmoke/pubs/tamarstudy.pdf, **2001**.
7. Norwood, R. Launceston City Council, *pers. comm.* **2004**.
8. Working Party, Report on an investigation by an expert working party into air pollution, environmental health and respiratory diseases, Launceston and upper Tamar Valley, Tasmania, 1991-94, Launceston City Council, Launceston, **1996**.
9. Power, M. Air pollution dispersion within the Tamar Valley, Ph.D. Thesis, University of Tasmania, Hobart, **2001**.
10. Environment Australia, National Pollution Inventory: Summary report of fifth year data 2002-2003, Environment Australia, Canberra, http://www.npi.gov.au/publications/fifth-report/pubs/npi-year-5-2002-03.pdf, **2004**.
11. Berko, H.N. Technical report no. 2: Polycyclic aromatic hydrocarbons (PAHs) in ambient air in Australia, Environment Australia, Canberra, www.deh.gov.au/atmosphere, **1999**.
12. Ayers, G.P.; Keywood, M.D.; Gras, J.L.; Cohen, D.; Garton, D.; Bailey, G.M. Chemical and physical properties of Australian fine particles: A pilot study, Environment Australia, Canberra, http://www.dar.csiro.au/publications/CSIRO_AFP.pdf, **1999**.
13. Keywood, M.D.; Ayers, G.P.; Gras, J.L.; Gillett, R.W.; Cohen, D.D. Size distribution and sources of aerosol in Launceston, Australia, during winter 1997, *J. Air & Waste Manage. Assoc.* **2000**, 50, 418-427.
14. Kleeman, M.J.; Schauer, M.J.; Cass, G.R. Size and composition distribution of fine particulate matter emitted from wood burning, meat charbroiling, and cigarettes, *Environ. Sci. Technol.* **1999**, 33(20), 3516-3523.
15. Fine, P.M.; Cass, G.R.; Simoneit, B.R.T. Chemical characterization of fine particle emissions from fireplace combustion of woods grown in the Northeastern United States, *Environ. Sci. Technol.* **2001**, 35(13), 2665-2675.

16. Gras, J.L.; Keywood, M.D.; Ayers, G. Factors controlling winter-time aerosol light scattering in Launceston, Tasmania, *Atmos. Environ.* **2001**, 35, 1881-1889.
17. Galbally, I.E.; Gillett, R.W.; Bentley, S.T.; Powell, J.; Lawson, S.; Weeks, I.A.; Selleck, P.; Boast, K.; Coram, S. Technical report no. 8. Personal monitoring of selected VOCs: The contribution of woodsmoke to exposure, Environment Australia, Canberra, www.deh.gov.au/atmosphere, **2004**.
18. $2 million in Federal funding to help Launceston residents breathe easier, Media Release, 29 July 2001, Sen. Jocelyn Newman, http://www.ea.gov.au/minister/env/2001/mr29jul201.html.
19. Shepherd, D. Review of Launceston air quality forecasts, March 2003, Bureau of Meteorology, Hobart, **2003**.
20. Henry, R.C.; Lewis, C.W.; Hopke, P.K.; Williamson, H.J. Review of receptor model fundamentals, *Atmos. Environ.* **1984**, 18(8), 1507-1515.
21. Schulze, R.H. Dispersion modeling using personal computers, *Atmos. Environ.* **1990**, 24A(8), 2051-2057.
22. Levy, J.I.; Spengler, J.D.; Hlinka, D.; Sullivan, D.; Moon, D. Using CALPUFF to evaluate the impacts of power plant emissions in Illinois: model sensitivity and implications., *Atmos. Environ.* **2002**, 36, 1063-1075.
23. Desiato, F. A long-range dispersion model evaluation study with Chernobyl data, *Atmos. Environ.* **1992**, 26A(15), 2805-2820.
24. USEPA, Support Center for Regulatory Air Models, http://www.epa.gov/scram001.
25. Barna, M.G.; Gimson, N.R. Dispersion modelling of a wintertime particulate pollution episode in Christchurch, New Zealand, *Atmos. Environ.* **2002**, 36, 3531-3544.
26. Cooper, J.A.; Watson, J.G. Receptor oriented methods of air particulate source apportionment, *J. Air Poll. Control Assoc.* **1980**, 30(10), 1116-1125.
27. Watson, J.G. Overview of receptor model principles, *JAPCA* **1984**, 34(6), 619-623.
28. Gordon, G.E. Receptor models, *Environ. Sci. Technol.* **1988**, 22(10), 1132-1142.
29. Watson, J.G.; Robinson, N.F.; Fujita, E.M.; Chow, J.C.; Pace, T.G.; Lewis, C.; Coulter, T., CMB8: Applications and validation protocol for $PM_{2.5}$ and VOCs, Desert Research Institute, http://www.epa.gov/scram001/.
30. Mitra, A.P.; Morawska, L.; Sharma, C.; Zhang, J. Chapter two: methodologies for characterisation of combustion sources and for quantification of their emissions, *Chemosphere* **2002**, 49(9), 903-922.
31. Zhang, J.; Morawska, L. Combustion sources of particles: 2. Emission factors and measurements methods, *Chemosphere* **2002**, 49(9), 1059-1074.
32. CMB8 user's manual, United States Environmental Protection Agency, http://www.epa.gov/scram001.
33. Chow, J.C.; Watson, J.G. Review of $PM_{2.5}$ and PM_{10} apportionment for fossil fuel combustion and other sources by the chemical mass balance receptor model, *Energy and Fuels* **2002**, 16(2), 222-260.
34. Watson, J.G.; Zhu, T.; Chow, J.C.; Engelbrecht, J.; Fujita, E.M.; Wilson, W.E. Receptor modeling application framework for particle source apportionment, *Chemosphere* **2002**, 49, 1093-1136.

35. Ramdahl, T. Retene - a molecular marker of wood combustion, *Nature* **1983**, 306, 580-582.
36. McDonald, J.D.; Zielinska, B.; Fujita, E.M.; Sagebiel, J.C.; Chow, J.C.; Watson, J.G. Fine particle and gaseous emission rates from residential wood combustion, *Environ. Sci. Technol.* **2000**, 34(11), 2080-2091.
37. Currie, L.A.; Klouda, G.A.; Gerlach, R.W. Radiocarbon: Nature's tracer for carbonaceous pollutants, in *Proceedings of the 1981 International Conference on Residential Solid Fuels: Environmental impacts and solutions*, Cooper, J.A. and Malek, D., Editors. **1982**, Oregon Graduate Center: Beaverton, Oregon. p. 365-385.
38. Klinedinst, D.B.; Currie, L.A. Direct quantification of $PM_{2.5}$ fossil and biomass carbon within the Northern Front Range Air Quality Study's domain, *Environ. Sci. Technol.* **1999**, 33(23), 4146-4154.
39. Currie, L.A.; Klouda, G.A.; Schjoldager, J.; Ramdahl, T. The power of ^{14}C measurements combined with chemical characterization for tracing urban aerosol in Norway, *Radiocarbon* **1986**, 28(2A), 673-680.

Chapter 2

Polycyclic Aromatic Hydrocarbons in Launceston Ambient Air and Tamar Estuary Sediments

Chapter 2

Polycyclic Aromatic Hydrocarbons in Launceston Ambient Air and Tamar Estuary Sediments

2.1 Introduction

2.1.1 Overview & Health Effects

Polycyclic aromatic hydrocarbons (PAHs) are a class of organic compounds containing two or more fused benzene rings (Figure A.1, Appendix A). They are found in petroleum products and are also formed during incomplete combustion of both fossil and biomass fuels. Although PAHs are ubiquitous in the environment, anthropogenic activity is by far the main source of these compounds in urban areas.

Hundreds of different PAHs have been identified, and the USEPA has included 16 PAHs in a list of "priority pollutants" (Table 2.1). Benzo(a)pyrene in particular is the most widely reported of these, due to its potent carcinogenic effects.

Table 2.1 PAHs included in USEPA list of priority pollutants, and their relative carcinogenic potential (1-5; – not known or inactive).

Naphthalene	(–)	Benzo(a)anthracene	(1)
Acenaphthene	(–)	Chrysene	(1)
Acenaphthylene	(–)	Benzo(b)fluoranthene	(2)
Fluorene	(–)	Benzo(k)fluoranthene	(–)
Anthracene	(–)	Benzo(a)pyrene	(4)
Phenanthrene	(–)	Dibenz(a,h)anthracene	(3)
Fluoranthene	(–)	Indeno(1,2,3-cd)pyrene	(1)
Pyrene	(–)	Benzo(ghi)perylene	(1)

Adapted from Kennish [1].

Much attention has been given to these compounds in recent times due to their carcinogenic and mutagenic effects [2, 3]. Of particular concern is the transport and fate of PAHs emitted to the atmosphere from combustion sources, and a review undertaken on-behalf of Environment Australia outlined potential problems of atmospheric PAHs [4]. It has been estimated that about 30 lung cancers per year are caused by airborne PAHs in Sydney [5]. Consumption of contaminated food is also of concern, especially from seafood. Bivalves (mussels and oysters) are particularly good at concentrating heavy metals [6] and PAHs [7, 8], and are used as biomarkers for these groups of pollutants. Appreciable amounts of PAHs are also imparted to smoked foodstuffs during the smoking process and from artificial smoke flavouring [9]. Grilling of meat is also a source of atmospheric [10] and ingestable [11] PAHs.

2.1.2 Formation

PAHs are formed predominantly through thermal decomposition of organic material during incomplete combustion of fossil and biomass fuels. A number of

mechanisms for PAH formation have been proposed, and are included in a review by Mastral and Callen [12]. Mechanisms include creation of free-radicals from the "cracking" of char, which quickly re-combine to form more stable aromatic ring structures, or through a Diels-Alder type reaction of alkenes and subsequent dehydrogenation. There is also a temperature dependence on the total amount of PAHs produced, reaching a maximum at around 900^{o}C from combustion of phenols and lignin under an inert atmosphere [13]. The PAH content of car exhaust has been shown to co-vary with the PAH content of the fuel [14]. Although combustion destroyed the majority (>95%) of fuel borne PAHs, it was estimated that greater than 50% of emitted PAHs were formed during the combustion process.

2.1.3 PAHs in Air

Once released to the atmosphere, PAHs can undergo a variety of chemical and physical changes. Firstly, they will partition between the particle- and vapour-phases according to their volatility, and ultimately they will either degrade or be removed from the atmosphere through deposition to the earth's surface, where soils and sediments act as final sinks.

2.1.3.1 Vapour-particle partitioning

The distribution of airborne organic pollutants between the particle- and vapour-phases tends to mirror the vapour pressure of the compounds [15], and in order to completely assess the true nature of airborne contamination, both particle- and vapour-phases must be collected. Particle-phase compounds are collected by

drawing air through filters, while adsorbents such as polyurethane foam (PUF) or Amberlite XAD-2 resin (a hydrophobic styrene co-polymer) are placed behind the filter to collect compounds in the vapour-phase.

Chuang *et al.* compared the collection efficiencies of PUF and XAD-2 resins as adsorbents for vapour-phase PAHs and found that XAD-2 had a higher collection efficiency for the more volatile PAHs, and that collection efficiency increased for both adsorbents as the ambient temperature decreased [16]. XAD-2, however, has a much higher flow resistance making it less practical for high-volume samplers.

The inherent nature of air sampling creates a problem known as "blow-off", where PAHs originally collected in the particle-phase volatilise as additional air is drawn through the filter [17]. Higher flow-rates have been found to reduce the amount of particle-phase PAHs collected on glass-fibre filters [18].

2.1.3.2 Degradation of atmospheric PAHs

Photodegradation has been shown to be a major pathway for decomposition of PAHs, through formation of nitro- and oxy- derivatives [19, 20]. Kamens and co-workers have investigated the decay of PAHs within an outdoor Teflon-film chamber [21, 22, 23]. They found that the decay rate was proportional to the sunlight intensity, which had a much greater influence on PAH decay than either O_3 or NO_2 concentrations. Temperature was also found to be a major factor in the decay of woodsmoke associated PAHs, which suggests that only small losses would be expected during colder winter months.

Photodegradation rates are also increased in the presence of certain organic compounds [24, 25]. Degradation occurred approximately seven times faster in the presence of methoxyphenols, a class of compounds emitted in large quantities from woodburning, than in the presence of hexadecane, which is representative of diesel and automobile exhaust. Little degradation occurred when these tests were carried out in the dark.

Stabilisation of combustion derived PAHs can occur through binding with co-formed particles, with a fraction potentially trapped within the particles themselves [26].

2.1.3.3 Deposition of atmospheric PAHs

PAHs emitted to the atmosphere will ultimately be degraded or deposited to the earth's surface. Two mechanisms for PAH deposition from the atmosphere have been investigated in numerous studies: dry- and wet- deposition. Dry deposition involves the transfer of vapour- and particulate- phase compounds from the atmosphere either through gaseous exchange or under gravity [27]. Wet deposition on the other hand is relatively fast, involving "washout" during periods of rain. Rain periods also act to wash PAHs deposited to the ground into waterways, a process known as "urban runoff" [28]. McVeety and Hites used a chemical mass balance (CMB) method to show that although it is a much slower process, total dry deposition to a small lake exceeded wet deposition by a factor of ten [29]. A similar PAH distribution found between the vapour- and water-dissolved-phases also shows the dominance of gaseous exchange [30].

Global atmospheric transport allows pollution from heavily urbanised and industrialised areas to impact upon pristine regions, possibly many thousands of kilometres away. The impact of atmospheric transport has been assessed by measuring levels in remote mountain lakes scattered throughout Europe [31] and deep sea sediments in the Pacific Ocean [32]. Decreasing concentration gradients were observed with increasing distance from the source in the direction of the prevailing winds.

2.1.4 PAHs in Sediment

Sediments tend to act as sinks for many anthropogenic pollutants. Input of PAHs to waterways and sediments arise from sources such as urban runoff, industrial and sewage discharges, creosote treated woods, and direct deposition from the atmosphere. Many studies have focussed on the impact from established industries, such as aluminium smelters [33, 34] and coal fired power stations [35]. Other studies have looked at the immediate and lasting effects from the grounding of an oil tanker [36], or from forest fires [37].

Not all studies have focussed on heavily polluted regions, however. Total PAH levels in rivers of north Siberia and the Arctic Ocean were, as expected, extremely low, and were thought to have been atmospherically transported from more industrialised areas of Russia and Europe [38]. Other Arctic regions haven't faired so well, with PAH levels in the Beaufort Sea north of Canada indicating extensive contamination from petroleum exploration [39].

2.1.4.1 Sediment cores

The relative inertness of PAHs bound to sediments make them good tracers for gauging historical anthropogenic contributions to local environments through the collection of sediment cores (for example [31, 33, 40-46]).

Changes in PAH sources over time can also be reconstructed through changes in PAH compound ratios and CMB models on sediment cores [47-50], although an assumption that source profiles have remained constant must be made. See Chapter 2.1.5 for further discussion on sourcing PAHs.

In a study of lakes situated in urban areas of the USA, Van Metre *et al.* found that PAH levels have increased over the past decade [51]. This was noted to be contrary to previous studies, and the authors suggested that increased traffic density due to urbanisation was the main cause.

Lima *et al.* reconstructed the flux of PAHs to the Pentaquamscutt River basin (Rhode Island, USA) by sectioning a core into thin (5 mm) slices, allowing a high temporal resolution to be obtained [52]. Essentially very low and constant concentrations were observed from the bottom of the core, which dated from 1820, to around 1900. At this time, levels of most compounds increased, showing several peaks in concentration, with an overall maximum occurring around 1960. Some smaller peaks, which had not been observed previously, correlated well with historical events such as the Great Depression in the 1930s and another immediately preceding the 1973 oil embargo. Levels slowly decreased until the mid 1990s where they increased sharply, again probably due to increasing traffic density. Changes in

the relative abundances of different PAHs also coincided with historical events such as high use of coal during the Great Depression, the increasing use of oil and gas from the 1950s, and automobile emission control technology from the 1970s onwards.

2.1.4.2 Sediment – pore-water partitioning

Partitioning between the sedimentary and aqueous phases plays an important role in determining PAH reactivity, mobility and bioavailability in sediments. The more water soluble PAHs tend to associate less with sedimentary particles, and have been found to be depleted in sediments relative to particles suspended in the water column [53].

Sedimentary pore-water concentrations have been shown to be much lower than those predicted from solubility constants alone [54]. The presence of sedimentary organic matter [33, 55, 56] and elemental carbon (EC) [57-59] can account for some of these anomalies. Going one step further, Accardi-Dey and Gschwend have shown that incorporating both absorption into organic matter and adsorption onto elemental carbon can explain the higher than expected distribution coefficients [60, 61]. Elemental carbon (also known as "soot", or "black" carbon) is formed exclusively by combustion sources, and pyrogenic (combustion derived) PAHs are less available than petrogenic (petroleum derived) PAHs for degradation and biological uptake because of the strong association with co-formed EC [57]. In addition, the radiocarbon (^{14}C) content of EC and PAHs in a number of Standard Reference Materials was found to be similar ($f_M < 0.1$), indicating that both were primarily derived from fossil fuel combustion [62] (see Chapter 4.1.5). Hence a

positive relationship between levels of PAHs and EC in sediment suggests that pyrogenic sources have dominated inputs of PAHs.

2.1.4.3 Degradation of PAHs in sediment

A number of studies have investigated degradation rates of PAHs in sediments. The aerobic biodegradation half-life of phenanthrene in sediments has been shown to range between 0.6 and 5.8 days [63]. Degradation was found to be much faster in the absence of sediment, showing some sort of stabilising effect by either the particles themselves or other compounds present. Readman *et al.* found that microbial degradation occurs fastest for lower molecular weight compounds [64], although in a further study the same authors found that the uniformity of PAH levels throughout a core from an estuary in the UK implied they were chemically inert to the surrounding conditions, and "unavailable" for degradation or partitioning [40].

Another study has shown that native phenanthrene and chrysene bioavailability decreases through sequestration as soils age, and that freshly spiked PAHs degraded substantially faster than native PAHs [65]. This view is shared by others, as discussed in a critical-review article [66]. This implies that the majority of degradation and bioavailability studies, which use spiked compounds as their testing material, may be overestimating degradation rates and potential toxicities of PAHs in natural sediments.

2.1.5 Methods for Determining Sources of PAHs

For regulatory bodies to be effective in regulating and monitoring pollution, there is a need to understand the relative contribution from potential sources. There are a number of ways to deduce the origins of PAHs, including isomer ratios, numerical models, and isotopic composition.

The presence of marker PAHs and variations in isomer ratios have commonly been used to differentiate between pyrogenic and petrogenic derived sources. For example, coronene and benzo(ghi)perylene are emitted in large amounts from automobiles [67, 68], and retene is formed exclusively from the burning of softwoods [69]. Commonly used source ratios are the Phen/Anth and FluA/Pyr ratios [36, 45, 70, 71], while others have used alkylated to parent PAH ratios [72], relative abundances of dimethylphenanthrene isomers [73], or ternary plots [7, 74]. The use of ratios is somewhat limited however, due to the large range of values observed for many sources.

The Phen/Anth ratio has been shown to be temperature dependant [70], with higher temperatures (combustion) producing lower ratios (4-10) when compared to lower temperature geological formation of petroleum products (>10). The FluA/Pyr ratio has been determined experimentally, with values >1 typical for combustion- and <1 for petroleum- sources [75, 76]. Freeman & Cattell found FluA/Pyr ratios ranging 0.8-1.0 for burning Australian native hardwoods [77], and samples collected from a Brisbane car-park had a FluA/Pyr of 0.60 [78]. Coal combustion has been found to have lower Phen/Anth and FluA/Pyr ratios than woodburning [79]. A review of

some ratios from atmospheric and non-atmospheric sources is included by Maher & Aislabie [7].

Witt and Trost found a strong correlation between BaP levels and copper and lead in coastal sediments of Germany [44], and suggested they were associated with airborne particles originating from combustion processes, most likely vehicle exhaust. With the complete removal of lead from petrol in Australia, it can no longer be used as a tracer for vehicular emissions.

Chemical mass balance (CMB) models and other numerical models have been used to apportion PAH sources in both sedimentary and atmospheric environments. These models apportion receptor concentrations by estimating the linear contribution from each source. To successfully apply a CMB model, the chemical composition of emissions from sources must be known, and to that end a number of PAH fingerprinting studies have been completed [50, 67, 80-82]. Most studies using the CMB method to apportion PAHs have found either coal combustion or automobile exhaust as the main contributors [30, 81, 83, 84].

A further requirement of a CMB is that there is no alteration in the composition of the target compounds between the source and the receptor. This assumption is also required when using PAH ratios for sourcing. One group of researchers has consistently used Nap in its CMB calculations [48, 49, 85], presumably to apportion woodburning as they report Nap as comprising a high proportion (~75%) of PAHs emitted from woodburning. However, the use of Nap in CMB models for sediments is questionable due to the potential for large losses due to its high vapour-pressure,

solubility and reactivity which should invalidate its use in CMBs, a view shared by others [86].

Differentiation between "fossil" and "biomass" sources of PAHs is now achievable by measuring the carbon-14 content of individual compounds (see Chapter 4). In the past, the requirement of relatively large sample sizes (>1 mg) meant that only the total organic fraction of air samples could be analysed for ^{14}C. The increased sensitivity of accelerator mass spectrometer (AMS) has allowed sample sizes <10 μg to be measured. Coupled to preparative capillary gas chromatography, determination of the ^{14}C abundance of individual compounds is now possible. Reddy and co-workers analysed PAHs from a number of NIST Standard Reference Materials, and found they were derived mainly from combustion of fossil fuels, contrasting with the approximately 50% biomass nature of the total organic carbon fractions [62]. Further ^{14}C studies of PAHs where woodburning is a primary source of pollution may give a better indication of ratios from these source types.

2.1.6 Previous Studies of PAHs in Australia

2.1.6.1 Launceston and Tamar Valley

Two studies of PAH levels in the Tamar Estuary were identified in the "State of the Tamar Estuary" report in 1997 [87]. Both centred around the industrial area of Bell Bay at the northern end of the Estuary (Figure 1.1). Conflicting results between the studies were observed for both sediments and oysters, with BaP levels from the two studies reported as <1-300 ng/g and 550-12,220 ng/g for sediments, and <1-13 ng/g

and <1-1800 ng/g in oysters, respectively. The high levels found were attributed to the large amount of shipping in the area, plus effluent and runoff from an aluminium smelter, a manganese ferroalloy plant, and other local industries.

Three previous studies have measured PAHs in Launceston ambient air. An undergraduate student at the University of Tasmania found wintertime BaP levels ranged 0.2-2.4 ng/m^3 [88], and levels <1-5 ng/m^3 were found in seven low-volume air samples collected from two sites by this author as part of an Honours project, also at the University of Tasmania [89]. Concentrations in that study compared well with those found in samples collected with a co-located high-volume sampler. Concentrations of benzo(a)pyrene were reported as part of the Working Group study during 1991-93, and were generally 1-3 ng/m^3 during the winter, with a maximum level of 34 ng/m^3 [90].

Dated sediment cores taken from the Tamar Estuary at Rosevears (approximately 20 km north-west of Launceston) and Home Reach were analysed for PAHs as part of Honours work undertaken by the author [89]. The Home Reach core showed fluctuating PAHs levels over the past 50 years, with levels steadily decreasing in the past 20 years (Figure 2.1). The very low sedimentation rate subsequently determined for the Rosevears core meant that only the top 5-10 cm of the core could be dated using ^{210}Pb methods, corresponding to the period after European settlement in the area. Not surprisingly, levels of benzo(a)pyrene at Rosevears were extremely low (<2 ng/g) and were expected to represent background levels for the region.

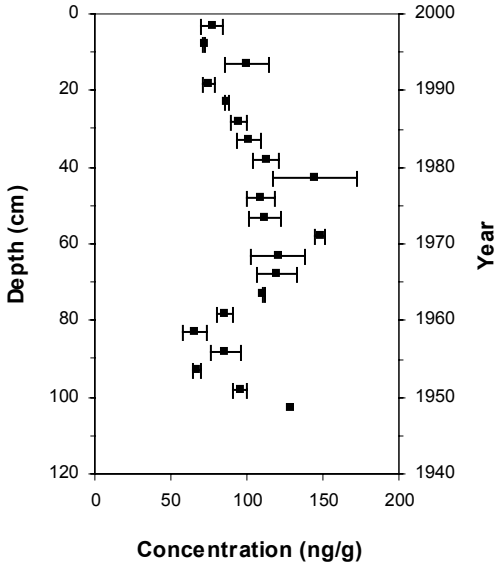

Figure 2.1 Concentration of benzo(a)pyrene in a sediment core taken from the upper Tamar Estuary during a previous study. Adapted from Jordan [89].

2.1.6.2 Other studies of PAHs in Australian sediments

A small number of studies investigating PAHs in sediments have been undertaken in Australia. Many are reviewed by Maher and Aislabie [7], with discussion of potential sources and degradation. This review showed that significant levels of PAHs have been observed in Australian sediments, and highlights the need to conduct further research in regions not yet studied.

Bagg *et al.* measured PAH levels in sediments in one remote and two urban regions of Victoria [91]. The highest concentrations of BaP (6.8 μg/g) were found near the mouth of the Yarra River, adjacent to the Port of Melbourne, but lower levels comparable to remote regions (20-60 ng/g) were found further upstream in residential areas. Kayal and Connell took sediment samples along a 40 km section

of the Brisbane River, Brisbane, with the highest levels (1.1 μg/g, BaP) found near the most urbanised area of the river [92]. It was concluded from isomer ratios that combustion sources dominated. Brown and Maher measured the levels of 13 PAHs from 20 sites in an estuary in the southern suburbs of Sydney [93], where levels of BaP ranged <1-1960 ng/g. Combustion sources linked to atmospheric particles were determined to be the major contributors at most sites, while marinas were identified as point sources of naphthalene. Work undertaken in Sydney Harbour indicated that urban runoff of combustion derived PAHs was the dominant source at the majority of the 124 sites investigated [94]. Samples taken near a petrochemical industrial site showed PAH ratios consistent with petrogenic origins, and the majority of sites were noted to have total PAH concentrations likely to cause some adverse biological effects.

2.1.7 Outline of Work to be Presented in this Chapter

The overall aim of this section of work was to determine if a dated sediment core from the Tamar Estuary could be used to estimate historical levels of air pollution in Launceston. PAHs were selected as tracers because they are produced from incomplete combustion (a major source of air pollution in urban regions), they have been studied extensively in the past because of their environmental persistence, and they exhibit a relatively linear relationship with atmospheric particulate matter [95]. In order to use a core to gauge historical air pollution, it was first verified that a link between the atmospheric and sedimentary levels of PAHs exists. To this end, compound ratios in air and surface sediments were compared. Ratios were also used to determine possible sources of the PAHs. It was also vitally important that the

ambient air samples collected were representative of atmospheric levels. Therefore a number of factors influencing the collection of airborne PAHs were investigated, including the vapour-particle phase distribution under different sampling conditions and the effect of different filter media.

2.2 Experimental

2.2.1 Sampling

2.2.1.1 Air

Air samples were collected using low- and high- volume samplers from a number of sites around Launceston. Low-volume samples were collected using a Q-Max personal sampling pump (Supelco, Figure 2.2) operating at 2.0-2.5 L/min at two sites; the Elphin samples were collected near the driveway of a residential house, approximately 10 m from Elphin Rd; the City samples were taken from the roof of an office located adjacent to a busy intersection (corner of Bathurst and York Streets, see Figure 2.3). The samples were collected approximately 2.5 m and 4 m above ground level, respectively. The sampling train consisted of a 37 mm diameter PTFE membrane filter (2 μm pore size with glass-fibre support pad, Supelco) or borosilicate glass-fibre filter (GFF, Gelman EPM 2000) housed in a plastic 3-piece cassette placed in front of an ORBO-43 adsorbent tube (containing 100 mg and 50 mg sections of XAD-2 resin, Supelco) to collect vapour-phase species. Samples were capped and stored in snap-lock plastic bags in a freezer. Sampling times varied from 9-66 hours.

Figure 2.2 Low-volume sampling pump, filter cassette and ORBO tube.

High-volume PM_{10} samples collected at Ti-Tree Bend were kindly donated by the Department of Primary Industries, Water and Environment (DPIWE, see Figure 1.7). The two samplers operate on alternate calender days (midnight-midnight) at 70 m^3/hour using borosilicate glass-fibre filters (EPM 2000, Gelman). After sampling, the filters were stored in plastic snap-lock bags before weighing at known humidity to determine the 24-hour average PM_{10} loading.

2.2.1.2 Sediment

Two sediment cores (2.79 m and 2.27 m) were collected from an undisturbed intertidal zone stabilised by reeds a few metres from the west bank of Home Reach, approximately 400 m south of the Trevallyn Power station (Figure 2.3) using a 1 m x 4 cm i.d. Livingstone corer. Each core was collected in four sections; 0-60, 60-126, 126-157 and 157-227 cm, and 0-63, 63-134, 134-198 and 198-279 cm. Collection of the lower sections of the core was accomplished by passing the corer through the upper sediment with the plunger held at the bottom of the corer. At the required starting depth, the outer casing of the corer was pressed further into the

sediment while holding the plunger steady. After sampling, the cores were extruded and wrapped in plastic wrap and aluminium foil for transportation to the laboratory, where they were refrigerated (4^{o}C).

The 2.27 m core was sectioned at 5 cm intervals, and the bottom 4 cm of each section stored in glass bottles for PAH analysis. The remaining 1 cm of each slice was set aside for future analysis. The 2.79 m core was cut into 10 cm slices, dried, ground, and a small amount set aside for heavy metals analysis [96]. The remaining portion of each slice was submitted for ^{210}Pb analysis at the Australian Nuclear Science and Technology Organisation (ANSTO), Sydney [96]. While improved time resolution can in theory be obtained by taking thinner slices of the core, the effect of the approximately 20 cm surface mixed layer (and high sedimentation rate) was expected to prevent higher time resolved details from being observed.

Surface sediment (0-4 cm) was collected at three sites on the Tamar Estuary and at one site on the North Esk River (Figure 2.3).

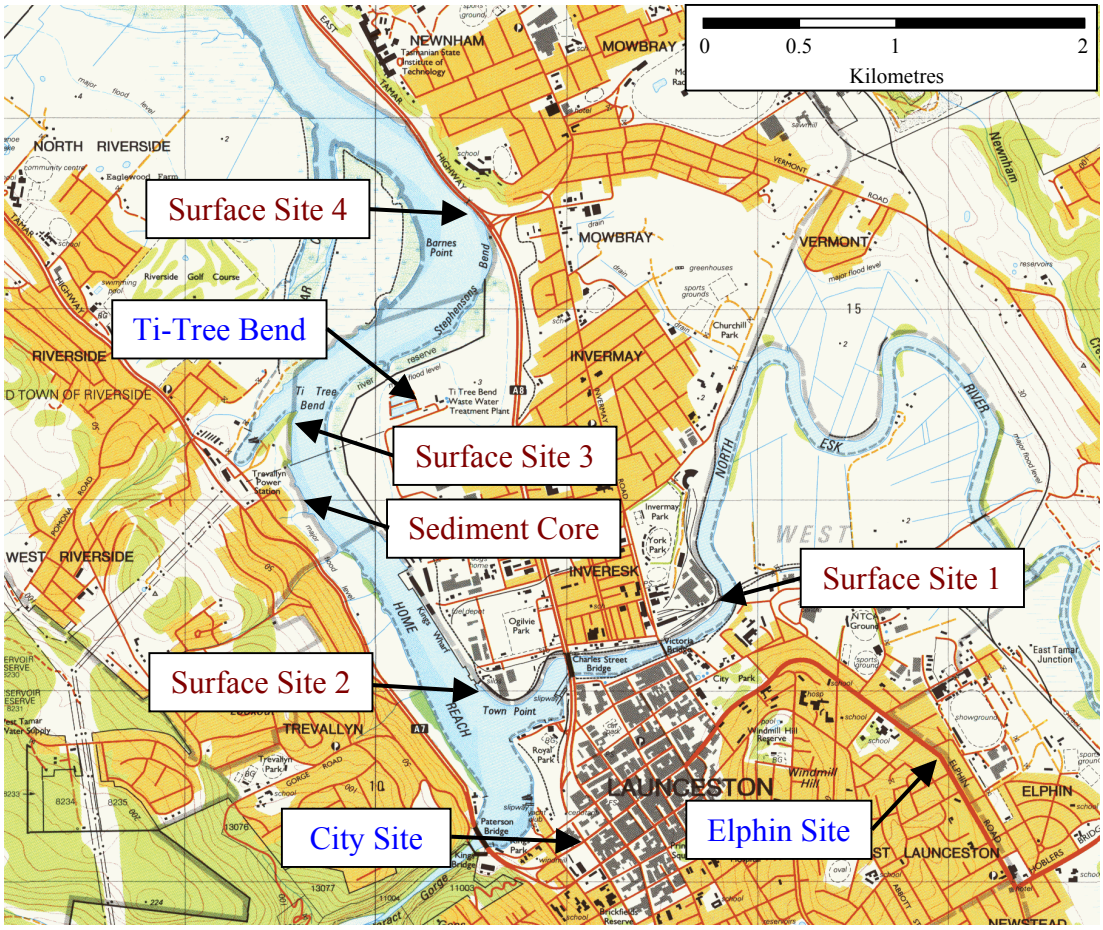

Figure 2.3 Location of air and sediment sampling sites, Launceston and upper Tamar Estuary. Source: Tasmap #5041, Hobart.

2.2.2 Extraction of PAHs

2.2.2.1 Air samples

A similar procedure to that employed by Colombini *et al.* was used to extract the air samples [97]. Filters were extracted in a 10 mL 1:1 mixture of dichloromethane (DCM) and acetone for 30 minutes in an ultrasonic bath. For low-volume samples, the entire filter was used, while a small portion (3 x 3 cm) was cut from the high-volume filters. After extraction, the filter was removed and rinsed with DCM, and the extract evaporated to dryness with a gentle stream of air (cleaned through a bed

of XAD-2 resin). Acetonitrile (1 mL) was added, the sample ultrasonicated, and the final extract filtered through a 0.45 μm syringe filter into an HPLC autosampler vial.

The XAD-2 adsorbent beds were transferred to vials and extracted with 1 mL of acetonitrile for 30 minutes in an ultrasonic bath, and similarly filtered into vials.

2.2.2.2 Sediment samples

The extraction method for sediments was similar to that of the air samples. Wet sediment samples (5-6 g) were extracted by adding 4 mL acetone, shaking vigorously for approximately 30 seconds, then adding 6 mL DCM and placing in an ultrasonic bath for 30 mins. The solvent was decanted, and the procedure repeated an additional three times. The combined extracts were gently evaporated to dryness under a gentle stream of XAD-2 cleaned air, 1 mL acetonitrile was added and ultrasonicated briefly, and filtered through a 0.45 μm syringe filter into an HPLC autosampler vial.

The weight percentage of water in the sediment was 61.2 ± 2.6% w/w (mean ± 1σ) averaged over the entire core, determined by drying 2-3 g sediment at 60^{o}C until constant weight.

2.2.3 HPLC Analysis

HPLC analyses were conducted on a GBC Winchrom system using an LC-1150 pump and LC-1650 autosampler connected to a 2 cm C-18 guard column followed

by a 25 cm x 4.6 mm i.d. x 5 μm particle C-18 Supelcosil LC-PAH column (Supelco). A linear solvent gradient from 60-100% acetonitrile in water over 22 minutes was employed at a flow-rate of 1.2 mL/min. Detection was accomplished using an LC-1205 UV absorbance detector operated at 254 nm, and an LC-1255 fluorescence detector using a timed wavelength program (Table 2.2). The fluorescence wavelength program was selected by scanning excitation (200-320 nm) and emission (300-460 nm) spectra of each compound as the apex of the peak passed through the fluorescence detector. Standards were prepared in acetonitrile, and quantification was based on a linear-least-squares fit from a four- or five- point external calibration curve. Peak identification was based on comparison of retention times with a standard solution of target PAHs. Confirmation of peak identity and purity was performed on selected samples by scanning the fluorescence excitation and emission spectra of the peaks. Typical chromatograms and fluorescence spectra are shown in Figures A.2 and A.3 (Appendix A), respectively.

Table 2.2 Fluorescence wavelength program used in HPLC analysis.

Target Compound	**λ excitation** (nm)	**λ emission** (nm)
Naphthalene	222	330
Fluorene	252	310
Phenanthrene	250	358
Anthracene	250	400
Fluoranthene	282	450
Pyrene	276	394
Benzo(a)anthracene	292	396
Benzo(a)pyrene	284	410
Dibenz(a,h)anthracene	292	402

2.2.4 Method Validation

Target analytes were not detected in any method or solvent blanks (Figure A.2, Appendix A).

Validation of the extraction method for air samples has been undertaken previously [89]; the desorption efficiency from the ORBO tubes averaged 90.9 ± 5.0%, and varied from 52 ± 0.7% (BaP) to 145 ± 7% (Nap).

To determine the recovery of the analytes for the sediment extraction method, 20 μL of a standard solution was spiked into a vial containing extraction solvent only and extracted as usual. Recoveries were generally very good (Figure 2.4), except for naphthalene and fluorene, which are apparently too volatile. This was also reported by Song *et al.* for a similar procedure [98]. Oxidation through the use of a stream of air in place of the usual N_2 for evaporation did not seem to be significant.

Spiked samples have been shown to overestimate extraction efficiencies relative to native PAHs [99], and are thus not necessarily representative of real-world conditions. As such, the extraction method was also tested on aliquots of Standard Reference Material (SRM) IEAE-383 Marine Sediment [100]. This SRM was selected as the levels of PAH were similar to those found in the Tamar Estuary core (Table A.1, Appendix A). To simulate the influence of water on the extraction efficiency, approximately 60% w/w water was added to aliquots of the SRM and extracted as usual. The mean extraction efficiencies for most of the compounds determined in this study are slightly lower than the reference 95% confidence

intervals (Table A.1, Appendix A). Although it is clear from Figure 2.4 that the presence of the water did not significantly influence the extraction efficiency, all sediment samples were corrected for the mean SRM wet extraction efficiency of each compound.

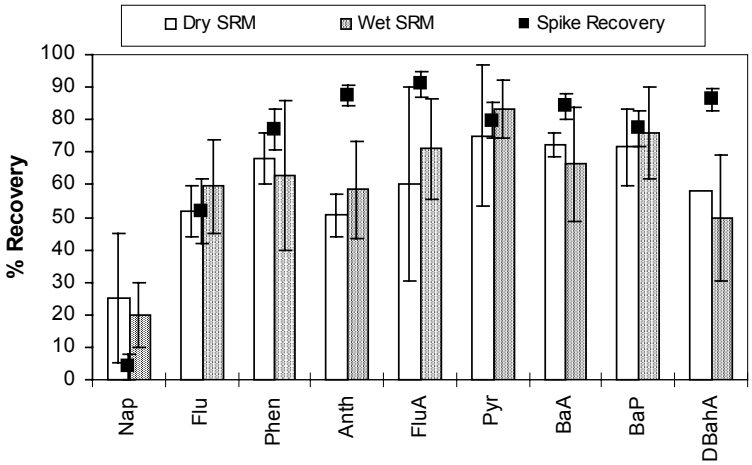

Figure 2.4 Recovery of PAHs from SRM IEAE-383 (n = 3 dry, n = 6 wet), and of spiked PAHs (n = 3), mean ± 1σ.

As HPLC coupled with fluorescence detection allows very good specificity and selectivity for PAHs, a clean-up procedure to remove polar components from the extract was not deemed necessary [89]. Indeed, Sisovic & Fugas also found that clean-up was not required, thus reducing costs and analysis time [101], although it presumably reduces the lifetime of the guard column.

2.2.5 ^{210}Pb Dating of Sediment Core

Lead-210 dating was undertaken on the 2.79 m core by staff at the Australian Nuclear Science and Technology Organisation (ANSTO), Sydney [102]. A sedimentation rate of 1.74 ± 0.12 cm yr^{-1} was determined for the top 190 cm,

ignoring the discontinuities in the profile (Figure 2.5), and was assumed to be constant for sediments deposited below 190 cm. This is similar to the ~2 cm yr^{-1} determined from a 60 cm core collected nearby in a previous study [89, 96].

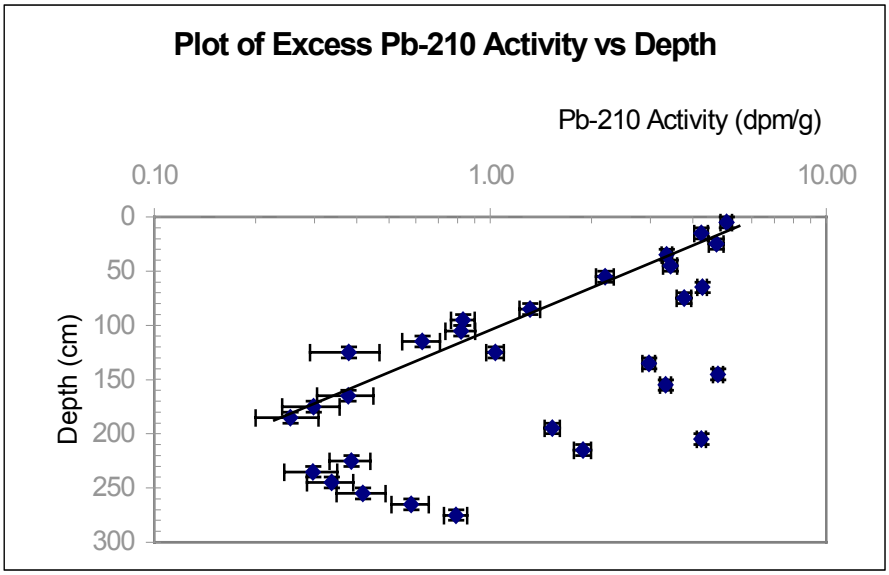

Figure 2.5 Depth profile of excess ^{210}Pb in sediment core. Adapted from Seen *et al.* [96].

The discontinuities within the profile exhibit ^{210}Pb activities similar to that found at the surface, and correspond to the top portion of each core section. Seen *et al.* concluded this was probably due to fibrous matter at the surface which transported a plug of sediment down with the corer to the top of each core section [96].

To check whether the PAH-core was also contaminated in this way, the zinc concentration profile of that core was determined for comparison with the profile in the ^{210}Pb-core [96]. Briefly, 0.2 g of dried, ground sediment was extracted with 5 mL concentrated HNO_3 for 4 hours at 90-95^oC. The extract was filtered, rinsed with 10% HNO_3 and ultra-high purity water, and diluted accurately by weight to

approximately 35 g. Analyses were conducted by flame atomic absorption spectroscopy (Varian SpectrAA 300).

Contamination during sampling as discussed above explains both the presence of surface ^{210}Pb activity and the high zinc concentration at the top of each section of the ^{210}Pb-core (Figure 2.6). In contrast, the zinc profile of the PAH-core does not show any significant surface contamination at the top of each core section.

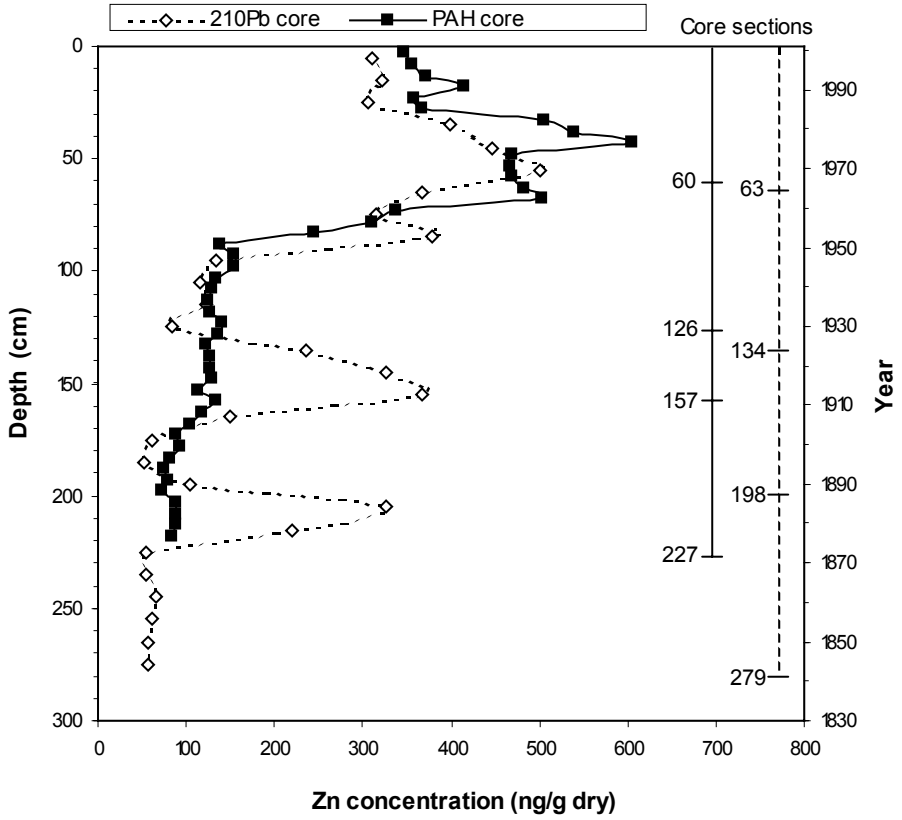

Figure 2.6 Zinc concentration in ^{210}Pb- (2.79 m) and PAH- (2.27) cores, and depth of each core section.
Data for the ^{210}Pb core from Seen *et al.* [96].

2.2.6 Loss-on-ignition and Elemental Carbon Analysis

The loss-on-ignition (LOI) and elemental carbon (EC) content of the sediment core was determined using a combination of the methods of Gustafsson *et al.* [57], and Klinedinst and Currie [103]. Briefly, 0.3-0.5 g of dried sediment was combusted at 375^{o}C for 24 hours in a muffle furnace, with a slow stream of air entering at the bottom front of the furnace and exiting at the top rear. The mass lost during this combustion was operationally defined as "loss-on-ignition", and represents the volatile fraction that is lost during combustion at 375^{o}C, and is not limited to carbon. Isolation of the EC fraction was then performed on a sub-sample of the combusted sediment by removing carbonates with HCl fumes; 15 mL concentrated HCl was placed in the centre of twelve 0.02-0.05 g samples inside a sealed desiccator for 24 hours. The HCl was then replaced with NaOH pellets to neutralise the acidic fumes and desiccate the samples. Elemental carbon was then defined as the carbon remaining after the combustion and acidification steps, and was determined using a Leco CHNS-932 analyser.

A slight negative co-variation between LOI and EC was found ($r^2 = 0.12$, $p = 0.08$), indicating that charring of organic matter during the combustion process did not present a problem, presumably because there was a sufficient excess of oxygen. This is in contrast to the results of Gelinas *et al.* who found a slight positive co-variation ($r^2 = 0.35$) for a similar thermal method for the removal of organic carbon [104].

2.3 Results and Discussion

2.3.1 PAHs in Air

2.3.1.1 Concentration of PAHs in Launceston ambient air

More than 40 low-volume ambient air samples were collected from two sites in Launceston, with the majority taken at the Elphin site during the winter months. Mean, and maximum and minimum concentrations for vapour- and particle- phase PAHs found at the Elphin site are shown in Table 2.3; full results are presented in Table A.2, Appendix A.

Table 2.3 Concentration of vapour- and particle- phase PAHs during winter at the Elphin site, mean and range (ng/m^3).

	Nap	Flu	Phen	Anth	FluA	Pyr	BaA	BaP
Vapour-phase								
Mean	276	6.54	7.65	2.09	0.84	0.52	-	-
Min	*61.9*	*2.04*	*2.67*	*0.34*	*<0.08*	*<0.05*	-	-
Max	*701*	*16.7*	*20.1*	*6.80*	*3.16*	*1.81*	-	-
Particle-phase								
Mean	1.29	0.19	1.10	0.24	1.79	0.97	1.78	2.36
Min	*<0.44*	*<0.06*	*<0.12*	*<0.03*	*<0.11*	*<0.12*	*<0.10*	*0.13*
Max	*3.54*	*0.73*	*6.27*	*1.34*	*7.80*	*2.43*	*8.12*	*11.4*

The average measured winter concentration of BaP was 2.36 ng/m^3, and is obviously greater than the 0.3 ng/m^3 "investigation level" set down by the Federal Government [105], although the annual average would be expected to be much lower. The maximum concentration of BaP measured during 2001-03 was only one third of the highest ever recorded in Launceston; 34 ng/m^3 during the winter of 1992 [90]. The concentrations of target PAHs were within the range found in previous studies [88-

90], and were similar to those found in Sydney (BaP averaged 1.4 and 2.1 at two sites, and peaked at 10 ng/m^3) [5].

Concentrations of all PAHs were much lower during the summer compared to the winter. This is to be expected, as pollution levels are much lower during the warmer months. Higher solar intensity and increased temperatures would also degrade a larger proportion of airborne PAHs [23]. Although bushfires present another source of woodsmoke from time to time during the summer, the smoke plumes are generally transported from many kilometres away. A sample collected on a day when bushfire smoke from Victoria (~500-600 km to the north, across Bass Strait) impacted Launceston had extremely low levels of PAHs, despite a relatively high PM_{10} loading (48 μg/m^3, 26/1/03, Table A.2, Appendix A).

2.3.1.2 Factors affecting the collection of airborne PAHs

A number of factors associated with the sampling process can influence the apparent concentration of PAHs collected from ambient air. Sampling variability, degradative effects of the filter media, vapour partitioning on various components of the sampling system, and the effect of sampling flow-rate were investigated.

Sampling variability

Three paired samples were collected using parallel PTFE filters to gauge the degree of sampling and analysis variability. Comparison of the paired PTFE samples shows that sampling variability of both the particle- and vapour- phase concentrations was relatively small (Figure 2.7). Vapour-phase naphthalene and fluorene had the lowest variability (5-7%), whereas pyrene in the vapour-phase had

the greatest variability (51%), probably due to the low concentrations found. The relative variation in particle-phase concentrations averaged 20% (11-27%).

Filter media

A further five paired samples were collected using parallel PTFE and glass-fibre filters to determine if the filter media had any effect on the collection of PAHs. The GFFs generally collected lower amounts of particle-phase PAHs (1-51% lower), especially at higher concentrations (Figure 2.7). The concentrations of PAHs found on the ORBO tubes placed behind the GFFs showed no significant difference to those behind PTFE filters.

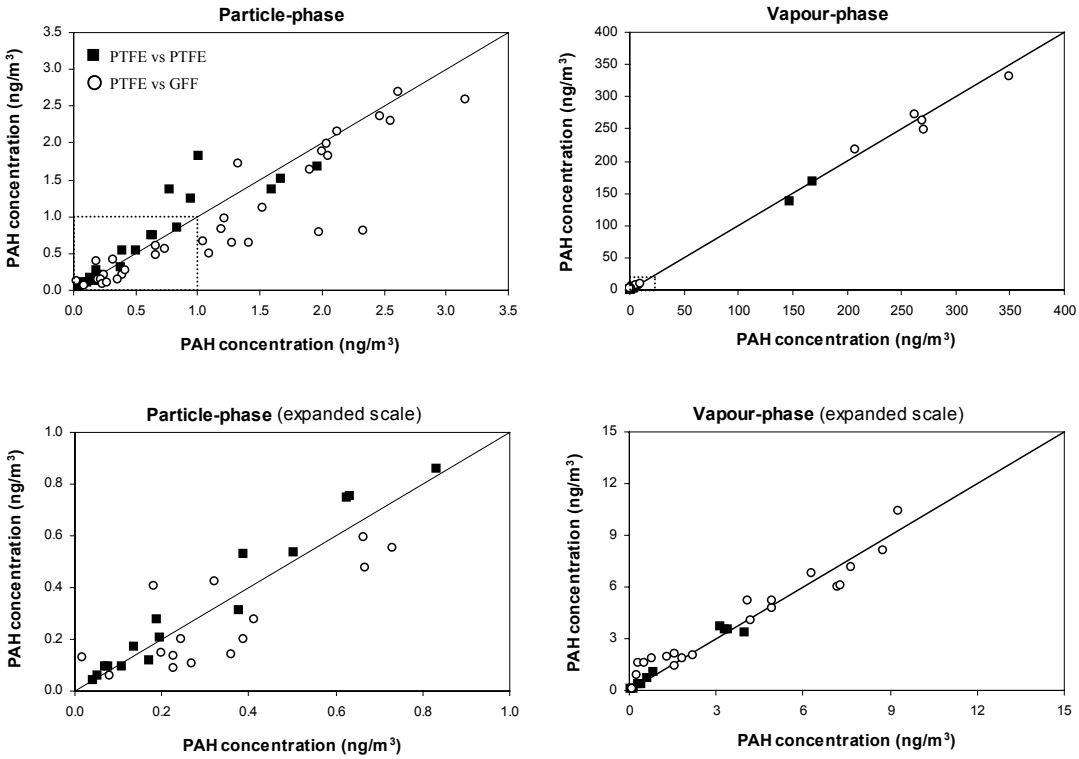

Figure 2.7 Comparison of paired air samples.

Each point represents the concentrations of a single compound from paired samples (GFF concentration on the y-axis). The line indicates a 1:1 ratio. The bottom graph of each set has an expanded scale of the upper graph.

PTFE filters have been found previously to have higher PAH recoveries than five other filter types, including glass-fibre and quartz filters [106]. The glass-fibre type substrates are thought to have more "active" surfaces, and coupled with a higher specific surface area they are prone to greater degradative losses than the inert PTFE surfaces. There is conflicting evidence of the role that the filter material plays in the collection of PAHs sampled in the presence of other compounds, however. For example, Grosjean *et al.* found that very little degradation occurred on either glass-fibre or Teflon filters during sampling when exposed to O_3, NO_2, or SO_2 [107]. Schauer *et al.* on the other hand found that O_3 alone or when combined with NO_2 substantially degraded surface-bound BaP on GFFs, while NO_2 itself caused negligible losses [108]. A further study found that gas adsorption caused higher levels of PAHs to be found on GFFs compared to PTFE filters [109]. It is evident that there is by no means a consensus on the effect of the filter media in the collection of PAHs.

Vapour-particle partitioning

Partitioning presents a problem when investigating airborne PAHs, as both particle- and vapour- phase components need to be collected. As atmospheric PM_{10} and PAH levels are generally very low (ng-μg/m^3), high-volume samplers are commonly employed to collect a sufficiently large sample to be of practical use. Because these samplers typically run at flow-rates of ~0.5-2.5 m^3/min, loss of particle-phase PAHs through "blow-off" is a concern. Losses of up to 90% for the relatively non-volatile BaP have been reported from a high-volume sampler [110]. With the increasing sensitivity of modern analytical techniques it has become possible to use smaller and cheaper medium- (~10-50 L/min) and low- (~1-5 L/min) volume apparatus. The

lower flow reduces the extent of volatilisation, but even still, the vapour-particle distribution of FluA and Pyr has been shown to vary with temperature (50-90% on the filter) [21]; less volatile compounds were found exclusively in the particle-phase.

Comparison of summer and winter samples collected at the Elphin site show no distinct difference between the particle/vapour ratios of Phen and Anth. Although there is a marked difference in the ratios for FluA and Pyr (Table 2.4). It is apparent that Phen and Anth are collected mainly in the vapour-phase, even at the lower ambient temperatures during winter. On the other hand, the majority of FluA and Pyr were found on the filters during winter, and on the ORBO tubes or in approximately equal amounts, during the summer.

Table 2.4 Partitioning of semi-volatile PAHs at the Elphin site; comparison of summer and winter particle/vapour ratios.

		Phen	**Anth**	**FluA**	**Pyr**
Winter	Mean	0.15	0.15	2.71	3.80
(n = 28)	*Min*	*0.02*	*0.04*	*0.81*	*0.96*
	Max	*0.67*	*0.60*	*8.21*	*9.74*
Summer	Mean	0.13	0.32	0.41	0.96
(n = 6)	*Min*	*0.05*	*0.07*	*<0.08*	*<0.71*
	Max	*0.19*	*0.91*	*0.75*	*1.35*

Low-volume sampling generally employs a filter housed in a 37 mm plastic cassette. Under industrial workplace conditions (i.e. steelworks and aluminium plants), PAHs have been found to be retained on the inner walls of this type of cassette [111]. On average, 29% of the collected BaP was found on the walls with the remainder on the filter, whereas the semi-volatile Pyr was found partitioned between the glass-fibre filter (25%), XAD-2 adsorbent (42%) and the cassette walls (33%). The authors

suggested that studies employing these cassettes risk underestimating PAH levels, even where a backup adsorbent is included. To check the extent of cassette wall adsorption, a number of cassettes were rinsed with methanol, and prepared in the same way as the filter extracts. The proportions found adsorbed on the cassette walls in this study were much lower than previously reported, and BaA and BaP were detected on the cassette walls in only one sample (Table 2.5).

If the plastic cassette walls can adsorb vapour-phase compounds, then so too could the glass-fibre support pads placed behind the PTFE filters, and the walls of the glass tube containing the XAD-2 resin. While very little adsorbed species were detected on the walls of the glass tube, large amounts of FluA and Pyr were collected by the support pads (Table 2.5). Not surprisingly, the highest proportions of compounds adsorbed on the pad, cassette and tube were detected in summer samples (seasonal variation not shown in Table 2.5, see Table A.2 in Appendix A for full results).

Table 2.5 Distribution of compounds collected on components of the sampling system (range, % of total compound collected, n = 6).

	Nap	Flu	Phen	Anth	FluA	Pyr	BaA	BaP
PTFE filter	0.2 - 0.5	0.3 - 7	5 - 15	4 - 16	0 - 25	11 - 28	86 - 100	94 - 100
Support pad	0 - 0.8	0.8 - 8	7 - 15	2 - 21	35 - 79	42 - 72	0 - 14	0
Cassette wall	0.2 - 1.0	0 - 5	0 - 14	0 - 13	0	0	0 - 9	0 - 6
XAD-2	97 - 99	55 - 99	45 - 88	38 - 92	10 - 65	9 - 47	0	0
Glass tube	0.3 - 0.9	0 - 35	5 - 11	4 - 12	0	0	0	0

The distribution of the various compounds can be explained in terms of their vapour-pressures. The more volatile Nap and Flu pass through the filter as vapours,

and are too volatile to remain adsorbed onto the pads; they are "blown-off" both the filter and pad. The slightly lower volatility of Phen and Anth means that a proportion remains adsorbed on the pad, even though the majority of these compounds pass through to the XAD-2 resin. The still lower vapour-pressures of FluA and Pyr allow a substantial proportion to be blown-off the PTFE filter, but are sufficiently non-volatile to allow them to be trapped by the more "active" surface of the pad. BaA and BaP are non-volatile enough to be retained on the filter (associated with the particulate matter).

This shows that, at least for ambient studies where high temperatures are not encountered, cassette wall- and glass tube- adsorption do not significantly reduce the observed particle- or vapour- phase concentrations of airborne PAHs. However, the adsorptive properties of the support pads require further investigation.

High-volume samples

Twenty-one high-volume samples (PM_{10}) collected by DPIWE at Ti-Tree Bend were analysed for PAHs in the same manner as the low-volume samples. The PAH concentrations found in the high-volume samples were considerably lower than from low-volume samples collected during periods with similar PM_{10} loadings (Table 2.6, full results from the high-volume samples are shown in Table A.3, Appendix A). This is most likely because of "blow-off". Thus it is essential when collecting PAHs with high-volume samplers that compounds in the vapour-phase are collected in addition to the particles, otherwise concentrations will be severely underestimated. A small portion of this discrepancy is probably due to the enhanced degradation

caused by the glass-fibre filters themselves, but this obviously cannot account for all the losses observed.

Table 2.6 Comparison of mean particle-phase PAH concentrations collected during winter using high- and low- volume samplers (ng/m^3).

PM_{10} (μg/m^3)	Sampler	n	Nap	Flu	Phen	Anth	FluA	Pyr	BaA	BaP
>60	high-vol	6	-	0.01	0.18	0.01	0.05	0.09	0.26	0.83
	low-vol	1	-	-	-	0.09	1.77	1.34	1.76	1.89
50 - 60	high-vol	1	-	0.01	0.03	0.01	0.04	0.02	0.20	0.68
	low-vol	7	0.58	0.07	1.47	0.38	1.68	0.93	1.96	2.43
40 - 50	high-vol	5	-	-	0.10	0.01	0.02	0.11	0.06	0.23
	low-vol	14	0.68	0.15	0.75	0.19	2.75	1.15	1.49	2.06
30 - 40	high-vol	3	-	0.01	0.07	0.01	0.02	0.02	0.14	0.26
	low-vol	8	0.64	0.13	0.38	0.12	0.94	0.72	1.43	1.98
<30	high-vol	2	-	-	-	0.01	0.02	0.03	0.03	0.06
	low-vol	13	0.69	0.11	0.60	0.13	0.74	0.52	0.80	0.97

From the above discussions, it appears that high-volume samplers do not necessarily collect representative samples of PAHs from ambient air. The incorporation of a vapour-phase collection media (e.g. polyurethane foam [112]) would alleviate some of the problems. Consequently, the following discussions will use data collected with the low-volume sampler only.

2.3.2 Sources of PAHs to Launceston Air and Tamar Estuary sediments

In order to verify that a dated sediment core could be used as a record of historical air pollution, it was necessary to confirm that the sedimentary PAHs were

representative of those found in the overlying atmosphere. Compound ratios have been commonly used as a means of identifying sources of PAHs, however, previous sourcing studies have only been able to differentiate two broad source categories; pyrogenic and petrogenic sources (see Chapter 2.1.5). Pyrogenic sources comprise emissions from combustion processes, such as automobile exhaust and woodsmoke, and are usually emitted to the atmosphere. Petrogenic sources on the other hand, are based on fossil fuels and their derivatives, including unburnt petrol, oil, tyres and brake lining, and are not normally found in the air (except for volatile components).

As previously mentioned in Chapter 2.1.5, the Phen/Anth ratio is generally >10 for petrogenic and <10 for pyrogenic sources, and FluA/Pyr <1 for petrogenic and >1 for pyrogenic sources. A plot of Phen/Anth vs FluA/Pyr for ambient air samples and surface sediment samples shows pyrogenic sources to be the dominant source of atmospheric and surface sedimentary PAHs (Figure 2.8). Overall, the ratios found in this study were similar to those found in sediments elsewhere in Australia [7, 92].

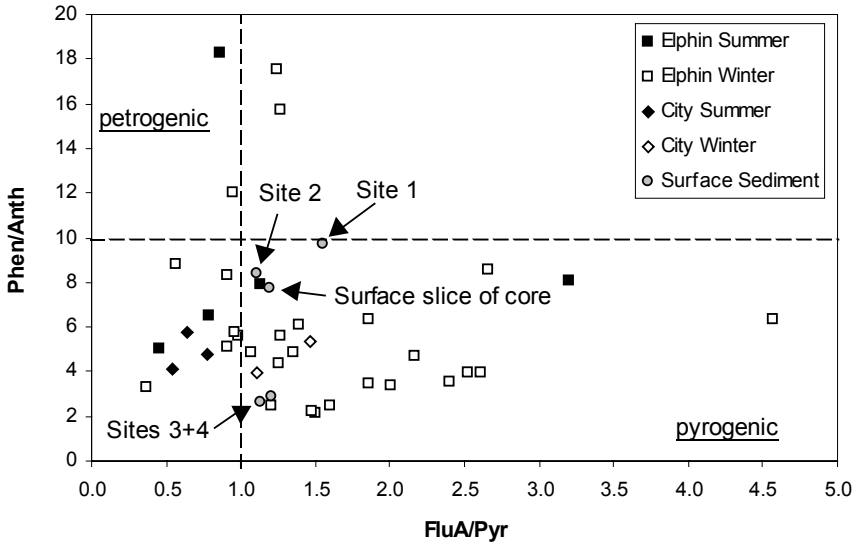

Figure 2.8 Source diagnostic ratios of PAHs in Launceston air and surface sediments of the Tamar Estuary.

Atmospheric deposition has been previously shown to be a main source of PAHs in sediments and soils in other regions [85, 113, 114]. For example, studies have shown similarity between PAH signatures in air and those found in urban runoff [28], and both the dissolved and sedimentary phases [30]. The similarity in PAH ratios between surface sediments of the Tamar Estuary and Launceston air indicates that the sediment probably reflects levels of PAHs in the atmosphere.

Woodsmoke also exhibits similar ratios to the atmospheric and sedimentary samples, (Table 2.7, and Figure 3.11 in Chapter 3.3.2), indicating that woodburning is likely to be a major source of PAHs in Launceston. However, as the atmospheric ratios are similar for both winter and summer months, it appears that these two ratios alone cannot sufficiently distinguish woodsmoke from other pyrogenic sources. The corresponding ratio's for the sum of the particle- and vapour- phases were very similar to those calculated for the particle-phase only, and have not been included in Table 2.7.

PAH source ratios calculated from other studies undertaken in Australia are compared to those found in the current study (Table 2.7). The values for the road are assumed to be representative of automobile exhaust, as they were also similar to those found in an underground carpark in the same study [78]. While the BaA/BaP ratio also appears unable to differentiate between woodburning and automobile exhaust, the Pyr/BaP ratio was significantly higher for automobile exhaust. The three air samples collected during the summer at the city site (a busy intersection) had Pyr/BaP ratios of 32, 4.5 and 3.2, suggesting that the notion that higher ratios might be characteristic of automobile exhaust, although the two lower values are not

significantly different to that of woodsmoke. The Pyr/BaP ratios found in samples collected at the Elphin site were even lower than woodsmoke, suggesting that automobile exhaust was probably not a significant source of PAHs in suburban areas of Launceston at any time of the year. This is consistent with the National Pollution Inventory assessment that vehicle exhaust contributes less than 8% of total PAH emissions in Launceston (Table 1.2).

Table 2.7 PAH source diagnostic ratios in Launceston ambient air compared with previous studies undertaken in Australia, mean ± 1σ.

	Winter Air [a]	Summer Air [a]	Surface Sediments [b]	Wood Burning [c]	Wood Burning [d]	Adjacent to Busy Road [e]
Phen/Anth	5.2 ± 2.8	6.9 ± 1.2	4.6 ± 3.2	5.5 ± 3.4	-	-
FluA/Pyr	1.2 ± 0.9	0.9	1.2 ± 0.1	0.9 ± 0.3	0.8 - 1.0	0.7 ± 0.2
BaA/BaP	0.8 ± 0.1	0.5 ± 0.4	0.8 ± 0.1	1.4 ± 0.4	0.5 - 1.4	1.0
Pyr/BaP	0.5 ± 0.2	1.3 ± 1.4	1.4 ± 0.1	2.9 ± 1.0	1.0 - 13.4	23 ± 6.3

[a] current study, Elphin low-volume samples, particle-phase only, n = 26 winter, n = 6 summer.
[b] current study, surface sites 2-4.
[c] current study, particle-phase only, see Chapter 3.3.2, n = 31.
[d] range of values for different combustion conditions, particle-phase only [77].
[e] sum vapour- and particle- phases [78], n = 3.

2.3.3 PAHs in Tamar Estuary Sediments

2.3.3.1 Spatial trends - surface sediments

Relative uniformity in PAH levels was seen at three of the surface sites, although a slight decreasing trend downstream is evident for most of the compounds (Figure 2.9). Site 1 had considerably higher levels of contamination, particularly of Phen, FluA and Pyr, probably due to proximity to disused rail-yards and gas-works.

Although the rail-yards closed in 1983 and coal-gas production ceased circa 1982, seepage of oils, coals and tars would be expected to continue for many years.

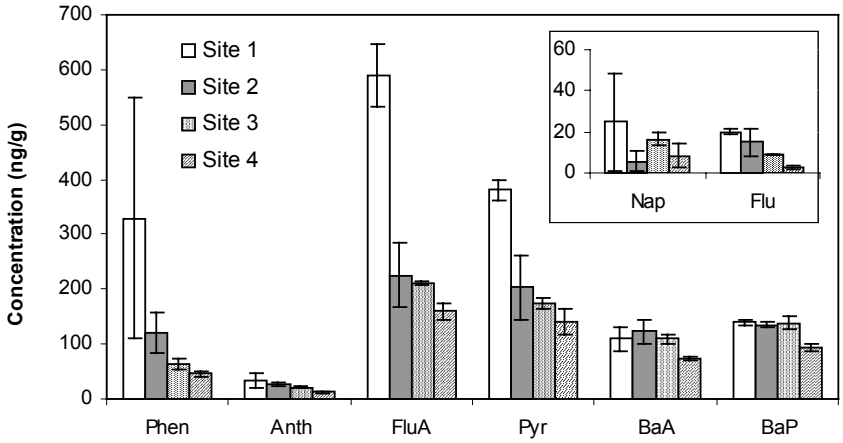

Figure 2.9 PAH concentrations is upper Tamar Estuary surface sediments. See Figure 2.3 for location of sites.

2.3.3.2 Temporal trends - sediment core

As the sediments of the Tamar Estuary reflect PAH levels found in the overlying atmosphere, the sediment core can provide an indication of historical levels of air pollution in Launceston.

Similar down-core concentration profiles were found for most of the target PAHs (Figure 2.10). Naphthalene is an exception, having a relatively low and essentially scattered concentration profile. This is probably due to its higher volatility, aqueous solubility and biodegradability, allowing it to be removed from the particle-phase much more readily.

The following discussion will focus mainly on BaP, as the other compounds follow the same general trends. In fact, the total PAH concentration can be estimated from the BaP levels alone (Figure 2.11), which may be useful if costs and analysis time must be minimised.

Concentrations at the bottom of the core were very low, and were dated to pre-1890. These can probably be considered as background levels for the region, as they were similar to those found in sections of a very old core (pre-1800) taken from the Tamar Estuary at Rosevears (approximately 20 km north-west of Launceston) during a previous study [89].

Fluctuating but steadily increasing levels are observed from the 1890s until around 1940. After a slight decrease, a massive increase in concentration is evident, which drops to previous levels again within 5-6 years. Two more peaks occur in the upper section of the core, the larger around 1970 and a smaller peak ca. 1985.

The top section of this core exhibits similar PAH concentration profiles to that found in a 1.0 m core taken nearby during a earlier study (Figure 2.1, [89]), though the concentration peaks observed in the current core at the surface and at 30 cm were not as well defined in the earlier core.

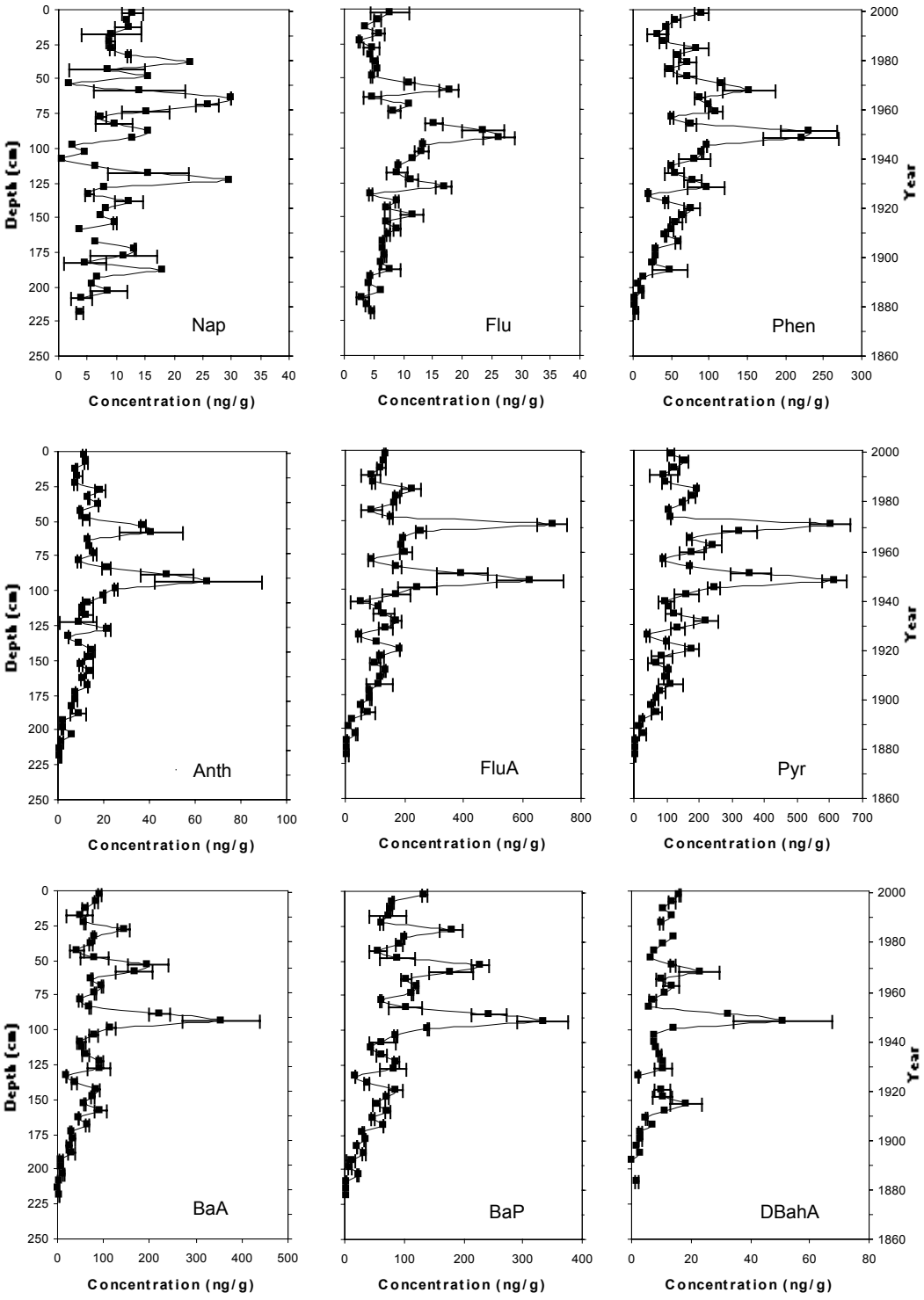

Figure 2.10 Down-core PAH concentration profiles and approximate year of deposition.

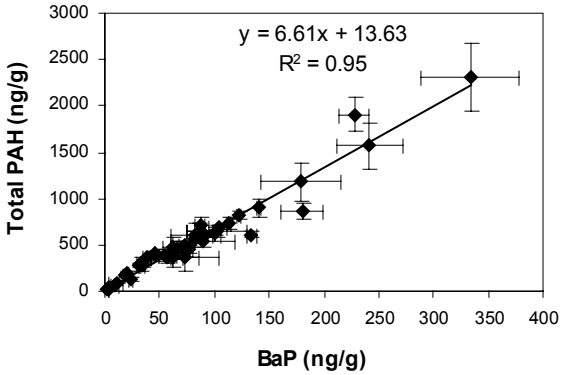

Figure 2.11 Correlation between benzo(a)pyrene and total PAH concentration in sediment core (ng/g dry weight).

Overall, the relative contribution of sources over time has remained relatively unchanged, as evidenced by the depth profile of source diagnostic ratios (Figure 2.12). The core exhibits similar ratios to those found in the air and in the surface sediments (pyrogenic), with woodsmoke the most likely source based on the low Pyr/BaP ratio. Residential and industrial coal burning was common in Launceston in the early 20th century and would have been expected to be a significant pollution source. In spite of this, the Pyr/BaP ratio in the sediments was lower than that observed by Oanh *et al.* [79] from burning coal briquettes (7.2).

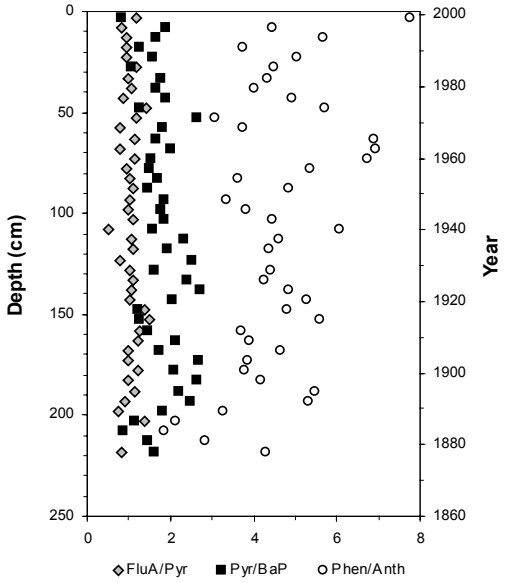

Figure 2.12 Down-core trends in PAH source diagnostic ratios.

Despite the constant down-core profiles in concentration and source ratios, changes in the relative abundance (%w/w of total PAH) of several PAHs occurs throughout the core (Figure 2.13). Nap and Flu show significantly higher abundances at the bottom of the core, while FluA, Pyr, and to a lesser extent BaA and BaP, tend to decrease slightly towards the bottom of the core.

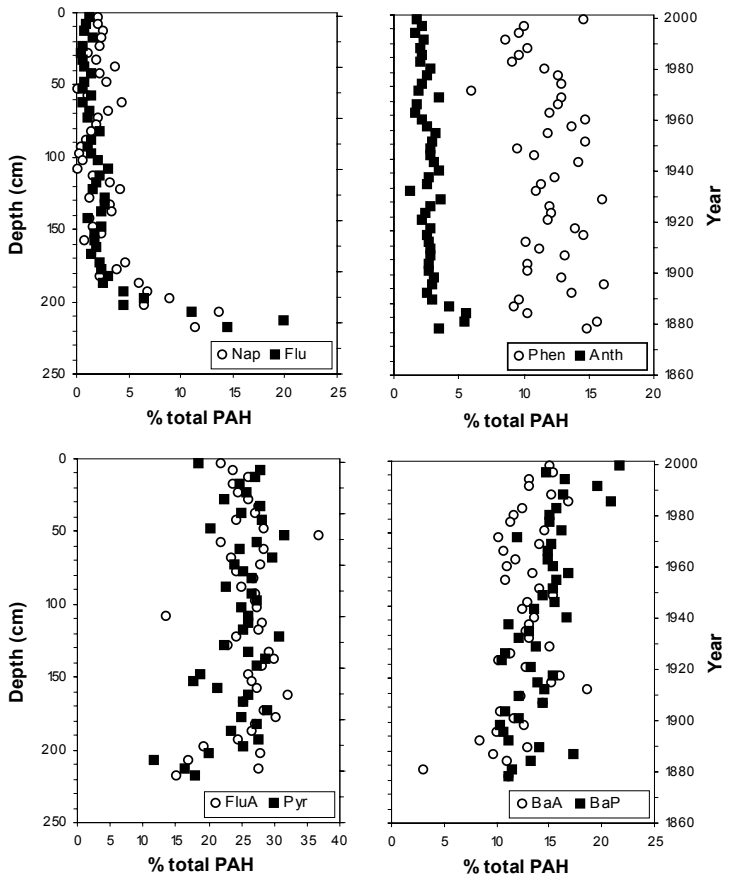

Figure 2.13 Down-core trends in relative abundances of PAHs.

The higher abundances of the smaller PAHs in the deeper sediments indicates that the effect of degradation is minimal in the Tamar Estuary environment. This reinforces the proposal that combustion sources contribute the majority of PAHs to

the Tamar Estuary, where the compounds are trapped within co-formed particles during the combustion process and thus are not "available" for degradation [40].

Co-variation of PAHs and elemental carbon (EC) through co-formation has been proposed as an indicator of pyrogenic sources [57, 114], while loss-on-ignition (LOI) has also been shown to correlate with PAHs in sediments [115]. The LOI and EC profiles in the sediment core are shown in Figure 2.14, with standard deviations shown for samples where replicates were performed. No down-core trends can be seen for either LOI or EC, although slightly higher LOI values were obtained in the lower slices of the core.

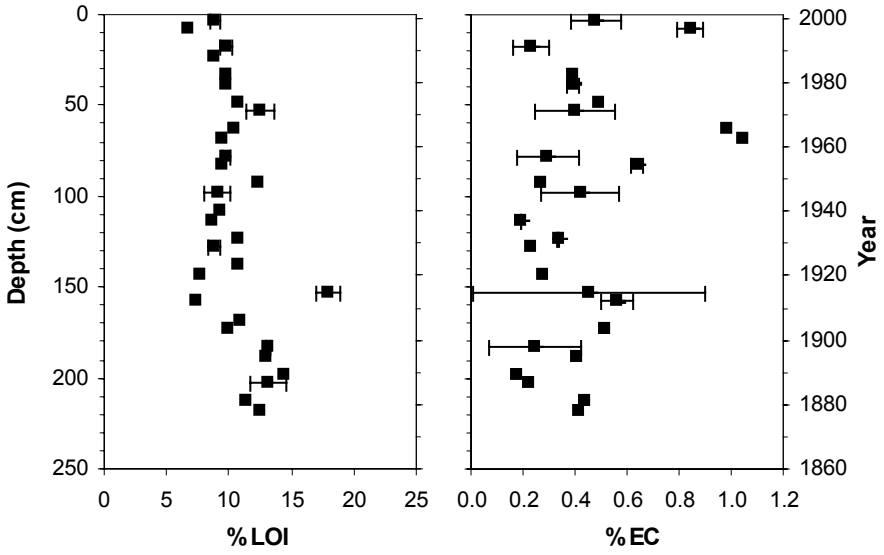

Figure 2.14 Down-core profiles of loss-on-ignition and elemental carbon, mean ± 1σ.

The scatterplot of total PAH concentration versus LOI seems to be grouped into two clusters (Figure 2.15); one consisting of slices with high PAH levels (1900-present) and the other with low levels (pre-1900). Neither shows any correlation to PAH within their clusters. Ingress of plant roots and detritus is the most likely cause of

the relatively consistent levels of LOI throughout the core. Total PAH levels throughout the core also appear to be non-correlated with EC. A study of PAHs in sediments near Sydney, Australia, also found little or no correlation with LOI or EC [93]. This lack of correlation may be due to a number of factors. Firstly, it may indicate that combustion sources are only a small contributor to total PAH levels, but this seems unlikely from the results of the earlier ratio comparisons. Alternatively, there is no guarantee that there is a strict correlation between EC and PAHs from woodburning. This is plausible, because although not directly reported in a recent Australian study of woodheater emissions, there appeared to be no correlation between the emission factors for particle-bound PAHs and "black carbon" [116].

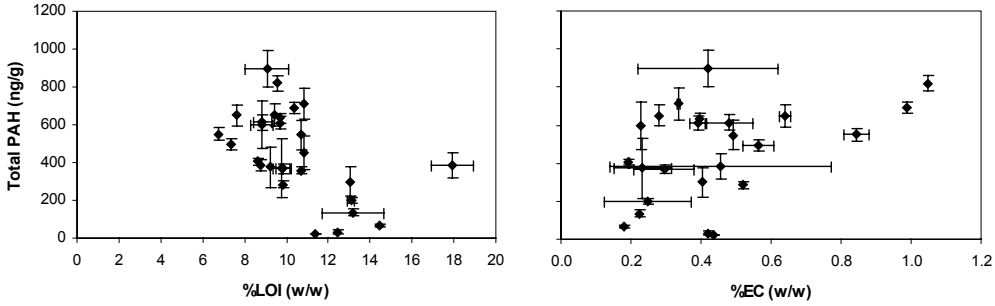

Figure 2.15 Total PAH concentration versus loss-on-ignition and elemental carbon content in sediment core, mean ± 1σ.
Slices 11, 18 and 19 (55, 90 and 95 cm respectively) were excluded from the correlation graphs due to their extremely high PAH concentrations.

2.3.3.3 Possible reasons for historical fluctuations in PAH levels

The constant down-core PAH ratios indicates there was probably only one major source of PAHs throughout the last 150 years, quite possibly woodsmoke. Although

localised short-term sources such as oil spills would create the peaks in the concentration profile, affected slices did not exhibit petrogenic ratios.

Anthropogenic activity has been proposed as producing a similar PAH concentration profile in sediments of the Pentaquamscutt River, a comparable tidal estuary in Rhode Island, USA [52] (Chapter 2.1.4.1). Levels began rising around 1900 with an overall maximum in 1959, with smaller peaks observed in 1934 and 1974. Relatively constant levels were found between 1983-1996, but levels rose again at the surface (1999). Pyrogenic PAH source ratios were observed throughout the entire core, and atmospheric transport of exhaust from nearby roadways was believed to be the major source. A decrease in the 1970s was ascribed to improved automobile efficiency and the 1973 oil embargo, while the recent increase was attributed to a combination of increasing population and rising fossil fuel consumption.

A slow and constant increase in zinc levels in the Tamar Estuary is also seen from the early 1890s, again with a massive increase in concentration in the late 1940s and early 1950s (Figure 2.16). The concentration increase and peaks in zinc in the PAH core tend to lag behind the peaks in PAH concentration by about 6-9 years, and may be due to differences in the nature of the pollution sources or different modes of transport into, and diagenesis in, the estuarine environment.

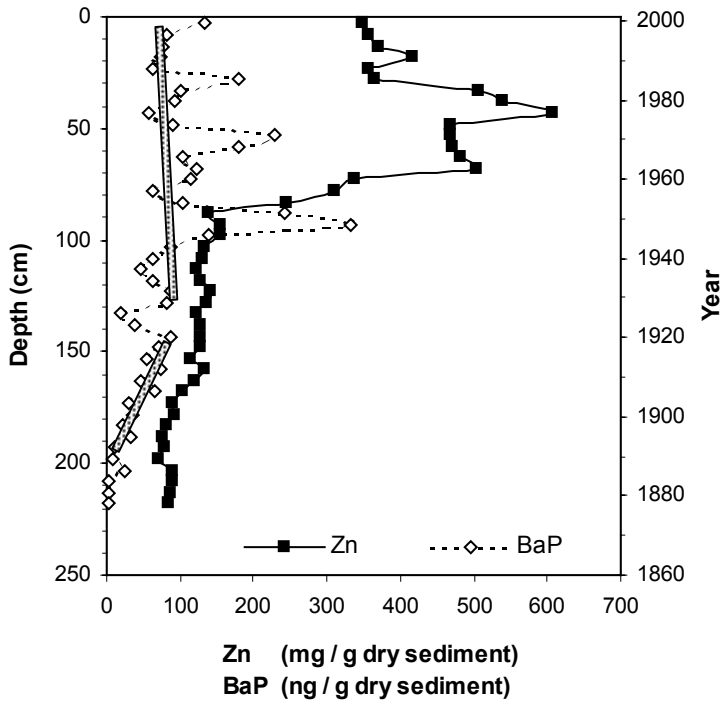

Figure 2.16 Comparison of zinc and benzo(a)pyrene concentration profiles in the PAH (2.27 m) sediment core.
Shaded line indicates possible overall trend in BaP concentration, ignoring peaks.

Although increases in the concentration of heavy metals in river sediment in New South Wales, Australia, have been attributed to increased rainfall [117], the lack of a peak for either PAHs or zinc coinciding with the largest flood of the 20th century (1929) makes it unlikely that flooding contributed to the large amounts of PAHs. Degradative losses of PAHs during atmospheric transport from bushfires (Chapter 2.3.1.1) discounts these as the source of the peaks [37], even though the peak centred around 1970 appears consistent with extensive bushfires in Tasmania in 1967. Analysis of the mean monthly air temperatures for Launceston gives no indication of significantly colder weather (and thus greater woodheater use) during the periods in question. Thus it is unlikely that the observed peaks in PAH concentrations arose from natural causes.

The fact that both PAH and heavy metal concentrations increased markedly around the 1940s and 1950s suggests that industrialisation and urbanisation were the most likely causes of the recent sedimentary profile for these contaminants. The immediate area surrounding the upper Estuary underwent an expansion of industries during and following World War Two, and post-war immigration and a rapid increase in the birth-rate led to an average annual increase of 3.2% in state population over five years; the largest seen since the 1860s and more than three times the average growth over the previous 25 years [118]. Nevertheless, this still does not explain the peaks for the PAHs.

The overall trend, excluding the peaks, is of PAH levels increasing from the late 19th century to a maximum around the 1920s-40s and decreasing slightly since that time. This suggests that air pollution in Launceston has changed little in the past 80 years despite constant urban and industrial growth. The lack of an unequivocal explanation for the spikes in concentrations precludes any definitive conclusions being drawn from those data points.

2.3.3.4 Other methods for determining the contribution of woodsmoke to air pollution

PAHs are not ideal tracer compounds for woodsmoke as they are produced from many combustion sources and are present in petroleum products. While differentiation between woodburning and automobile exhaust may be possible using the Pyr/BaP ratio, PAHs are unreliable in giving a quantitative breakdown of pollution sources.

An ideal chemical tracer for woodburning is the cellulose combustion product levoglucosan (see Chapter 3). A relationship with the "charcoal record" in a dated sediment core from the Amazon region confirmed that levoglucosan can be used to trace historical forest fires [119]. For that reason, a small number of Tamar Estuary sediment core slices were analysed for levoglucosan by extracting ~3 g of dried, crushed sediment ultrasonically with three successive 20 mL portions of methanol (30 mins each). The samples were centrifuged and the solvent decanted after each portion. The total extract was rotary evaporated to a few millilitres before concentrating with a gentle stream of air (XAD-2 cleaned). The extracts were analysed by GC-MS using the same conditions described in Chapter 3.2.2, and in addition by selected-ion-monitoring (SIM) of the m/z 60 ion (Figure 3.8).

While levoglucosan was quantified in Launceston ambient air samples (see Chapter 3.3.5), it was not detected in any of the sediment core slices analysed, presumably because the it has a very low response factor in the underivatised form [119]. Further discussion on levoglucosan as a tracer for woodsmoke is presented in Chapter 3.

Carbon-14 analysis of individual PAHs is a recently developed technique that allows a relatively unambiguous determination of "biomass" and "fossil fuel" based sources [62, 120]. It has been applied to PAHs from both sediments and ambient aerosols, although it is not a commonly used technique mainly because of the high cost of sample preparation and analysis. The use of ^{14}C as a tracer for biomass combustion is discussed in Chapter 4.

2.4 Conclusion

A sediment core from the Tamar Estuary has allowed an historical profile of air pollution in Launceston to be constructed, through the similarity of atmospheric and sedimentary PAH profiles. PAH concentrations in the dated sediment core were found to be relatively constant over the past 70-80 years, except for a number of short-term peaks in concentration. The constant source ratios throughout the core indicates that the Tamar Estuary has had only one major source of PAHs during the last 150 years, although the exact make-up of the sources could not be determined with any certainty. Traditional compound ratios (Phen/Anth and FluA/Pyr) indicated that pyrogenic sources have dominated input of PAHs to Launceston air and sediments, but could not differentiate between automobile exhaust and woodburning. Incorporating the Pyr/BaP ratio suggested that woodburning was the most likely major source, although it is unlikely that changes in woodburning alone could account for the large peaks in PAH concentrations observed. The lack of similar fluctuations prior to the 1940s implies that urbanisation and industrialisation, rather than climatic or weather related issues, were the principal causes of these peaks.

The lack of distinct source reconciliation allowed by PAHs severely limits their usefulness in source apportionment studies. Methods that are more specific to woodburning have been developed in the last few decades, including the cellulose combustion product levoglucosan, and carbon-14 analysis. These topics will be discussed in Chapters 3 and 4, respectively.

Sampling of atmospheric PAHs has been shown to be influenced by a number of factors. Comparison of filter media showed that glass-fibre filters tended to collect slightly lower concentrations of particle-phase PAHs compared to PTFE filters, but that vapour-phase concentrations were uneffected. As expected, greater partitioning of semi-volatile PAHs to the vapour-phase was observed in the summer months when air temperatures were higher, and lower particle-phase concentrations were collected by high-volume samplers because of "blow-off".

2.5 References

1. Kennish, M.J. *Practical handbook of estuarine and marine pollution*. **1997,** Boca Raton: CRC Press.
2. PAHs health review, National Environment Protection Council, Canberra, http://www.ephc.gov.au/pdf/Air_Toxics/PAH_Health_Review.pdf, **2003**.
3. Kalf, D.F.; Crommentuijn, T.; van de Plassche, E.J. Environmental quality objectives for 10 polycyclic aromatic hydrocarbons (PAHs), *Ecotox. Environ. Safety.* **1997**, 36, 89-97.
4. Berko, H.N. Technical report no. 2: Polycyclic aromatic hydrocarbons (PAHs) in ambient air in Australia, Environment Australia, Canberra, www.deh.gov.au/atmosphere, **1999**.
5. Freeman, D.J.; Cattell, F.C.R. The risk of lung cancer from polycyclic aromatic hydrocarbons in Sydney air, *Med. J. Aust.* **1988**, 149, 612-615.
6. Hayes, W.J.; Anderson, I.J.; Gaffoor, M.Z.; Hurtado, J. Trace metals in oysters and sediments of Botany Bay, Sydney, *Sci. Total Environ.* **1998**, 212(1), 39-47.
7. Maher, W.A.; Aislabie, J. Polycyclic aromatic hydrocarbons in nearshore marine sediments of Australia, *Sci. Total Environ.* **1992**, 112(2-3), 143-164.
8. Webster, L.; Angus, L.; Topping, G.; Dalgarno, E.J.; Moffat, C.F. Long-term monitoring of polycyclic aromatic hydrocarbons in Mussels (Mytilus edulis) following the Braer oil spill, *The Analyst* **1997**, 122, 1491-1495.
9. Garcia Falcon, M.S.; Gonzalez Amigo, S.; Lage Yusty, M.A.; Lopez de Alda Villaizan, M.J.; Simal Lozano, J. Enrichment of benzo[a]pyrene in smoked food products and determination by high-performance liquid chromatography - fluorescence detection, *J. Chromatog. A.* **1996**, 753, 207-215.
10. Rogge, W.F.; Hidlemann, L.M.; Mazurek, M.A.; Cass, G.R.; Simoneit, B.R.T. Sources of fine organic aerosol. 1. Charbroilers and meat cooking operations, *Environ. Sci. Technol.* **1991**, 25(6), 1112-1125.
11. Kazerouni, N.; Sinha, R.; Hsu, C.H.; Greenberg, A.; Rothman, N. Analysis of 200 food items for benzo[a]pyrene and estimation of its intake in an epidemiologic study, *Food and Chemical Toxicology* **2001**, 39(5), 423-436.
12. Mastral, A.M.; Callen, M.S. A review on polycyclic aromatic hydrocarbon (PAH) emissions from energy generation, *Environ. Sci. Technol.* **2000**, 34(15), 3051-3057.
13. Sharma, R.K.; Hajaligol, M.R. Effect of pyrolysis conditions on the formation of polycyclic aromatic hydrocarbons (PAHs) from polyphenolic compounds, *J. Anal. Appl. Pyrolysis* **2003**, 66(1-2), 123-144.
14. Westerholm, R.N.; Alsberg, T.E.; Frommelin, A.B.; Strandell, M.E.; Rannug, U.; Winquist, L.; Grigoriadis, V.; Egebaeck, K.E. Effect of fuel polycyclic aromatic hydrocarbon content on the emissions of polycyclic aromatic hydrocarbons and other mutagenic substances from a gasoline-fueled automobile, *Environ. Sci. Technol.* **1988**, 22(8), 925-30.
15. Yamasaki, H.; Kuwata, K.; Miyamoto, H. Effects of ambient temperature on aspects of airborne polycyclic aromatic hydrocarbons, *Environ. Sci. Technol.* **1982**, 16(4), 189-194.

16. Chuang, J.C.; Hannan, S.W.; Wilson, N.K. Field comparison of polyurethane foam and XAD-2 resin for air sampling for polynuclear aromatic hydrocarbons, *Environ. Sci. Technol.* **1987**, 21(8), 798-804.
17. Coutant, R.W.; Brown, L.; Chuang, J.C.; Riggin, R.M.; Lewis, R.G. Phase distribution and artifact formation in ambient air sampling for polynuclear aromatic hydrocarbons, *Atmos. Environ.* **1988**, 22(2), 403-409.
18. Knecht, U.; Woitowitz, H.J. PAH-losses from glass fiber filters under the conditions of different air volume sampling: results of field evaluations in occupational atmospheres, *Fresenius Z. Anal. Chem.* **1988**, 331, 8-13.
19. Brorstrom, E.; Grennfelt, P.; Lindskog, A. The effect of nitrogen dioxide and ozone on the decomposition of particle-associated polycyclic aromatic hydrocarbons during sampling from the atmosphere, *Atmos. Environ.* **1983**, 17(3), 601-605.
20. Jang, M.; McDow, S.R. Products of benz(a)anthracene photodegradation in the presence of known organic constituents of atmospheric aerosols, *Environ. Sci. Technol.* **1997**, 31(4), 1046-1053.
21. Kamens, R.M.; Perry, J.M.; Saucy, D.A.; Bell, D.A.; Newton, D.L.; Brand, B. Factors which influence polycyclic aromatic hydrocarbon decomposition on wood smoke particles, *Environ. Int.* **1985**, 11, 131-136.
22. Kamens, R.M.; Guo, Z.; Fulcher, J.N.; Bell, D.A. Influence of humidity, sunlight, and temperature on the daytime decay of polyaromatic hydrocarbons on atmospheric soot particles, *Environ. Sci. Technol.* **1988**, 22(1), 103-108.
23. Kamens, R.M.; Fulcher, J.N.; Zhishi, G. Effect of temperature on wood soot PAH decay in atmospheres with sunlight and low NO_x, *Atmos. Environ.* **1986**, 20(8), 1579-1587.
24. McDow, S.R.; Sun, Q.; Vartiainen, M.; Hong, Y.; Yao, Y.; Fister, T.; Yao, R.; Kamens, R.M. Effect of composition and state of organic components on polycyclic aromatic hydrocarbon decay in atmospheric aerosols, *Environ. Sci. Technol.* **1994**, 28(12), 2147-2153.
25. Jang, M.; McDow, S.R. Banz(a)anthracene photodegradation in the presence of known organic constituents of atmospheric aerosols, *Environ. Sci. Technol.* **1995**, 29(10), 2654-2660.
26. Eiceman, G.A.; Vandiver, V.J. Adsorption of polycyclic aromatic hydrocarbons on fly ash from a municipal incinerator and a coal-fired power plant, *Atmos. Environ.* **1983**, 17(3), 461-465.
27. Odabasi, M.; Sofuoglu, A.; Vardar, N.; Tasdemir, Y.; Holson, T.M. Measurement of dry deposition and air-water exchange of polycyclic aromatic hydrocarbons with the water surface sampler, *Environ. Sci Technol.* **1999**, 33, 426-434.
28. Hoffman, E.J.; Mills, G.L.; Latimer, J.S.; Quinn, J.G. Urban runoff as a source of polycyclic aromatic hydrocarbons to coastal waters, *Environ. Sci. Technol.* **1984**, 18(8), 580-587.
29. McVeety, B.D.; Hites, R.A. Atmospheric deposition of polycyclic aromatic hydrocarbons to water surfaces: a mass balance approach, *Atmos. Environ.* **1988**, 22(3), 511-536.
30. Simcik, M.F.; Eisenreich, S.J.; Lioy, P.J. Source apportionment and source/sink relationships of PAHs in the coastal atmosphere of Chicago and Lake Michigan, *Atmos. Environ.* **1999**, 33, 5071-5079.

31. Fernandez, P.; Vilanova, R.M.; Martinez, C.; Appleby, P.; Grimalt, J.O. The historical record of atmospheric pyrolytic pollution over Europe registered in the sedimentary PAH from remote mountain lakes, *Environ. Sci. Technol.* **2000**, 34(10), 1906-1913.
32. Ohkouchi, N.; Kawamura, K.; Kawahata, H. Distributions of three- to seven-ring polynuclear aromatic hydrocarbons on the deep sea floor in the central Pacific, *Environ. Sci. Technol.* **1999**, 33(18), 3086-3090.
33. Smith, J.N.; Levy, E.M. Geochronology for polycyclic aromatic hydrocarbon contamination in sediments of the Saguenay Fjord, *Environ. Sci. Technol.* **1990**, 24, 874-879.
34. Næs, K.; Oug, E. Multivariate approach to distribution pattern and fate of polycyclic aromatic hydrocarbons in sediments from smelter-affected Norwegian fjords and coastal waters, *Environ. Sci. Technol.* **1997**, 31(5), 1253-1258.
35. Heit, M. The relationship of a coal fired power plant to the levels of polycyclic aromatic hydrocarbons (PAH) in the sediment of Cayuga Lake, *Water, Air, and Soil Poll.* **1985**, 24, 41-61.
36. Webster, L.; McIntosh, A.D.; Moffat, C.F.; Dalgarno, E.J.; Brown, N.A.; Fryer, R.J. Analysis of sediments from Shetland Island voes for polycyclic aromatic hydrocarbons, steranes and triterpanes, *J. Environ. Monit.* **2000**, 2, 29-38.
37. Gabos, S.; Ikonomou, M.G.; Schopflocher, D.; Fowler, B.R.; White, J.; Prepas, E.; Prince, D.; Chen, W. Characteristics of PAHs, PCDD/Fs and PCBs in sediment following forest fires in northern Alberta, *Chemosphere* **2001**, 43(4-7), 709-719.
38. Fernandes, M.B.; Sicre, M.-A. Polycyclic aromatic hydrocarbons in the Arctic: Ob and Yenisei Estuaries and Kara Sea Shelf, *Estuarine, Coastal and Shelf Sci.* **1999**, 48, 725-737.
39. Yunker, M.B.; Snowdon, L.R.; Macdonald, R.W.; Smith, J.N.; Fowler, M.G.; Skibo, D.N.; Mclaughlin, F.A.; Danyusheveskaya, A.I.; Petrova, V.I.; Ivanov, G.I. Polycyclic aromatic hydrocarbon composition and potential sources for sediment samples from the Beaufort and Barents Seas, *Environ. Sci. Technol.* **1996**, 30, 1310-1320.
40. Readman, J.W.; Mantoura, R.F.C.; Rhead, M.M. A record of polycyclic aromatic hydrocarbon (PAH) pollution obtained from accreting sediments of the Tamar Estuary, U.K.: Evidence for non-equilibrium behaviour of PAH, *Sci. Total Environ.* **1987**, 66, 73-94.
41. Eisenreich, S.J.; Capel, P.D.; Robbins, J.A.; Bourbonniere, R. Accumulation and diagenesis of chlorinated hydrocarbons in lacustrine sediments, *Environ. Sci. Technol.* **1989**, 23(9), 1116-1126.
42. Latimer, J.S.; Quinn, J.G. Historical trends and current inputs of hydrophobic organic compounds in an urban estuary: The sedimentary record, *Environ. Sci. Technol.* **1996**, 30(2), 623-633.
43. Van Metre, P.C.; Callender, E.; Fuller, C.C. Historical trends in organochlorine compounds in river basins identified using sediment cores from reservoirs, *Environ. Sci. Technol.* **1997**, 31(8), 2339-2344.
44. Witt, G.; Trost, E. Polycyclic aromatic hydrocarbons (PAHs) in sediments of the Baltic Sea and of the German coastal waters, *Chemosphere* **1999**, 38(7), 1603-1614.

45. Mitra, S.; Dellapenna, T.M.; Dickhut, R.M. Polycyclic aromatic hydrocarbon distribution within Lower Hudson River estuarine sediments: Physical mixing *vs* sediment geochemistry, *Estuarine, Coastal and Shelf Science* **1999**, 49, 311-326.
46. Schneider, A.R.; Stapleton, H.M.; Cornwell, J.; Baker, J.E. Recent declines in PAH, PCB, and taxophene levels in the northern Great Lakes as determined from high resolution sediment cores, *Environ. Sci. Technol.* **2001**, 35(19), 3809-3815.
47. Su, M.-C.; Christensen, E.R.; Karls, J.F. Determination of PAH sources in dated sediments from Green Bay, Wisconsin, by a chemical mass balance model, *Environ. Poll.* **1998**, 98, 411-419.
48. Su, M.-C.; Christensen, E.R.; Karls, J.F.; Kosuru, S.; Imamoglu, I. Apportionment of polycyclic aromatic hydrocarbon sources in lower Fox River, USA, sediments by a chemical mass balance model, *Environ. Tox. Chem.* **2000**, 19(6), 1481-1490.
49. Li, K.; Christensen, E.R.; van Camp, R.P.; Imamoglu, I. PAHs in dated sediments of Ashtabula River, Ohio, USA, *Environ. Sci. Technol.* **2001**, 35(14), 2896-2902.
50. Li, A.; Jang, J.-K.; Scheff, P.A. Application of EPA CMB8.2 model for source apportionment of sediment PAHs in Lake Calumet, Chicago, *Environ. Sci. Technol.* **2003**, 37(13), 2958-2965.
51. Van Metre, P.C.; Mahler, B.J.; Furlong, E.T. Urban sprawl leaves its PAH signature, *Environ. Sci. Technol.* **2000**, 34(19), 4064-4070.
52. Lima, A.L.C.; Eglinton, T.I.; Reddy, C.M. High-resolution record of pyrogenic polycyclic aromatic hydrocarbon deposition during the 20th century, *Environ. Sci. Technol.* **2003**, 37(1), 53-61.
53. Gevao, B.; Jones, K.C.; Hamilton-Taylor, J. Polycyclic aromatic hydrocarbon (PAH) deposition to and processing in a small rural lake, Cumbria UK, *Sci. Total Environ.* **1998**, 215(3), 231-242.
54. McGroddy, S.E.; Farrington, J.W. Sediment porewater partitioning of polycyclic aromatic hydrocarbons in three cores from Boston Harbor, Massachusetts, *Environ. Sci. Technol.* **1995**, 29, 1542-1550.
55. Maruya, K.A.; Risebrough, R.W.; Horne, A.J. Partitioning of polynuclear aromatic hydrocarbons between sediments from San Francisco Bay and their porewaters, *Environ. Sci. Technol.* **1996**, 30, 2942-2947.
56. Macrae, J.D.; Hall, K.J. Comparison of methods used to determine the availability of polycyclic aromatic hydrocarbons in marine sediment, *Environ. Sci. Technol.* **1998**, 32(23), 3809-3815.
57. Gustafsson, O.; Haghseta, F.; Chan, C.; MacFarlane, J.; Gschwend, P.M. Quantification of the dilute sedimentary soot phase: Implications for PAH speciation and bioavailability, *Environ. Sci. Technol.* **1997**, 31(1), 203-209.
58. Naes, K.; Axelman, J.; Naf, C.; Broman, D. Role of soot carbon and other carbon matrices in the distribution of PAHs among particles, DOC, and the dissolved phase in the effluent and recipient waters of an aluminum reduction plant, *Environ. Sci. Technol.* **1998**, 32(12), 1786-1792.

59. Mitra, S.; Dickhut, R.M.; Kuehl, S.A.; Kimbrough, K.L. Polycyclic aromatic hydrocarbon (PAH) source, sediment deposition patterns, and particle geochemistry as factors influencing PAH distribution coefficients in sediments of the Elizabeth River, VA, USA, *Marine Chem.* **1999**, 66, 113-127.
60. Accardi-Dey, A.; Gschwend, P.M. Assessing the combined roles of natural organic matter and black carbon as sorbents in sediments, *Environ. Sci. Technol.* **2002**, 36(1), 21-29.
61. Accardi-Dey, A.; Gschwend, P.M. Reinterpreting literature sorption data considering both adsorption into organic carbon and adsorption onto black carbon, *Environ. Sci. Technol.* **2003**, 37(1), 99-106.
62. Reddy, C.M.; Pearson, A.; Xu, L.; McNichol, A.P.; Benner, B.A., Jr.; Wise, S.A.; Klouda, G.A.; Currie, L.A.; Eglinton, T.I. Radiocarbon as a tool to apportion the sources of polycyclic aromatic hydrocarbons and black carbon in environmental samples, *Environ. Sci. Technol.* **2002**, 36(8), 1774-1782.
63. Yuan, S.Y.; Chang, J.S.; Yen, J.H.; Chang, B.-V. Biodegradation of phenanthrene in river sediment, *Chemosphere* **2001**, 43, 273-278.
64. Readman, J.W.; Mantoura, R.F.C.; Rhead, M.M.; Brown, L. Aquatic distribution and heterotrophic degradation of polycyclic aromatic hydrocarbons (PAH) in the Tamar Estuary, *Estuarine, Coastal and Shelf Sci.* **1982**, 14, 369-398.
65. Carmichael, L.M.; Christman, R.F.; Pfaender, F.K. Desorption and mineralization kinetics of phenanthrene and chrysene in contaminated soils, *Environ. Sci. Technol.* **1997**, 31(1), 126-132.
66. Alexander, M. Aging, bioavailability, and overestimation of risk from environmental pollutants, *Environ. Sci. Technol.* **2000**, 34(20), 4259-4265.
67. Daisey, J.M.; Cheney, J.L.; Lioy, P.J. Profiles of organic particulate emissions from air pollution sources: Status and needs for receptor source apportionment modeling, *J. Air Poll. Contol Assoc.* **1986**, 36(1), 17-33.
68. Rogge, W.F.; Hidlemann, L.M.; Mazurek, M.A.; Cass, G.R.; Simoneit, B.R.T. Sources of fine organic aerosol. 2. Noncatalyst and catalyst-equipped automobiles and heavy-duty diesel trucks, *Environ. Sci. Technol.* **1993**, 27(4), 636-651.
69. Ramdahl, T. Retene - a molecular marker of wood combustion, *Nature* **1983**, 306, 580-582.
70. Budzinski, H.; Jones, I.; Bellocq, J.; Pierard, C.; Garrigues, P. Evaluation of sediment contamination by polycyclic aromatic hydrocarbons in the Gironde Estuary, *Marine Chem.* **1997**, 58, 85-97.
71. Baumard, P.; Budzinski, H.; Michon, Q.; Garrigues, P.; Burgeot, T.; Bellocq, J. Origin and bioavailability of PAHs in the Mediterranean Sea from mussel and sediment records, *Estuarine, Coastal and Shelf Sci.* **1998**, 47, 77-90.
72. Sporstøl, S.; Gjøs, N.; Lichtenthaler, R.G.; Gustavsen, K.O.; Urdal, K.; Oreld, F.; Skel, J. Source identification of aromatic hydrocarbons in sediments using GM/MS, *Environ. Sci. Technol.* **1983**, 17, 282-286.
73. Benner, B.A.; Wise, S.A.; Currie, L.A.; Klouda, G.A.; Klinedinst, D.B.; Zweidinger, R.B.; Stevens, R.K.; Lewis, C.W. Distinguishing the contributions of residential wood combustion and mobile source emissions using relative concentrations of dimethylphenanthrene isomers, *Environ. Sci. Technol.* **1995**, 29(9), 2382-2389.

74. Macías-Zamora, J.V.; Mendoza-Vega, E.; Villaescusa-Celaya, B.C. PAHs composition of surface marine sediments: a comparison to potential local sources in Todos Santos Bay, B.C., Mexico, *Chemosphere* **2002**, 46, 459-486.
75. Sicre, M.A.; Marty, J.C.; Saliot, A.; Aparicio, X.; Grimalt, J.; Albaiges, J. Aliphatic and aromatic hydrocarbons in different sized aerosols over the Mediterranean Sea: Occurrence and origin, *Atmos. Environ.* **1987**, 21(10), 2247-2259.
76. Zhou, J.L.; Maskaoui, K. Distribution of polycyclic aromatic hydrocarbons in water and surface sediments from Daya Bay, China, *Environ. Poll.* **2003**, 121(2), 269-281.
77. Freeman, D.J.; Cattell, F.C.R. Woodburning as a source of atmospheric polycyclic aromatic hydrocarbons, *Environ. Sci. Technol.* **1990**, 24, 1581-1585.
78. Muller, J.F.; Hawker, D.W.; Connell, D.W. Polycyclic aromatic hydrocarbons in the atmospheric environment of Brisbane, Australia, *Chemosphere* **1998**, 37(7), 1369-1383.
79. Oanh, N.T.K.; Reutergardh, L.B.; Dung, N.T. Emission of polycyclic aromatic hydrocarbons and particulate matter from domestic combustion of selected fuels, *Environ. Sci. Technol.* **1999**, 33, 2703-2709.
80. Li, C.K.; Kamens, R.M. The use of polycyclic aromatic hydrocarbons as source signatures in receptor modeling, *Atmos. Environ.* **1993**, 27A(4), 523-532.
81. Singh, A.K.; Gin, M.F.; Ni, F.; Christensen, E.R. A source-receptor method for determining non-point sources of PAHs to the Milwaukee Harbor Estuary, *Water Sci. Technol.* **1993**, 28(8-9), 91-102.
82. Khalili, N.R.; Scheff, P.A.; Holson, T.M. PAH source fingerprints for coke ovens, diesel and gasoline engines, highway tunnels, and wood combustion emissions, *Atmos. Environ.* **1995**, 29(4), 533-542.
83. Christensen, E.R.; Rachdawong, P.; Karls, J.F.; Van Camp, R.P. PAHs in sediments: Unmixing and CMB modeling of sources, *J. Environ. Engin.* **1999**, Nov, 1022-1032.
84. Kavouras, I.G.; Koutrakis, P.; Tsapakis, M.; Lagoudaki, E.; Stephanou, E.G.; von Bear, D.; Oyola, P. Source apportionment of urban particulate aliphatic and polynuclear aromatic hydrocarbons (PAHs) using multivariate methods, *Environ. Sci. Technol.* **2001**, 35(11), 2288-2294.
85. Christensen, E.R.; Irwan, A.L.; Ab Razak, A.; Rachdawong, P.; Karls, J.F. Sources of polycyclic aromatic hydroacrbons in sediments of the Kinnickinnic River, Wisconsin, *J. Great Lakes Res.* **1997**, 23(1), 61-73.
86. Dickhut, R.M.; Canuel, E.A.; Gustafson, K.E.; Liu, K.; Arzayus, K.M.; Walker, S.E.; Edgecombe, G.; Gaylor, M.O.; MacDonald, E.H. Automative sources of carcinogenic polycyclic aromatic hydrocarbons associated with particulate matter in the Chesapeake Bay region, *Environ. Sci. Technol.* **2000**, 34(21), 4635-4640.
87. Pirzl, H.; Coughanowr, C. State of the Tamar Estuary: a review of environmental quality data to 1997, Supervising Scientist Report 128, Supervising Scientist, Canberra, **1997**.

88. Mollison, J.C. Polycyclic aromatic hydrocarbons associated with woodsmoke in Launceston, 1990, Honours Thesis, School of Applied Science, University of Tasmania, Launceston, **1991**.
89. Jordan, T.B. Polycyclic aromatic hydrocarbon distribution in Launceston air and upper Tamar Estuary sediment, Honours Thesis, School of Applied Science, University of Tasmania, Launceston, **2000**.
90. Working Party, Report on an investigation by an expert working party into air pollution, environmental health and respiratory diseases, Launceston and upper Tamar Valley, Tasmania, 1991-94, Launceston City Council, Launceston, **1996**.
91. Bagg, J.; Smith, J.D.; Maher, W.A. Distribution of polycyclic aromatic hydrocarbons in sediments from estuaries of South-eastern Australia, *Aust. J. Freshwater Res.* **1981**, 32, 65-73.
92. Kayal, S.I.; Connell, D.W. Occurence and distribution of polycyclic aromatic hydrocarbons in surface sediments and water from the Brisbane River estuary, Australia, *Estuarine, Coastal and Shelf Sci.* **1989**, 29, 473-487.
93. Brown, G.; Maher, W. The occurrence, distribution and sources of polycyclic aromatic hydrocarbons in the sediments of the Georges River Estuary, Australia, *Org. Geochem.* **1992**, 18(5), 657-68.
94. McCready, S.; Slee, D.J.; Birch, G.F.; Taylor, S.E. The distribution of polycyclic aromatic hydrocarbons in surficial sediments of Sydney Harbour, Australia, *Marine Pollution Bulletin* **2000**, 40(11), 999-1006.
95. Sisovic, A.; Fugaš, M. Smoke concentration as an indicator of polycyclic aromatic hydrocarbons levels in the air, *Environ. Monit. Assess.* **1997**, 45, 201-207.
96. Seen, A.; Townsend, A.; Atkinson, B.; Ellison, J.; Harrison, J.; Heijnis, H. Determining the history and sources of contaminants in sediments in the Tamar Estuary, Tasmania, using ^{210}Pb and stable Pb isotope analysis, *Environ. Chem.* **2004**, 1(1), 49-54.
97. Colombini, M.P.; Fuoco, R.; Giannarelli, S.; Tremine, M.; Abete, C.; Vincentini, M.; Berti, S. Determination of polyaromatic hydrocarbons in atmospheric particulate samples by HPLC with fluorescence detection: A field application, *Microchemical J.* **1998**, 59, 228-238.
98. Song, Y.F.; Jing, X.; Fleischmann, S.; Wilke, B.-M. Comparative study of extraction methods for the determination of PAHs from contaminated soils and sediments, *Chemosphere* **2002**, 48, 993-1001.
99. Burford, M.D.; Hawthorne, S.B.; Miller, D.J. Extraction rates of spiked versus native PAHs from heterogeneous environmental samples using supercritical fluid extraction and sonication in methylene chloride, *Anal. Chem.* **1993**, 65, 1497-1505.
100. Carvalho, F.P.; Villeneuve, J.-P.; Cattini, C. Determination of organochlorine compounds, petroleum hydrocarbons, and sterols in a sediment sample, IAEA-383. Results of an intercomparison exercise, *Inter. J. Environ. Anal. Chem.* **1999**, 75(4), 315-329.
101. Sisovic, A.; Fugaš, M. Comparative evaluation of procedures for the determination of PAH in low-volume samples, *Environ. Monit. Assess.* **1991**, 18, 235-241.
102. Heijnis, H. ^{230}Th/^{234}U & ^{210}Pb dating, in *Technical workshop on Quaternary dating methods*, ANSTO: 13-14 October **1994**.

103. Klinedinst, D.B.; Currie, L.A. Carbon isotopic analysis of the Northern Front Range Air Quality Study's summer and winter 1996-1997 program, CRC Project No. A-20, NIST, Gaithersburg, **1998**.
104. Gelinas, Y.; Prentice, K.M.; Baldock, J.A.; Hedges, J.I. An improved thermal oxidation method for the quantification of soot/graphitic black carbon in sediments and soils, *Environ. Sci. Technol.* **2001**, 25(17), 3519-3525.
105. National Environmental Protection Council, National environment protection measure (ambient air quality), http://www.ephc.gov.au/.
106. Lee, F.S.-C.; Pierson, W.R.; Ezike, J. The problem of PAH degradation during filter collection of airborne particulates - An evaluation of several commonly used filter media, in *Polynuclear Aromatic Hydrocarbons: Chemistry and biological effect. Chem. Biol. Eff., Int. Symp., 4th*, Columbus, OH: Battelle Press, **1979**.
107. Grosjean, D.; Fung, K.; Harrison, J. Interactions of polycyclic aromatic hydrocarbons with atmospheric pollutants, *Environ. Sci. Technol.* **1983**, 17(11), 673-679.
108. Schauer, C.; Niessner, R.; Poschl, U. Polycyclic aromatic hydrocarbons in urban air particulate matter: Decadal and seasonal trends, chemical degradation, and sampling artifacts, *Environ. Sci. Technol.* **2003**, 37(13), 2861-2868.
109. Hart, K.M.; Pankow, J.F. Comparison of n-alkane and PAH concentrations collected on quartz fiber and Teflon membrane filters in an urban environment, *J. Aerosol Sci.*. **1990**, 21, S377-S380.
110. Peters, J.; Seifert, B. Losses of benzo(a)pyrene under the conditions of high-volume sampling, *Atmos. Environ.* **1980**, 14, 117-119.
111. Lafontaine, M.; Vu-Duc, T.; Delsaut, P.; Morele, Y. Aerosols deposits on the inner cassette walls during PAH sampling: Underestimation of the inhaled fraction and of the occupational risk, *Polycyclic Aromat. Compd.* **1999**, 17, 221-228.
112. Keller, C.D.; Bidleman, T.F. Collection of airborne polycyclic aromatic hydrocarbons and other organics with a glass fiber filter-polyerethane foam system, *Atmos. Environ.* **1984**, 18(4), 837-845.
113. Park, J.-S.; Wade, T.L.; Sweet, S. Atmospheric distribution of polycyclic aromatic hydrocarbons and deposition to Galveston Bay, Texas, USA, *Atmos. Environ.* **2001**, 35, 3241-3249.
114. Mai, B.; Qi, S.; Zeng, E.Y.; Yang, Q.; Zhang, G.; Fu, J.; Sheng, G.; Peng, P.; Wang, Z. Distribution of polycyclic aromatic hydrocarbons in the coastal region off Macao, China: Assessment of input sources and transport pathways using compositional analysis, *Environ. Sci. Technol.* **2003**, 37(21), 4855-4863.
115. Viguri, J.; Verde, J.; Irabien, A. Environmental assessment of polycyclic aromatic hydrocarbons (PAHs) in surface sediments of the Santander Bay, northern Spain, *Chemosphere* **2002**, 48, 157-165.
116. Gras, J.; Meyer, C.; Weeks, I.; Gillett, R.; Galbally, I.; Todd, J.; Carnovale, F.; Joynt, R.; Hinwood, A.; Berko, H.; Brown, S. Technical report no. 5: Emissions from domestic solid fuel burning appliances, Environment Australia, Canberra, www.deh.gov.au/atmosphere, **2002**.

117. Harrison, J.; Heijnis, H.; Caprarelli, G. Historical pollution variability from abandoned mine site, Greater Blue Mountains World Heritage Area, New South Wales, Australia, *Environ. Geol.* **2003**, 43(6), 680-687.
118. Australian Bureau of Statistics, Historical tables: Population - Population, Tasmania, 1820 to 2001, www.abs.gov.au.
119. Elias, V.O.; Simoneit, B.R.T.; Cordeiro, R.C.; Turcq, B. Evaluating levoglucosan as an indicator of biomass burning in Carajás, Amazônia: A comparison to the charcoal record, *Geochim. Cosmochim. Acta.* **2001**, 65(2), 267-272.
120. Currie, L.A.; Eglinton, T.I.; Benner, B.A., Jr.; Pearson, A. Radiocarbon "dating" of individual chemical compounds in atmospheric aerosol: First results comparing direct isotopic and multivariate statistical apportionment of specific polycyclic aromatic hydrocarbons, *Nucl. Instrum. Methods Phys. Res., Sect. B* **1997**, 123(1-4), 475-486.

Chapter 3

Characterisation of the Organic Composition of Woodsmoke

Chapter 3

Characterisation of the Organic Composition of Woodsmoke

3.1 Introduction

3.1.1 Chemical Composition of Wood

Wood is a complex material that cannot be defined in terms of specific chemical structures. All woods are composed of cells that provide mechanical strength and the means of transporting and storing nutrients and water. The cell walls are made up of varying proportions of cellulose and hemicelluloses contained within lignin (Figure 3.1).

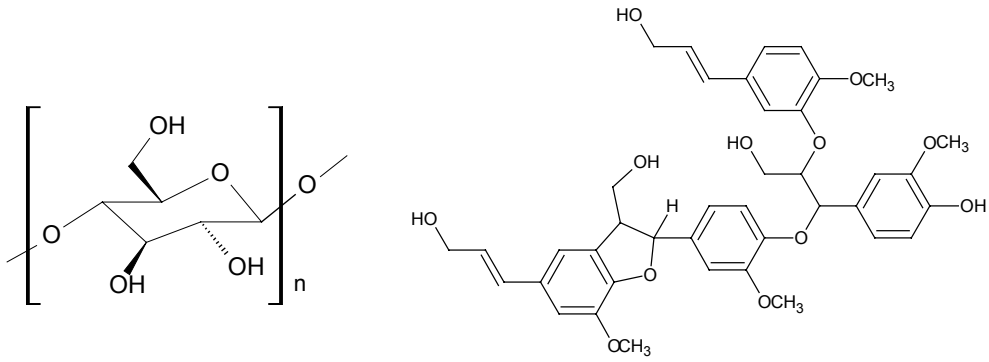

Cellulose Lignin

Figure 3.1 Simplified representative chemical structures of cellulose and lignin. Adapted from Sjöström [1].

Cellulose is the main component of wood (Table 3.1), and is composed of linear polymeric chains of β-D-glucopyranose sugar units (n = 7-12 x 10^3). The hemicelluloses comprise around 20-30% w/w of wood, and are heterogeneous polysaccharides (n = 100-200) made primarily from the monosaccharides D-glucose, D-mannose, D-galactose, D-xylose, and L-arabinose [1]. Lignin, a complex natural polymer principally made up of ether-linked p-hydroxyphenyl-propane, coniferyl alcohol and sinapyl alcohol units, provides the structural support of wood fibres. Apart from these major constituents, woods contain small amounts of other organic compounds such as aromatics, alcohols, terpenes and many carbonyl-containing compounds. Inorganic compounds such as carbonates, silicates, phosphates, and some metals (e.g. Ca, K, Mg, Fe) are also present in trace amounts.

Table 3.1 Chemical composition of various wood species (%w/w).

Common name	Species	Cellulose	Hemi-celluloses	Lignin	Residual + extractives
Blue gum	*Eucalyptus globulus*	51.3	25.2	21.9	1.6
River red gum	*Eucalyptus camaldulensis*	45.0	19.2	31.3	4.5
Black wattle	*Acacia mollissima*	42.9	33.6	20.8	2.7
Douglas fir	*Pseudotsuga menziesii*	38.8	26.3	29.3	5.6

Adapted from Sjöström [1].

3.1.2 Wood Combustion Process

The combustion of wood is a very complex and chaotic process, but can be thought of as occurring in four distinct stages [2, 3]. At most times throughout the burning process, all four will be occurring simultaneously. The endothermic processes of drying and volatilisation occurs as the wood is heated, firstly at the surface, and then deeper in the wood through outward diffusion of water. Drying is followed by

thermal decomposition or solid-particle pyrolysis when temperatures are greater than 100^{o}C, and becomes exothermic above 280^{o}C. The different constituents of wood tend to undergo pyrolysis at different temperatures; cellulose 330-380^{o}C, hemi-celluloses 230-330^{o}C, lignin 230-500^{o}C. Combustion of cellulose and hemi-cellulose begins with the breakdown of the glycosidic bonds between the individual sugar units, and further breakdown of the rings proceeds through a multitude of possible reaction pathways. High temperatures favour volatile compound producing reactions, while lower temperatures produce larger amounts of char.

Pyrolysis and oxidation of volatilised compounds then occurs, and it is this stage that is characterised by visible flames above the surface of the wood. Most of the gas-phase reactions occur through free-radical pathways, ultimately producing CO_2, H_2O, and other incomplete combustion products. Once the majority of volatile compounds have been driven out of the wood, oxygen is able to penetrate to the charred surface and combustion continues, again through free radical oxidation. This stage is characterised by “hot coals” or oxidation of char, very clean combustion, and no visible flame.

The moisture content of the wood plays an integral role throughout the combustion process. It increases the energy required to heat the wood to pyrolysis temperatures, reduces the rate of char oxidation, and tends to increase the amount of char formed.

The typical heat output from burning hardwoods is 19 MJ/kg, and 20 MJ/kg for softwoods [4]. Due to their lower density, softwoods tend to burn faster than

hardwoods, and also tend to produce significantly more smoke. As such, softwoods are not as popular as hardwoods for home heating in Australia [5].

3.1.3 Emissions from Woodburning

3.1.3.1 Particulate emissions

Smoke is a ubiquitous and unwanted by-product of woodburning, released because complete combustion is rarely obtained in most situations. There are many concerns about the health impacts of woodsmoke, mainly because the very small size of the smoke particles allows them to penetrate deep into the lungs. The size distribution of particles has been found to be similar when burning different wood species, with a mode diameter of ~0.1 μm [6], although particles were found to get progressively smaller throughout the burn-cycle in a wood stove [7].

The amount of particulate matter (PM) produced from wood combustion varies depending on a number of factors. These include the design of the appliance, the species and moisture content of the wood, and the airflow conditions within the combustion zone. Woodheaters operated with insufficient airflow (i.e. "incomplete" combustion) produce significantly more particulate matter than when operated with sufficient airflow ("complete" combustion) [8]. Higher emissions are also observed when burning pine compared to eucalyptus, and it was noted that the moisture content did not play a large role in determining the overall particle emission factor (PEF, mass of particles per dry mass of wood burned).

3.1.3.2 Organic composition of woodsmoke

The health impact of woodsmoke is not limited to the particles alone, and a wide range of toxic inorganic and organic compounds are also emitted as gases or adsorbed onto the particles [9, 10].

There have been numerous studies undertaken to characterise the composition of emissions from wood burning. Most studies have focussed on those compounds found in the particulate-phase, mainly because most ambient air quality guidelines concentrate on airborne particulate matter. Vapour-phase organics are emitted in substantial amounts, however, with one study finding compounds in the vapour-phase dominated those in the particle-phase by a factor of almost ten (Table 3.2) [11].

Table 3.2 Emission rates of vapour- and particle- phase compounds from fireplace combustion of softwoods and hardwoods, (mg/kg dry wood burned).

	Softwood	Hardwood
Vapour-phase		
alkanes + alkenes	801	1092
furans	447	822
carbonyls	890	1293
alcohols	1201	3388
resins & terpenoids	292	42
sesquiterpenes	140	4.0
halogenated	236	237
aromatics	653	658
phenols	164	264
guaiacols	247	216
PAHs	43	108
unidentified VOC	245	389
Particle-phase		
mass (g/kg)	5.14	5.66
organic carbon	3007	3580
elemental carbon	774	398
nitrate	6.8	10
sulfate	10	27
ammonium	5.5	5.1
chloride	7.5	10
potassium	18	67
sodium	1.4	1.1
guaiacols	143	233
syringols	6.0	755
PAHs	36	59

Adapted from McDonald *et al.* [11].

A number of chemical compounds have been proposed as woodsmoke specific tracers. Most are breakdown products of cellulose or lignin, or other components that may be particular to different types of wood. Khalil and Rasmussen reviewed the use of three different woodsmoke tracers (elemental and organic carbon, and methyl chloride), finding good agreement between the three [12]. Polycyclic aromatic hydrocarbons (PAHs) are frequently quantified due to their carcinogenic nature, but are also produced during any incomplete combustion process (Chapter 2). Whereas PAHs possibly have limited application as markers for wood combustion, retene (1-methyl-7-isopropylphenanthrene) is a PAH produced

exclusively from the degradation of abietic acid found in softwoods [13]. The high resin and abietane content of coniferous woods (softwoods) also leads to terpenoids and resin acids being produced in significant quantities during combustion of these woods [14, 15]. The relative abundances of the 1,6- and 1,7- dimethylphenanthrene isomers have also been used to distinguish woodburning (softwood) contributions to ambient pollution [16].

Another class of compounds identified as specific woodsmoke tracers are the methoxyphenols. They are formed during the pyrolysis of lignin, and consist mainly of para-substituted compounds based on two main parent compounds; guaiacol and syringol (Figure 3.2). First identified in woodsmoke by Hawthorne and co-workers [17, 18], guaiacols are emitted in almost equal amounts from both softwood and hardwood burning, while syringols are found at much lower levels in softwood smoke.

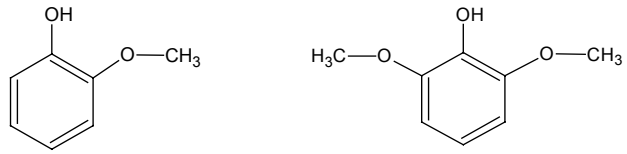

Guaiacol Syringol

Figure 3.2 Chemical structure of parent methoxyphenols found in woodsmoke.
More structures are shown in Figure B.1, Appendix B.

Several recent studies have attempted to identify as many individual compounds from as many compound classes as possible. Compounds quantified included trace metals, ionic species, alkanes, alkenes, alcohols, organic acids, esters, guaiacols, syringols, benzaldehydes, PAHs, sugar derivatives, furans, and terpenoids. Two of

these reports were part of larger studies characterising the chemical composition of various pollution sources [19, 20].

Fine *et al.* quantified over 250 elemental, organic and inorganic compounds in fine particles emitted from the fireplace combustion of 22 different wood species [21-23]. Differences in the concentrations of certain organic compounds emitted from the different species was expected to allow region-specific (USA) differentiation of woodsmoke pollution.

Composite emission profiles were constructed using statistical methods from emissions data collected by McDonald *et al.* [11]. From the various combustion conditions tested (burn-rate, wood species and appliance design), distinct composite profiles based on softwood, hardwood and synthetic log combustion in a fireplace, and hardwood combustion in a woodstove, were identified.

Schauer *et al.* presented the vapour-particle distribution of woodheater emissions, sampled using a dilution tunnel and residence-time chamber [20]. The distribution was found to be similar to that expected from the vapour-pressures and partition coefficients of the compounds. Hays *et al.* found vapour-phase methoxyphenol emissions from open burning of various wood species were around three times greater than the particle-phase emissions [24].

Aromatic and polar compounds make up a large proportion of the organic compounds emitted from woodburning, the majority of which are derived from the pyrolysis of cellulose or lignin. Some of these compounds are too polar for

conventional gas chromatography (GC) methods, but can be converted to various derivatives more amenable for analysis. Many aliphatic and resin acids have been quantified as methyl esters using diazomethane as the derivatising agent [21]. Nolte *et al.* converted many alcohols, sterols and sugars to their trimethylsilyl (TMS) ethers, identifying a number of compounds not previously detected in woodsmoke [25]. High-temperature-GC has also allowed many high-molecular weight compounds to be detected for the first time [26].

The cellulose breakdown product levoglucosan (Figure 3.3) has been proposed as a specific tracer for biomass combustion because of its almost ideal atmospheric pollution tracer qualities [27]; biomass combustion is the only known source, it is found exclusively in the particle-phase, and it is relatively resistant to degradation [28]. Its resistance to degradation is so great that it has been quantified in a sediment core and used as an indicator of forest fires [29]. Fluctuations in the levels of levoglucosan in the core were comparable to the more traditional technique of charcoal analysis, and large forest fires up to 7000 years ago were identified. Fireplace combustion of different wood species has shown that levoglucosan is emitted at relatively constant amounts per gram of organic carbon (OC); 99-168 mg/g OC from seven hardwood species, and 36-95 mg/g OC from five softwoods [21, 22]. A later study by the same authors targeting woods grown in the Western United States had much greater variability in levoglucosan emission fractions; 76-334 and 10-271 mg/g OC from six hardwoods and four softwoods, respectively [23].

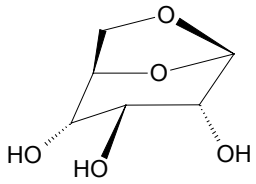

Figure 3.3 Chemical structure of levoglucosan (1,6-anhydro-β-D-glucose).

3.1.3.3 Studies undertaken in Australia

There exists quite extensive emissions data from wood burning in the US, but little work has been undertaken in other areas of the world. The most thorough study to date undertaken in Australia tested emissions from four different woodheaters using a variety of combustion conditions and wood characteristics [8]. Sampling was conducted using a dilution tunnel based Australian Standard 4013 [30] (see Figure 3.4), and included collection of integrated (total) and continuous (instantaneous) particle mass loadings, isocyanates, PAHs, aldehydes and ketones, and a variety of other organic and inorganic compounds. Continuous measurement of gaseous species (CO, NO_x, SO_2, CH_4, VOCs) was also undertaken. Particle emission factors (PEFs) varied from 0.2 to 30 g/kg wood burned, with higher mass loadings observed when operating the heaters with a restricted airflow, as expected. Pine woods also consistently produced higher PEFs. Emission factors for over 120 chemical species were reported, and a best estimate of average emissions was presented based on these results and data from a concurrent survey of woodburning households. Many relationships between emissions (of both particle-mass and chemical species), operating conditions, and over time were investigated. Qualitative differences between open and closed airflows were observed in the time series of many of the variables (e.g. PEF, combustion efficiency, power output, total VOC).

A literature review on the use of woodheating in Australia and around the world was compiled as part of the same series of Environment Australia reports as the above study [5]. Various policies and procedures from around Australia were outlined, along with current and possible future air quality guidelines. Emissions data from local and international studies were presented, but there was a perceived lack of speciated emissions data from woodburning under Australian conditions (i.e. local wood species and heater designs). The health impacts of wood smoke from both particulate matter and associated toxic compounds was also reviewed.

Emissions of PAHs were investigated from woodheaters burning Australian woods by Zou and co-workers [31]. Three Eucalyptus species and Radiata pine were tested under open and ½-closed airflow conditions. The vapour-particle phase distribution was determined from in-flue samples withdrawn without dilution, with vapour-phase compounds accounting for 88-98% of the total PAH mass emitted; primarily naphthalene. Softwoods consistently produced greater amounts of both vapour- and particle- phase PAHs than hardwoods, and increased emissions of most target compounds were observed when the heater was operated with a decreased airflow.

3.1.4 Outline of Work to be Presented in this Chapter

It is vital when undertaking source apportionment studies to understand how the composition of emissions from woodheaters change when using different models and combustion conditions so these effects can be taken into account. Differences in emission profiles have been observed when burning different species of wood [21-

23], between woodheaters and open combustion [24], and when using different models of woodheater [32]. The effect of the airflow setting (burn-rate) on the emission of organic compounds has not been fully investigated and is expected to be significant.

This chapter will present vapour- and particle- phase organic compound emission factors from woodheaters operated with different airflows. Quantification of the woodheater contribution to PM_{10} in Launceston will be made using levoglucosan, a specific tracer for woodsmoke.

A manuscript based on this work was accepted for publication in *Environmental Science and Technology*, 4 March 2005.

3.2 Experimental

3.2.1 Apparatus and Testing Procedure

3.2.1.1 Dilution tunnel

A dilution tunnel was built based on AS/NZS 4013 [30], as shown in Figures 3.4 and 3.5. The dimensions of the tunnel did not conform exactly to the Standard due to space limitations of the building housing the facility.

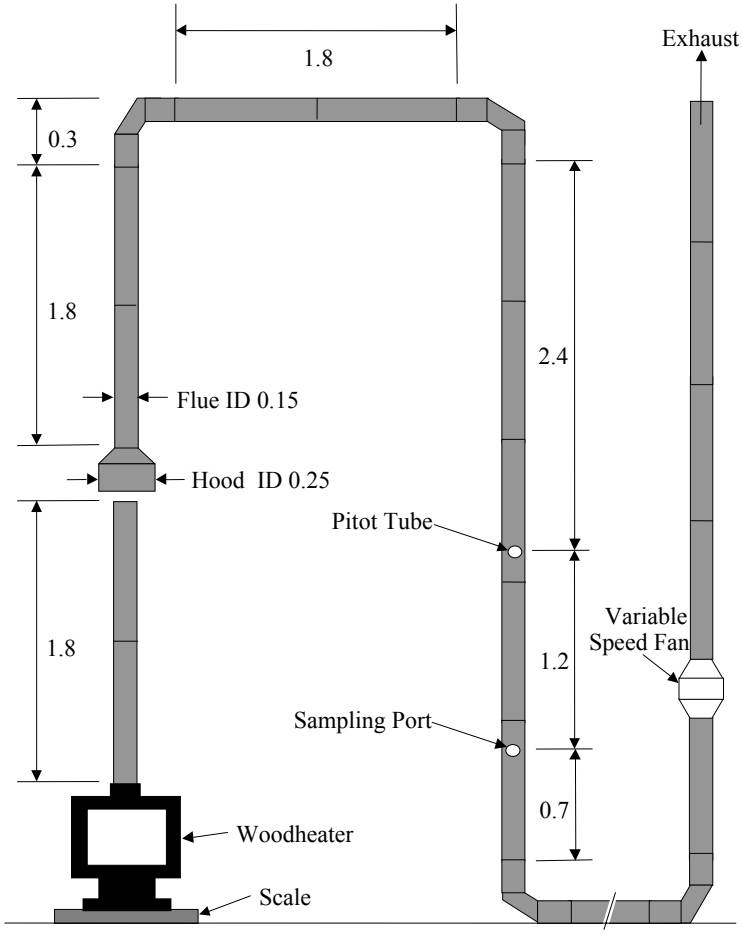

Figure 3.4 Dimensions of dilution tunnel.
Dimensions in metres, adapted from AS/NZS 4013 [30].

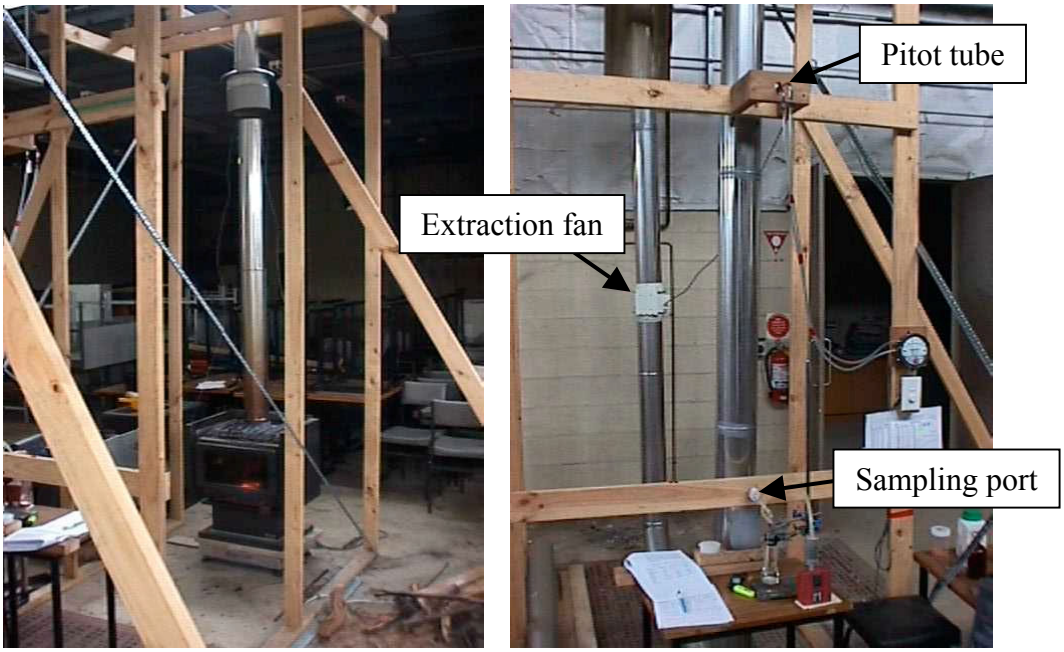

Figure 3.5 Dilution tunnel set-up.

A) Heater M1 on scales, showing chimney and smoke collection "hood" and supporting framework.

B) Flow measurement and sampling set-up, including pitot tube, sampling train and extraction fan.

The principle of the dilution tunnel is to collect the entire woodheater emissions and dilute it with a large amount of cooler air to allow the semi-volatile compounds to condense onto particles. Thus the cooled emissions will be closer to "real-world" conditions; i.e. after they have exited the flue and resided in the atmosphere for a period of time. Different dilution designs allow the emissions to mix with the cooler air from a few seconds to a few minutes, with the later utilising residence-time-chambers to further enhance the equilibration process [33]. The main disadvantages of these methods are the cost and complexity of the apparatus required.

Australian Standard 4013 is based on a simple dilution tunnel where the complete woodheater emissions are drawn into a total flow of approximately 6 m^3 per minute (~5.5 m/s) [30]. Samples are withdrawn iso-kinetically almost seven metres into the tunnel and are collected on glass-fibre filters. This standard is used in conjunction with other standards relating to the wood fuel and power output for the certification of woodheaters manufactured in Australia [34, 35].

A simpler method of emissions sampling is to withdraw samples directly from the hot flue-gasses without cooling. This method is relatively simple, requiring only access to the top or mid-section of the chimney, and is useful for testing appliances used in home and industrial settings when the appliances are operated under realistic conditions or when other sampling techniques are not easily implemented. A major drawback of in-flue sampling is that the emissions are still relatively hot, and thus have not had a chance to cool and allow semi-volatile compounds to condense onto particles.

3.2.1.2 Woodheater models tested

Three different models of woodheater were tested (Figure 3.6); two from Saxon Woodheaters, Australia (S1 and S2), a popular local manufacturer, and one from Masport Woodheaters, Australia (M1). Heaters S1 and M1 were approximately 20 years old, while heater S2 was a larger and much more modern design (about 5 years old). All were removed from use in homes in Launceston through the woodheater "buyback" scheme, and kindly donated by the Launceston City Council. Although they comprise only a small sample of the range of models available, they are representative of actual models currently used in Launceston.

Figure 3.6 Woodheater models used in emissions testing.
L-R: S1, S2, M1.

3.2.1.3 Firewood

The firewood, White Gum (*Eucalyptus viminalis*), was used in all the tests and was obtained from a local wood merchant. Although many households collect their own firewood, this was aimed to represent the typical species of wood burned locally. The average moisture content of the wood on a dry basis was 13.8 ± 0.9% w/w (mean ± 1σ, n = 6), measured by drying portions (30-200 g) at 105^{o}C until constant weight was obtained.

3.2.1.4 Woodheater testing procedure

Each source test was started using a few sheets of newspaper and fallen twigs from a Eucalyptus tree outside the building, followed by larger kindling cut from a log of the test wood. Each test load consisted of a single charge of fuel (typically 2-3 logs) being added to hot coals, usually 23-27% of the mass of the test load. A short period of "pre-combustion" was allowed before setting the airflow conditions and initiation of sampling, in a similar manner to Gras *et al.* [8], ensuring sustainable combustion throughout the test period. Typically, 10-15% of the test load was pre-

burnt for closed and ½-closed airflow conditions, with 1-5% pre-burnt for open-airflow conditions.

The dilution tunnel flow-rate was measured using an s-type pitot tube connected to a magnehelic gauge (Models 160S-18 and 2000-00, respectively, both from Dwyer Instruments). The pitot tube was positioned at the centre of the flue, and was calibrated using a method based on AS/NZS 4323.1 [36]. Briefly, a dilution tunnel flow giving a static pressure of approximately 0.1" water was established, and a series of pressure readings were made while traversing the flue at 6.7%, 25%, 75% and 93.3% the flue diameter across two perpendicular axes. The cross-sectional flow calibration factor (F_p in Equation B.1, Appendix B) was calculated as the ratio of the centre pressure to the average of the 8 transverse readings. The dilution tunnel temperature was measured with a thermometer attached to the trailing edge of the pitot tube. Temperature-corrected flow-rates were then calculated using the equations given in the pitot tube product data sheet (Equation B.1, Appendix B). The dilution tunnel flow was monitored at intervals not exceeding 10 minutes to ensure that isokinetic sampling conditions were maintained.

Emissions were withdrawn iso-kinetically from the centre of the flue through a 1/8" ID stainless-steel probe (Figure 3.7). The sampling train consisted of one or two borosilicate glass-fibre filters (GFF, Gelman EPM2000) housed in separate plastic cassettes, followed by a tube containing 150 mg XAD-2 resin (ORBO-43 tube, Supelco, selected tests only), a cold-finger and finally silica gel housed in plastic cassettes (Figure 3.7). Silicone tubing was used to connect the sections of the sampling train. The cold-finger and silica gel were included to clean and dry the air

and provide the pump some protection from any damaging substances which may have passed through the filter and sorbent tube. In later tests using the newer and more efficient S2 heater, the diluted flue gas temperature reached over 60^{o}C and so further cooling was deemed necessary. To this end, a piece of cloth sitting in a beaker of water was draped over the sample probe immediately after exiting the flue to help cool the sample flow.

A) **B)**

Figure 3.7 Woodsmoke sampling apparatus.

A) Sampling probe and filter cassette (upper), and filter after sampling (lower).

B) Sampling train comprising filter cassette, ORBO tube, cold-finger, silica gel and pump.

Background samples were collected to assess any contamination arising from the dilution air, with no target compounds detected. Build-up of creosote in the tunnel resulted in very small amounts (<5% w/w) of some of the more volatile compounds

being detected in vapour-phase blanks, but were not subtracted from the test concentrations.

The potential for positive artefacts caused by gaseous adsorption onto the filters was assessed by analysing the backup filters used in selected tests. The total mass collected on the backup filter was typically less than 4% of the front filter. Only a small number of organic compounds were detected on the backup filters, generally at levels less than 1% of the front filter, although a small number of tests had levels of syringol, 4-methylsyringol, 4-ethylsyringol and 4-allylsyringol up to 6% of the front filter concentrations. As the levels were all very low, no corrections were made for gaseous adsorption on to the filters.

A summary of the woodheater emission tests is shown in Appendix B (Table B.1), followed by an example of the observations and calculations pro-forma used (Figure B.2).

3.2.2 Sample Extraction and Analysis

After sampling, filters were placed in a desiccator until constant weight (± 0.00020 g) was obtained on two consecutive readings; usually about 2-3 days. The filters were then stored in a freezer (-18^{o}C) in their cassettes until extraction, where they were allowed to thaw for 30 minutes before cutting into two or three sub-samples.

3.2.2.1 Organics by GC-MS

One of the filter portions (typically ½-¾) was extracted for gas chromatography-mass spectrometry (GC-MS) analysis using an ultrasonic bath and the following solvent scheme:

2 x 15 mL acetone	(5 mins each)
1 x 15 mL hexane	(5 mins)
1 x 15 mL dichloromethane (DCM)	(5 mins)
1 x 15 mL 1:1 DCM:acetone	(10 mins)

The solvent was decanted each time into a round-bottom flask, and the total extract was concentrated to approximately 2-3 mL using a rotary evaporator. The concentrate was then transferred to a vial with acetone rinsing, and concentrated to approximately 1 mL using a gentle stream of air (XAD-2 cleaned) while sitting the vial in luke-warm water (~30^{o}C). A portion of the extract was filtered into a GC-MS autosampler vial through glass wool in a pipette.

The resin from the XAD-2 sorbent tubes was transferred to a vial, and 10 mL of a 1:1 DCM:acetone mixture run into the vial through the tube and remaining glass wool plugs. The resin was then extracted ultrasonically for 10 minutes, the solvent transferred to a small round bottom flask, and the resin extracted for a further 10 minutes with 10 mL DCM. The extracts were combined and reduced in volume in the same manner as the filters.

Nonane and decane were used as internal and recovery standards, respectively. Decane recovery averaged 64 ± 22% (1σ, n = 40), and is considered a worst case recovery as it is more volatile than the vast majority of the target compounds.

Analyses were conducted at the Central Science Laboratory (CSL) University of Tasmania, using a Varian 3800 gas chromatograph coupled to a Varian 1200 triple quadrupole mass spectrometer, scanning from m/z 35-350 every 0.3 sec. Analytes were separated on a Varian VF-5ms column (25 m length, 0.25 mm diameter, 0.25 μm film) using helium as carrier gas. The GC oven was programmed from 60°C to 270°C at 6°C/min with a final 6 min hold. Identification and quantification of peaks was based on authentic standards where possible, and on mass-spectral libraries and interpretation of mass-spectra when standards were not available. Quantification was based on the area under the peak of a specific-ion (generally the base peak) for each target compound instead of the total-ion response in order to exclude possible co-eluting compounds. Compounds lacking standards were quantified by calculating the total-ion response from the quantification-ion, and then calculating the concentration using the total-ion response of compounds with similar structures and retention times.

Silylation of levoglucosan and other more polar compounds has been required in a number of previous studies in order to make them more amenable to GC analysis. An optimised method of silylation has been recently described and validated by Zdrahal *et al.*, showing a relative precision of 2-5% [37]. Levoglucosan was successfully quantified in this study, however, without derivitisation by selecting the m/z 60 base peak ion (Figure 3.8); the molecular ion (m/z 162) was extremely weak.

While the native compound showed poor peak shape, the data analysis software was still able to quantify it. Reducing sample handling and pre-treatment in this way minimises the potential for loss or contamination, while at the same time providing considerable time and cost savings. Silylation is still required when targeting some of the higher polarity compounds found in woodsmoke such as resin acids and sterols [25].

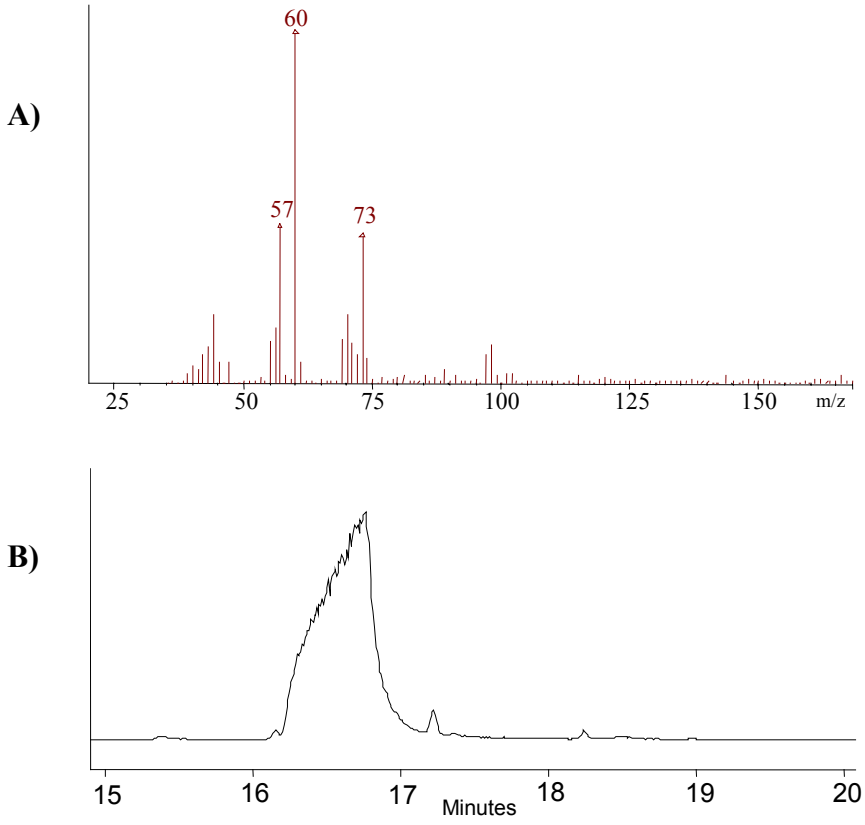

Figure 3.8 GC-MS analysis of levoglucosan.

A) Mass spectrum.

B) Selected-ion-chromatogram (m/z 60, 15-20 mins) of levoglucosan in woodsmoke extract.

3.2.2.2 PAHs by HPLC

A small number of particle-phase samples were analysed for PAHs by HPLC with fluorescence detection because it offers much greater sensitivity than the GC-MS

method used. Chrysene was not analysed by HPLC because it lacked an authentic standard (but could be identified from its mass spectrum), and BaP was not analysed by GC as its retention time was too long under the conditions employed.

A portion (typically ¼) of the selected filters was extracted in 15 mL 1:1 DCM:acetone for 30 minutes in an ultrasonic bath. The filter was removed and rinsed with DCM, and the extract evaporated to dryness under a gentle stream of purified air while sitting in luke-warm water (~30^{o}C). Acetonitrile (1 mL) was added, the vial ultrasonicated for 30 seconds, and the extract filtered through a 0.45 μm syringe filter into an autosampler vial. HPLC analysis of PAH extracts was conducted using the procedure outlined for ambient air samples in Chapter 2.2.3.

A total of 30 samples (including blanks) were analysed by both the HPLC and GC methods. The GC-MS method consistently gave slightly higher results, usually by about a factor of 2-3 (Table 3.3), which was most likely due to the different extraction solvents or the multi-point calibrations used for the HPLC analyses. Despite these discrepancies, the results given in Chapter 3.3.2 were from the GC-MS analyses to retain consistency, except for BaP which was taken from the HPLC analyses after multiplying the result by the average correction factor for BaA (2.5).

Table 3.3 Example comparison of PAH concentrations using HPLC and GC-MS.

	S1 closed		S2 open	
(mg/g PM)	HPLC	GC	HPLC	GC
Fluorene	0.005	-	0.001	-
Phenanthrene	0.042	0.103	0.007	0.014
Anthracene	0.010	-	0.002	-
Fluoranthene	0.011	0.032	0.072	0.214
Pyrene	0.012	0.038	0.080	0.382
Benzo(a)anthracene	0.004	-	0.043	0.096

3.3 Results and Discussion

A total of 36 emission tests were conducted using the three woodheater models. In order to assess the differences in emissions from each heater under varying airflow conditions, it was important to limit other sources of variability such as wood species and wood loading practices. It would however, be impossible to conduct tests encompassing all operating conditions encountered across the entire city.

3.3.1 Particle Emission Factors

The average overall burn-rates, particle emission factors (PEFs), and the proportion of the particle mass accounted for by the identified organic compounds from the three heaters are shown in Table 3.4. Heater S2 consistently had higher burn-rates than S1 and M1, indicating that this newer heater had a greater airflow for a given setting. In fact, heater S2 operated with a closed airflow had a similar burn-rate to S1 operated with a ½-closed airflow.

Table 3.4 Average overall burn-rates, particle emission factors, and percentage of particle mass accounted for by identified particle-phase organic compounds, mean ± 1σ.

	Number of tests	**Burn-rate** (kg/h)	**PEF** (g/kg)	**% mass accounted**
S1				
open	7	2.70 ± 0.64	13.5 ± 4.1	18 ± 5
½-closed	5	1.58 ± 0.76	30.6 ± 7.6	26 ± 7
closed	5	0.72 ± 0.20	33.6 ± 9.6	30 ± 8
S2				
open	5	3.52 ± 0.71	2.86 ± 1.60	19 ± 7
½-closed	3	2.15 ± 0.22	12.9 ± 7.3	28 ± 9
closed	5	1.42 ± 0.44	35.7 ± 9.6	54 ± 25
M1				
open	3	2.90 ± 0.21	2.50 ± 1.50	8 ± 3
½-closed	1	2.03	10.1	16
closed	2	1.06 ± 0.10	37.0 ± 3.7	18 ± 2

As expected, an inverse relationship between PEF and burn-rate is observed for all models tested (Figure 3.9), and is consistent with what is generally expected from woodheaters. The medium burn-rates (½-closed) using S2 and M1 produced PEFs intermediate between the two extremes, but for S1 they were not significantly different from the closed conditions, indicating that oxygen starved conditions are induced more easily with this heater. It also appears that the PEF reached a maximum at around 35-40 mg/kg when the burn-rate was less than 1.5 kg/h, irrespective of the heater model. The relative variability is fairly constant across all airflow settings (~30%), and there is little difference in the PEFs between the models for a given burn-rate. The main difference between the heater models seems to be the variation in the burn-rate at a given airflow setting.

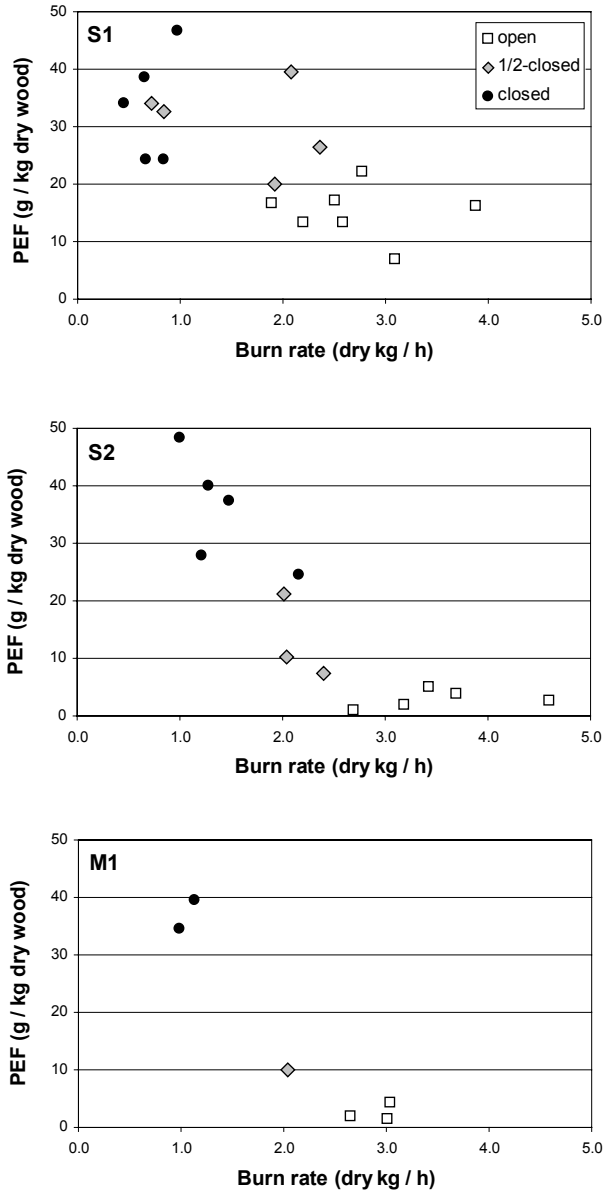

Figure 3.9 Variation in particle emission factor from woodheaters operated at different airflow settings, as a function of burn rate.

These emission factors are slightly higher than those reported by Gras and others under Australian conditions [8, 38]. Although it appears that none of these heaters would pass the current 4 g/kg emission limit (average of high-, medium-, and low-burns), these tests were not carried out in strict accordance with AS/NZS 4012 and

4013. Rather, the standards were used as a guide, with operating conditions altered to reflect commonly used operating conditions.

The proportion of the PM mass accounted for by the identified particle-phase compounds increased as the airflow setting was progressively closed (Table 3.4). While many of the differences are not significant at the one standard deviation level, the general trend holds for all heater models. The higher temperatures and greater oxygen availability encountered with the open tests presumably leads to a greater proportion of the organic compounds being burned, and would also lead to a greater vapour-phase distribution of semi-volatile organics. The remaining unaccounted mass is most likely composed of inorganic species, elemental carbon, and other high-molecular weight organic compounds which are either not extractable or not eluted under the chromatographic conditions employed.

3.3.2 Emission Factors of Organic Compounds

Typical chromatograms of vapour- and particle- phase woodheater emission extracts are shown in Figure 3.10. Detailed peak assignment for the particle-phase extract is shown in Figure B.3, Appendix B.

The emission factors for the organic compounds identified in this study are shown in Tables 3.5–3.7. Values are given as the mass of compound per kg of dry wood burned, presented as means with one standard deviation. Although emissions from woodheaters have in the past been assumed to not be normally distributed [39], standard deviations are reported here to at least give some measure of the variances

encountered. Compounds that were detected in only one test from each set do not have an associated standard deviation.

Table 3.7 includes a column indicating the quantification method used and the degree of confidence in identification, based on those quoted by Schauer *et al.* [20]:

a) positive, authentic quantitative standard, using response of selected ion.
b) probable library match, quantified using total-ion-current (TIC) of authentic standard with similar structure, molecular weight and retention time.
c) possible, identification using mass spectrum only and quantified using TIC of authentic standard with similar structure and molecular weight.

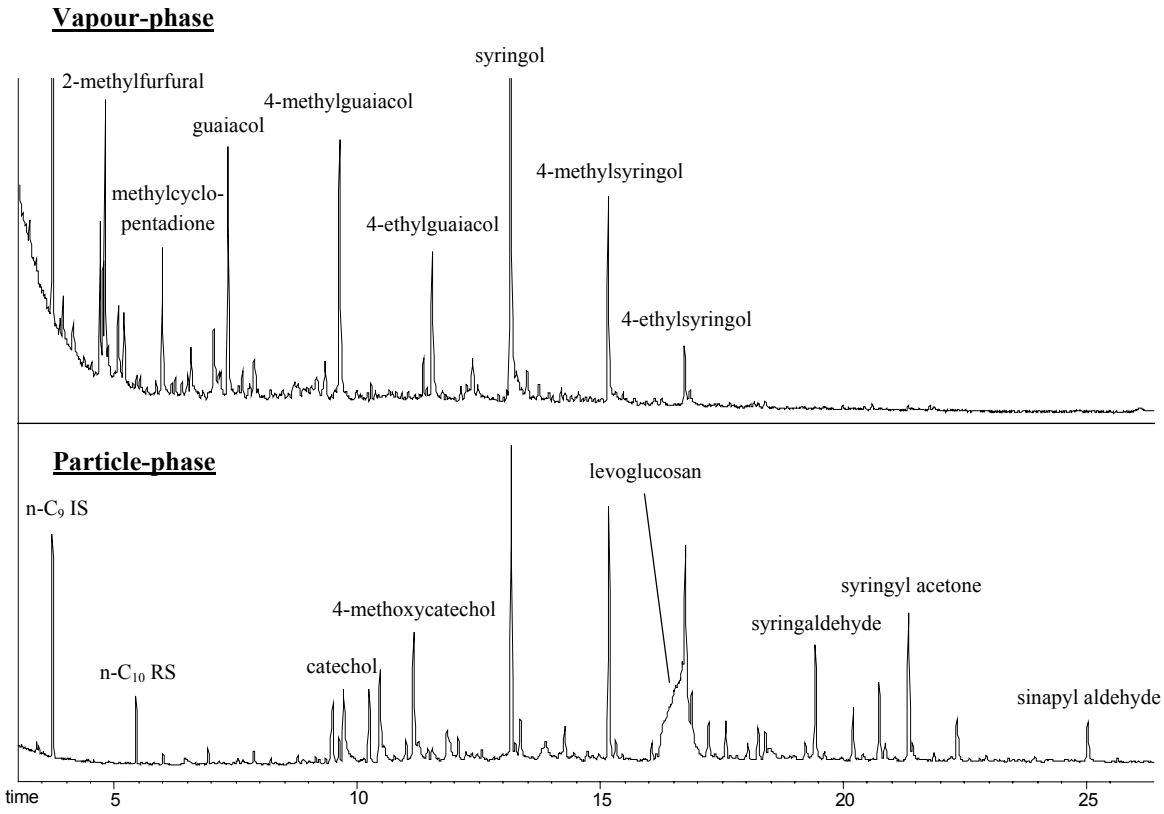

Figure 3.10 Total-ion-current gas chromatogram of vapour- and particle-phase organic compounds present in woodheater emissions.

Table 3.5 Organic emission factors from heater S1 operated with various airflows (mg/kg dry wood burned), mean ± 1σ. nd; not determined.

S1	OPEN		½-CLOSED		CLOSED	
	PARTICLE	VAPOUR	PARTICLE	VAPOUR	PARTICLE	VAPOUR
n-alkanes						
n-C20	0.17		0.57 ± 0.61		9.42 ± 11.9	
n-C21	0.14 ± 0.02		0.31 ± 0.14		6.41 ± 7.77	
n-C22	0.34 ± 0.09		1.73 ± 1.81		16.3 ± 2.0	
n-C23	0.40 ± 0.13		1.05 ± 0.95		20.2 ± 24.2	
n-C24	0.77 ± 0.50		1.19 ± 0.80		41.2 ± 45.9	
n-C25	1.09 ± 0.71		1.86 ± 1.30		45.9 ± 43.3	
n-C26	1.28 ± 0.99		1.11 ± 0.91		39.5 ± 33.4	
Furans						
2-methylfurfural	1.19 ± 1.97	35.4	0.56 ± 0.64	109 ± 43	0.51 ± 0.04	254 ± 168
5-hydroxymethylfurfural	343 ± 212		911 ± 750		1014 ± 453	
5-acetoxymethyl-2-furfural	6.44 ± 4.34	1.38	18.2 ± 15.8	2.07 ± 2.11	22.5 ± 8.23	4.49 ± 3.55
acetylmethylfuran	0.61	2.00		7.21 ± 3.86		16.9 ± 9.0
benzofuran		0.98		3.14 ± 1.17		3.39 ± 1.11
dimethylbenzofuran(s)		0.62		3.41 ± 1.70		5.53 ± 0.56
dibenzofuran	1.11	2.30	0.80	7.73 ± 0.52		5.05 ± 0.20
Benzaldehydes						
benzaldehyde	0.17	3.84		9.75 ± 3.54		4.91 ± 1.48
salicylaldehyde		18.7		35.9 ± 3.0		28.2 ± 11.5
p-hydroxybenzaldehyde	6.89 ± 2.73		12.5 ± 11.6		7.57 ± 5.81	
o- or m-methoxybenzaldehyde		0.37		3.50 ± 3.41		4.37 ± 1.34
cinnamaldehyde	0.29 ± 0.07	0.25	0.29	1.27 ± 0.41	0.56	1.23 ± 0.27
Guaiacols						
guaiacol	2.23 ± 4.35	24.5	2.19 ± 3.02	109 ± 74	2.02	205 ± 94
4-methylguaiacol	2.23 ± 3.87	7.39	1.90 ± 0.01	50.0 ± 39.3	7.66	80.0 ± 20.9
methylguaiacol B	0.56	1.24		7.82 ± 5.65		14.9 ± 3.6
4-ethylguaiacol	2.19 ± 2.60	5.55	7.56 ± 7.22	45.5 ± 35.2	8.38 ± 5.17	70.1 ± 1.5
4-propylguaiacol	1.66 ± 1.68	1.52	6.67 ± 6.21	11.5 ± 9.2	8.59 ± 3.85	21.2 ± 6.2
eugenol	0.81 ± 0.76		3.13 ± 2.14	3.19	2.33 ± 2.03	3.55 ± 0.19
cis-isoeugenol	0.72 ± 0.59		3.32 ± 2.71	1.08	3.41 ± 2.87	2.01
trans-isoeugenol	5.44 ± 4.00		22.6 ± 16.0		24.3 ± 17.7	1.98
vanillin	21.1 ± 10.3	0.63	49.6 ± 29.3		46.8 ± 11.4	2.09
acetovanillone	12.9 ± 6.4		37.9 ± 21.7		42.2 ± 6.5	0.53
guaiacyl acetone	32.1 ± 14.7		96.0 ± 48.1		115 ± 22	2.62
propionyl guaiacol	15.6 ± 11.3		41.1 ± 15.4		61.2 ± 50.2	
coniferyl aldehyde	10.7 ± 4.6		22.9 ± 11.4		25.2 ± 13.3	
Syringols						
syringol	183 ± 94	14.6	615 ± 305	72.5 ± 45.3	826 ± 159	128 ± 84
syringol B	2.85 ± 2.22		18.8 ± 15.3		23.3 ± 3.1	
syringol C	22.8 ± 14.1		94.9 ± 63.3		104 ± 21	
4-methylsyringol	151 ± 75	2.12	583 ± 301	20.9 ± 10.8	802 ± 155	48.8 ± 45.9
4-ethylsyringol	116 ± 54	0.98	398 ± 255	7.52 ± 3.53	696	19.4 ± 23.6
ethylsyringol B	1.19 ± 0.53		4.70 ± 3.12	0.46	7.44	0.67 ± 0.56
4-propylsyringol	16.3 ± 7.3	0.06	57.2 ± 33.1	0.28 ± 0.07	90.7 ± 23.4	2.63
4-allyl syringol	13.8 ± 6.9		40.1 ± 23.4		51.7 ± 26.2	0.77
allylsyringol B	8.40 ± 6.10		25.0 ± 10.3		36.1 ± 33.0	
allylsyringol C	26.3 ± 17.6		69.6 ± 34.4		113 ± 131	
syringaldehyde	91.0 ± 36.0		209 ± 112	0.21	225 ± 50	0.86
acetosyringone	47.0 ± 17.0		132 ± 65		165 ± 39	0.54
syringyl acetone	90.5 ± 35.9		244 ± 108		374 ± 56	1.25
propionyl syringol	5.23 ± 3.20		11.6 ± 3.1		22.8 ± 15.2	
sinapyl aldehyde	35.4 ± 13.6		78.3 ± 34.5		113 ± 66	

(Table 3.5 continued)	OPEN		½-CLOSED		CLOSED	
	PARTICLE	VAPOUR	PARTICLE	VAPOUR	PARTICLE	VAPOUR
Other Benzenes & Phenols						
phenol	3.43 ± 6.08	27.5	4.00 ± 6.57	78.0 ± 9.69	1.04	65.2 ± 29.3
o-cresol	3.56 ± 4.17	10.8	7.03	49.7 ± 13.4		50.7 ± 26.2
m- and p-cresol	2.96 ± 4.83	10.1	7.50 ± 10.7	49.2 ± 16.3	3.74 ± 1.67	45.3 ± 18.5
4-methoxyphenol	0.54		3.04	0.38		
3-methoxyphenol	10.7 ± 0.6		21.7 ± 17.8		21.4	
2-4-dimethylphenol	1.31 ± 1.46	2.30	3.22 ± 4.39	17.5 ± 8.2	1.23 ± 0.09	21.6 ± 7.6
2-6-dimethylphenol	0.28	0.60		3.38 ± 0.70		4.48 ± 1.42
3-5-dimethoxyphenol	0.80 ± 0.47	0.17	2.03 ± 1.11	0.53	2.29 ± 0.72	
catechol	142 ± 105		467 ± 364		384 ± 30	
4-methylcatechol	34.2 ± 33.6		156 ± 132		135 ± 10	
resorcinol	11.6 ± 3.9		21.4 ± 21.8		17.4	
hydroquinone	36.9 ± 22.6		84.2 ± 75.3		55.3 ± 32.8	
5-methylresorcinol	1.22		15.2		4.81 ± 3.18	
methoxycatechol	147 ± 86		576 ± 389		636 ± 101	
ethylbenzenediol	14.3 ± 17.5		65.0 ± 67.4		56.3 ± 4.3	
o-dimethoxybenzene	0.40 ± 0.19	0.37	1.72	1.47 ± 0.75		2.77 ± 1.01
1,2,3-trihydroxybenzene	111 ± 83		300 ± 237		197 ± 76	
dimethoxytoluene		2.30		12.0 ± 6.8	21.0	19.1 ± 2.5
propiophenone	0.27				0.17	
2'-hydroxyacetophenone	0.27 ± 0.13	1.16	1.31	4.17 ± 0.97		4.80 ± 1.12
4'-hydroxyacetophenone	2.42 ± 1.48		13.7		5.29 ± 0.99	
flopropione	1.57 ± 0.96		6.20 ± 4.24		8.12 ± 1.35	
3-phenoxyphenol	4.77 ± 1.87		11.3 ± 5.3		13.2 ± 3.6	
methylcyclopentadione	13.3 ± 20.8	8.18	39.1 ± 48.1	70.6 ± 43.6	38.3 ± 27.1	110 ± 26
PAHs						
naphthalene		4.91		23.4 ± 2.8		12.7 ± 3.4
acenaphthylene		0.81		8.41 ± 0.25		4.49 ± 1.92
acenaphthene		0.13		1.71 ± 0.01		0.87 ± 0.27
fluorene	0.34 ± 0.28	0.30	0.47 ± 0.01	2.08 ± 0.10	0.36	1.33 ± 0.11
phenanthrene	4.62 ± 3.31	1.21	9.05 ± 4.53	2.61 ± 1.83	4.78 ± 1.55	1.50 ± 0.09
anthracene	0.72 ± 0.34	0.11	1.30 ± 0.55	0.28 ± 0.13	0.97	0.20 ± 0.03
fluoranthene	1.66 ± 0.91		2.62 ± 1.17	0.09	1.65 ± 0.71	
pyrene	2.49 ± 1.47		3.93 ± 1.60		2.36 ± 1.41	
benzo(a)anthracene	0.58 ± 0.31		0.84 ± 0.31		0.66	
chrysene	0.74 ± 0.38		1.09 ± 0.47		0.77	
benzo(a)pyrene	0.50	nd	nd	nd	0.14	nd
methylnaphthalene A		0.90		6.98 ± 0.57		4.27 ± 0.38
methylnaphthalene B		0.60		4.71 ± 0.55		2.79 ± 0.41
dimethylnaphthalene(s)		0.30		2.31 ± 0.62		1.84 ± 0.18
trimethylnaphthalene(s)		0.14		1.77 ± 0.83		1.87 ± 0.62
1-naphthol			29.8		4.73	
2-naphthol	5.77 ± 4.32		18.0 ± 8.1		9.58	
biphenyl						
Sugars						
levoglucosan	738 ± 209		2026 ± 1017		3424 ± 1310	
1,4:3,6-dianhydro-β-D-glucose	76.5 ± 25.4		246 ± 150		272 ± 63	
115 sugar	55.9 ± 25.5		207 ± 241		305 ± 193	
Maltols						
maltol	20.8 ± 17.9	3.03	68.7 ± 55.4	12.7 ± 9.7	69.2 ± 33.2	18.8 ± 1.1
5-hydroxymaltol	69.1 ± 33.4		231 ± 154		218 ± 75	0.90
hydroxymaltol B	1.40 ± 1.21		6.22 ± 4.80		7.45 ± 4.47	0.77
hydroxymaltol C	2.39 ± 1.69		7.07 ± 3.23		11.5 ± 7.3	

Table 3.6 Organic emission factors from heater S2 operated with various airflows (mg/kg dry wood burned), mean ± 1σ. nd; not determined.

	OPEN		½-CLOSED		CLOSED	
	PARTICLE	VAPOUR	PARTICLE	VAPOUR	PARTICLE	VAPOUR
n-alkanes						
n-C20					6.51 ± 8.94	
n-C21					0.37	
n-C22			1.25		3.64 ± 3.02	
n-C23	0.05		1.23		1.84 ± 1.17	
n-C24			0.07		0.53	
n-C25					0.76	
n-C26						
Furans						
2-methylfurfural		149	0.51	545 ± 750	2.12 ± 2.28	150 ± 76
5-hydroxymethylfurfural	9.3 ± 12.0	358	392 ± 412	157 ± 189	1809 ± 1040	40.5 ± 38.7
5-acetoxymethyl-2-furfural	0.40	25.5	5.45 ± 7.86	70.1 ± 93.1	42.4 ± 34.1	10.2 ± 1.1
acetylmethylfuran		15.0		60.4 ± 83.3	1.29	16.2 ± 8.6
benzofuran		7.58		10.4 ± 13.6		1.91 ± 0.32
dimethylbenzofuran(s)		4.23		25.7 ± 35.5		6.66 ± 3.51
dibenzofuran		44.0		51.4 ± 68.1		5.11 ± 1.81
Benzaldehydes						
benzaldehyde		41.8		29.2 ± 37.0		4.42 ± 1.93
salicylaldehyde		122		161 ± 211		14.4 ± 16.4
p-hydroxybenzaldehyde	2.80 ± 3.27	3.69	7.00 ± 5.60		18.8 ± 13.3	
o- or m-methoxy benzaldehyde		12.0		29.6 ± 41.4		37.8 ± 44.3
cinnamaldehyde		6.84		14.4 ± 19.8	0.97 ± 0.90	1.76 ± 0.01
Guaiacols						
guaiacol	0.06	118	0.81 ± 1.07	730 ± 1015	19.5 ± 23.5	179 ± 90
4-methylguaiacol	0.07	45.7	0.21	406 ± 566	5.48	110 ± 48
methylguaiacol B		5.21		64.2 ± 89.3		18.9 ± 8.5
4-ethylguaiacol	0.11	42.9	1.68 ± 1.81	394 ± 549	21.1 ± 25.0	107 ± 46
4-propylguaiacol		11.8	2.52	150 ± 209	20.8 ± 24.9	39.9 ± 10.9
eugenol		4.59		30.6 ± 42.4	9.41	7.34 ± 0.01
cis-isoeugenol			0.92		6.33 ± 5.54	2.87
trans-isoeugenol	0.17		4.03 ± 4.12		41.8 ± 31.2	0.62
vanillin	3.65 ± 2.60	33.4	22.4 ± 18.0	45.8 ± 59.0	96.4 ± 55.0	8.75 ± 2.76
acetovanillone	2.79 ± 2.06	8.41	15.3 ± 13.8	5.22 ± 6.14	75.1 ± 40.4	1.35 ± 1.18
guaiacyl acetone	8.01 ± 5.90	20.9	47.0 ± 47.9	26.3 ± 33.5	199 ± 87	8.08 ± 2.47
propionyl guaiacol	0.71 ± 0.27	2.12	5.53 ± 4.97	0.43	60.4 ± 32.9	
coniferyl aldehyde	2.99 ± 0.28		10.3 ± 6.4		44.2 ± 30.5	0.86
Syringols						
syringol	6.47 ± 6.03	327	211 ± 266	1285 ± 1733	1257 ± 482	208 ± 56.6
syringol B	0.15		5.56 ± 7.95	4.10	50.9 ± 29.0	1.57
syringol C	2.11 ± 0.59	6.41	29.2 ± 35.1		203 ± 105	2.35
4-methyl syringol	6.98 ± 4.36	89.1	190 ± 216	430 ± 568	1194 ± 477	91.6 ± 43.9
4-ethyl syringol	5.83 ± 3.63	55.6	125 ± 137	198 ± 257	878 ± 510	42.4 ± 21.9
ethyl syringol B			0.58	7.62 ± 10.5	10.8 ± 5.5	1.41 ± 0.62
4-propylsyringol	1.04 ± 0.48	5.49	16.1 ± 16.2	12.4 ± 15.7	138 ± 79	3.19 ± 2.43
4-allylsyringol	1.41 ± 0.25		10.6 ± 8.7	0.86	73.1 ± 37.9	1.63 ± 1.56
allylsyringol B			4.48 ± 4.44		38.4 ± 16.3	
allylsyringol C	0.97 ± 0.49		3.40 ± 2.56		42.4 ± 32.2	
syringaldehyde	25.8 ± 2.7		97.4 ± 54.4	1.66 ± 1.74	400 ± 215	4.35 ± 5.12
acetosyringone	12.4 ± 2.9		53.2 ± 38.8		265 ± 133	2.36 ± 3.06
syringyl acetone	22.8 ± 5.7	1.35	113 ± 99		479 ± 177	5.68 ± 6.90
propionyl syringol	1.74 ± 0.54		4.24 ± 3.49		18.1 ± 6.8	0.90
sinapyl aldehyde	13.0 ± 1.9		36.5 ± 21.9		131 ± 89	3.54

(Table 3.6 continued)	OPEN		½-CLOSED		CLOSED	
	PARTICLE	VAPOUR	PARTICLE	VAPOUR	PARTICLE	VAPOUR
Other Benzenes & Phenols						
phenol	0.26	317	0.86 ± 1.14	415 ± 556	10.2 ± 14.0	65.5 ± 10.0
o-cresol		121		248 ± 340	17.1	44.8 ± 7.6
m- and p-cresol	0.21	144	0.83 ± 1.26	297 ± 406	17.8 ± 21.6	52.8 ± 4.34
4-methoxyphenol			0.87		5.55	1.36
3-methoxyphenol				42.8 ± 55.2	34.9 ± 27.4	4.32
2-4-dimethylphenol		45.1	0.45 ± 0.55	162 ± 224	8.07 ± 11.0	31.6 ± 8.5
2-6-dimethylphenol		6.37		24.7 ± 34.9		5.77 ± 2.24
3-5-dimethoxyphenol			0.86 ± 0.87	3.46 ± 4.54	7.25	0.67 ± 0.15
catechol	27.0 ± 33.7	136	193 ± 223	60.6 ± 73.9	814 ± 414	12.5 ± 14.5
4-methylcatechol	8.20 ± 10.2	4.64	57.9 ± 68.7	0.34	248 ± 132	3.62
resorcinol	5.11		16.5 ± 7.7		28.1 ± 19.8	
hydroquinone	12.8		41.7 ± 45.9		150 ± 100	
5-methylresorcinol	0.41		2.75 ± 2.95		7.21 ± 7.18	
methoxycatechol	9.15 ± 6.58	15.0	194 ± 235	75.5 ± 101	1255 ± 606	27.8 ± 28.8
ethylbenzenediol	7.22		23.9 ± 32.1		106 ± 60	
o-dimethoxybenzene		3.33		6.75 ± 9.26		3.28 ± 1.23
1,2,3-trihydroxybenzene	5.66		134 ± 200		531 ± 374	
dimethoxytoluene		11.2		93.0 ± 128		26.5 ± 10.7
propiophenone						
2'-hydroxyacetophenone		18.5		51.4 ± 70.2		10.2 ± 0.8
4'-hydroxyacetophenone	1.73		3.25 ± 2.24		9.69 ± 0.93	
flopropione	0.25 ± 0.08		1.89 ± 2.18		14.9 ± 7.7	
3-phenoxyphenol	1.28 ± 0.28		4.93 ± 2.89	0.61	23.4 ± 10.0	
methylcyclopentadione	0.52 ± 0.28	83.7	4.13 ± 6.05	514 ± 717	100 ± 141	126 ± 31
PAHs						
naphthalene		118		77.7 ± 101		7.05 ± 3.53
acenaphthylene		61.9		37.8 ± 50.3		2.31 ± 2.71
acenaphthene		6.88		7.91 ± 10.8		0.85
fluorene		16.1		12.3 ± 16.3		1.32 ± 0.82
phenanthrene	0.34 ± 0.40	97.3	1.82 ± 1.95	21.6 ± 24.5	5.54 ± 3.04	1.35 ± 1.50
anthracene		10.8	0.29 ± 0.21	2.22 ± 2.56	0.67	0.27
fluoranthene	1.59 ± 1.08	5.83	1.10 ± 0.28	0.32	1.36 ± 1.01	0.09
pyrene	2.91 ± 2.02	7.14	1.64 ± 0.24	0.30	2.27 ± 1.90	0.13
benzo(a)anthracene	0.67 ± 0.41		0.36 ± 0.06		0.34	
chrysene	0.83 ± 0.59		0.47 ± 0.07		0.67	
benzo(a)pyrene	0.55 ± 0.42	nd	0.39 ± 0.11	nd	0.22 ± 0.10	nd
methylnaphthalene A		22.5		29.4 ± 39.3		3.68 ± 0.32
methylnaphthalene B		15.7		19.8 ± 26.4		2.28 ± 0.32
dimethylnaphthalene(s)		4.42		12.5 ± 17.0		2.08 ± 0.30
trimethylnaphthalene(s)	0.12	2.48		11.8 ± 16.5		2.03 ± 0.46
1-naphthol	1.50	3.91	4.38 ± 2.99	1.64 ± 1.78		0.37
2-naphthol	2.51 ± 2.32	13.0	5.68 ± 3.75	0.75	10.7 ± 5.9	
biphenyl		75.3		86 ± 116		9.22 ± 0.76
Sugars						
levoglucosan	620 ± 320	26.7	1533 ± 872	5.76 ± 6.73	5216 ± 2843	86.5 ± 112
1,4:3,6-dianhydro-β-D-glucose	18.0 ± 13.2	57.3	105 ± 93	58.5 ± 72.6	456 ± 247	11.7 ± 8.9
115 sugar	26.9 ± 22.1		106 ± 95		570 ± 404	12.6
Maltols						
maltol	1.01	75.1	12.1 ± 19.0	180 ± 247	148 ± 128	39.2 ± 3.5
5-hydroxymaltol	1.05 ± 0.64	42.9	81 ± 105	22.8 ± 28.6	415 ± 313	7.85 ± 8.96
Hydroxymaltol B			1.55 ± 1.64		14.8 ± 13.9	
Hydroxymaltol C		59.2	1.91 ± 2.13	28.2 ± 34.5	17.5 ± 10.5	11.2 ± 12.6

Table 3.7 Organic emission factors from heater M1 operated with various airflows (mg/kg dry wood burned), mean ± 1σ. nd; not determined. See text for explanation of the identification code.

	code	OPEN		½-CLOSED		CLOSED	
		PARTICLE	VAPOUR	PARTICLE	VAPOUR	PARTICLE	VAPOUR
n-alkanes							
n-C20	a	0.21				0.18	
n-C21	b	0.31				0.32	
n-C22	a	0.89				1.83	
n-C23	a	1.24				0.82	
n-C24	a	1.92 ± 2.00				1.04 ± 0.92	
n-C25	b	4.03				1.29	
n-C26	b	1.90 ± 2.27					
Furans							
2-methylfurfural	b		14.7 ± 12.9	0.14	22.5	0.70 ± 0.52	126
5-hydroxymethylfurfural	b	3.62 ± 2.37	11.6 ± 8.0	221	0.00	1044 ± 348	
5-acetoxymethyl-2-furfural	b		1.08 ± 0.69	1.35	0.66	15.2 ± 6.6	4.95
acetylmethylfuran	c		1.41 ± 1.58		1.94		8.85
benzofuran	c		1.52 ± 1.30		2.28		2.98
dimethylbenzofuran(s)	c		1.05 ± 1.12		0.83		4.22
dibenzofuran	c		6.64 ± 4.60		8.19	15.1	5.24
Benzaldehydes							
benzaldehyde	a		4.99 ± 3.69		10.2		7.40
salicylaldehyde	a		14.7 ± 6.58		14.1		21.5
p-hydroxybenzaldehyde	a	0.39 ± 0.14	0.70 ± 0.28	4.60		6.68 ± 3.50	
o- or m-methoxybenzaldehyde	b		0.92 ± 0.67		0.49		2.60
cinnamaldehyde	a		0.63 ± 0.63		0.17	0.41	0.97
Guaiacols							
guaiacol	a		5.55 ± 4.99	0.09	16.0	1.90 ± 1.13	96.0
4-methylguaiacol	b		2.69 ± 1.70		8.77	2.91	56.0
methylguaiacol B	b		0.69 ± 0.72		8.71		9.64
4-ethylguaiacol	b		2.41 ± 1.57	0.10	7.24	5.10 ± 1.26	50.5
4-propylguaiacol	b		0.73 ± 0.58		2.62	4.20 ± 1.91	15.8
eugenol	a				0.92	0.80 ± 0.38	3.19
cis-isoeugenol	a					1.62 ± 0.33	1.29
trans-isoeugenol	a	0.04		0.84		14.2 ± 4.8	1.88
vanillin	a	0.21 ± 0.23	0.99 ± 0.59	5.80		29.1 ± 9.4	0.93
acetovanillone	a	0.27 ± 0.23	0.52 ± 0.02	4.11		27.7 ± 12.4	
guaiacyl acetone	b	0.55 ± 0.63	0.55	11.6		80.8 ± 30.0	1.43
propionyl guaiacol	c	0.13 ± 0.07		4.25		23.8 ± 2.1	
coniferyl aldehyde	a	0.19		2.37		8.71 ± 0.43	
Syringols							
syringol	a	1.45 ± 1.23	15.4 ± 9.86	46.1	36.2	435 ± 58.0	149
syringol B	b			0.70		8.82 ± 3.37	
syringol C	b	0.15		6.61		57.5 ± 26.8	
4-methylsyringol	b	1.08 ± 0.63	5.01 ± 4.70	46.9	13.2	399 ± 88	58.4
4-ethylsyringol	b	0.92 ± 0.49	2.22 ± 1.79	31.7		302 ± 106	23.4
ethylsyringol B	b					4.14	0.60
4-propylsyringol	b	0.13 ± 0.07	0.14	3.94	0.23	44.8 ± 21.7	1.04
4-allylsyringol	a			3.29		20.6 ± 4.5	
4-allylsyringol B	b	0.05		3.20		20.7 ± 5.4	
4-allylsyringol C	b	0.14 ± 0.09		16.5	2.91	99.0 ± 15.2	
syringaldehyde	a	2.48 ± 2.59	0.60	22.1		96.4 ± 17.2	
acetosyringone	a	1.66 ± 1.41		13.3		78.6 ± 22.4	
syringyl acetone	b	2.68 ± 2.66		29.7		167 ± 29	
propionyl syringol	b			2.09		7.97 ± 0.12	
sinapyl aldehyde	a	0.30 ± 0.19		8.06		27.5 ± 4.4	

(Table 3.7 continued)

	code	OPEN		½-CLOSED		CLOSED	
		PARTICLE	VAPOUR	PARTICLE	VAPOUR	PARTICLE	VAPOUR
Other Benzenes & Phenols							
phenol	a		30.3 ± 19.3	0.14	65.1	3.02 ± 2.81	67.6
o-cresol	a		7.48 ± 8.84		24.0	1.46 ± 1.18	43.4
m- and p-cresol	a		9.49 ± 11.1	0.12	25.3	4.68 ± 1.55	43.7
4-methoxyphenol	a					10.2	
3-methoxyphenol	a		3.03			18.5	
2-4-dimethylphenol	a		4.03 ± 4.87		11.0	2.70 ± 0.77	25.9
2-6-dimethylphenol	a		0.87 ± 0.92		1.53		4.24
3-5-dimethoxyphenol	a		0.23	0.13		1.52 ± 0.93	
catechol	a	0.53	3.01	69.4		292 ± 151	
4-methylcatechol	a			14.0		36.0 ± 15.2	
resorcinol	a	0.39 ± 0.29		11.4		13.2 ± 3.0	
hydroquinone	a	0.51 ± 0.19		27.6		80.2 ± 32.5	
5-methylresorcinol	a	0.05 ± 0.01		2.55		5.13 ± 1.19	
methoxycatechol	b	0.87 ± 0.38	0.31	39.8		401 ± 180	8.40
ethylbenzenediol	b			7.67		13.2 ± 4.62	
o-dimethoxybenzene	a		0.19				
1,2,3-trihydroxybenzene	a			39.6		105 ± 82	
dimethoxytoluene	b		1.76 ± 1.80		1.98		14.1
propiophenone	a						
2'-hydroxyacetophenone	a		1.51 ± 1.49				6.17
4'-hydroxyacetophenone	a	0.07 ± 0.05		1.14		3.11 ± 1.88	
flopropione	b			0.40		3.03 ± 2.13	
3-phenoxyphenol	c	0.18	0.65 ± 0.29	1.25		6.71 ± 2.60	
methylcyclopentadione	c		3.62 ± 1.44	0.36	16.85	27.8 ± .6	80.4
PAHs							
naphthalene	a		12.7 ± 8.7		24.9		17.4
acenaphthylene	a		1.71 ± 1.73		9.88		6.86
acenaphthene	a		0.41 ± 0.26		4.59		1.81
fluorene	a		0.50 ± 0.47		2.02		1.60
phenanthrene	a	0.06	4.67 ± 2.38	4.22	4.38	2.79 ± 0.92	1.46
anthracene	a		0.20	0.48	0.42	0.38	
fluoranthene	a	0.05 ± 0.03	0.62 ± 0.27	1.29		0.65 ± 0.23	
pyrene	a	0.07 ± 0.04	0.68 ± 0.27	2.01		1.00 ± 0.42	
benzo(a)anthracene	a	0.01		0.42		0.14 ± 0.03	
chrysene	b	0.02 ± 0.01		0.39		0.08	
benzo(a)pyrene	a	nd	nd	nd	nd	nd	nd
methylnaphthalene A	a		1.94 ± 2.14		5.99		5.24
methylnaphthalene B	a		1.36 ± 1.45		4.23		3.63
dimethylnaphthalene(s)	b		0.46 ± 0.53		1.19		2.04
trimethylnaphthalene(s)	b		0.20				0.38
1-naphthol	a	0.14	0.35	4.34		3.25	
2-naphthol	a	0.20 ± 0.03		5.37		4.87 ± 1.16	
biphenyl	a		9.32 ± 6.60		13.6		11.7
Sugars							
levoglucosan	a	196 ± 198	2.84 ± 1.08	779		2153 ± 10	
1,4:3,6-dianhydro-β-D-glucose	c	3.25 ± 3.55	9.71 ± 4.84	58.3	5.61	279 ± 26	10.8
115 sugar	c	4.81 ± 5.29		40.9		185 ± 43	
Maltols							
maltol	c		1.09	1.57	5.77	42.3 ± 25.0	14.0
5-hydroxymaltol	c	0.13	0.34	15.3		131 ± 68	
Hydroxymaltol B	c			0.09		4.00 ± 1.75	
Hydroxymaltol C	c			0.49		7.68 ± 3.5	

Just as the particle emission factors were influenced by the heater model and airflow setting, these factors also appear to influence the emission rates of most of the particle-phase organic compounds. It can be seen that there is a general trend of increasing particle-phase emission factors as the airflow is progressively closed, presumably because of the less efficient combustion conditions and lower temperatures encountered when operating with a closed airflow. The differences in organic emission factors between the airflow settings is smaller for S1 than either S2 or M1, consistent with the PEF results (Table 3.4). In terms of both PM and organic emissions, it appears that heater M1 is the least polluting model of the three tested.

The vapour-phase emission factors increased for heaters S1 and M1 as the airflow was closed, although there is little difference between ½-closed and closed for a number of compounds. Conversely, vapour-phase emissions tended to be greater (or remained constant) from heater S2 when operated with an increasing airflow. This difference probably reflects the complex effect of firebox temperature on combustion, and hence the relative quantity of compounds produced and destroyed. For example, a higher firebox temperature would lead to greater volatilisation of these compounds from the wood itself, with the higher airflow then quickly removing the vapours before they could combust. This is most likely the case early in the burn cycle, as total volatile-organic-compound (VOC) emissions have been found to be greatest within the first 10-30 minutes [8].

An overview of each of the chemical classes detailed in Tables 3.5–3.7 will now be presented, together with discussion on their suitability as tracers for woodsmoke.

n-Alkanes

The concentrations of the n-C_{20} – C_{26} alkanes were found to be low and highly variable, and collectively made up less than 0.5% of the total PM mass. As these compounds are found in emissions from other sources such as automobiles [40], and natural gas appliances [41], they are not specific tracers for woodsmoke and should be used cautiously in sourcing studies.

Furans

Substituted furan and furaldehyde compounds were found predominantly in the vapour-phase, although large amounts of 5-hydroxymethylfurfural were found in the particle-phase, comprising up to 5% of the total particle mass for the closed airflow tests.

Methoxyphenols

Substituted guaiacol and syringol compounds made up a large number of identified species. The most abundant compounds in this class were syringol, 4-methylsyringol, 4-ethylsyringol, syringaldehyde and syringyl acetone. Vanillin, acetovanillone, guaiacyl acetone and propionyl guaiacol dominated the particle-phase guaiacols, and there were large amounts of vapour-phase guaiacol, 4-methylguaiacol and 4-ethylguaiacol. The guaiacols were generally detected in greater quantities in the vapour-phase relative to the corresponding substituted syringols due to their higher volatilities.

Methoxyphenols, produced during the pyrolysis of lignin, have been suggested as specific tracers for woodsmoke, although there is evidence to suggest that their long-

term atmospheric stability may be limited [25, 42]. The low levels of methoxyphenols found in Launceston air (see Chapter 3.3.5) tends to confirm their atmospheric instability. It is therefore important that the stability of these compounds is investigated thoroughly if they are to be used as tracers in source apportionment studies.

Other Substituted Aromatic and Phenolic Compounds

Like the methoxyphenols, these compounds are also derived from the decomposition of lignin. Phenol made up 3-10% of the total mass of identified vapour-phase compounds, and other compounds with high emission rates were catechol, methoxy catechol, trihydroxybenzene, and the cresols. Significantly greater amounts of the benzaldehydes were emitted from heater S2.

Polycyclic Aromatic Hydrocarbons

This important class of compounds has been studied extensively from a multitude of combustion sources, including wood burning [39, 43]. Emission rates determined in this study were about the same or slightly higher than those found in previous studies burning Australian woods [8, 31, 44]. Levels of the particle-phase PAHs (BaA, Chrysene, BaP) were below 1.0 mg/kg wood burned, and were relatively consistent across the airflows. The high emissions of biphenyl, naphthalene, methylnaphthalenes and phenanthrene from heater S2 are noted in particular, consistent with reports that woodburning produces large amounts of the vapour-phase 2-3 ring (naphthalene - anthracene) PAHs [45].

Particle-phase PAHs were emitted from all three heaters at relatively constant amounts irrespective of the airflow setting. Conversely, heater S2 exhibited an increase in vapour-phase PAH emissions with increasing airflow. This can be explained by the temperature dependence on the rate of PAH formation, which increases with temperature up to 900^{o}C for the combustion of phenols and lignin [46]. These results are in contrast to a previous study undertaken in Australia [31], where emissions were higher under slower burning conditions. Yet, Morawska and Zhang note that while the total organic emissions decrease, the proportion of PAHs increases with increasing burn-rate [47].

The source diagnostic ratios Phen/Anth and FluA/Pyr found in woodsmoke were similar to those observed in Launceston ambient air (Figure 3.11, also see Figure 2.8 and Table 2.7 in Chapter 2.3.2), and there were no apparent differences between the airflow settings or heater models.

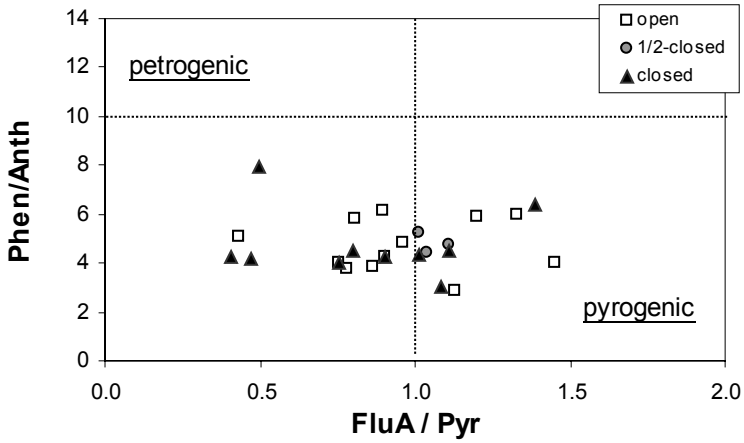

Figure 3.11 PAH source diagnostic ratios in particle-phase woodheater emissions (analysed by HPLC).

PAHs have been used in chemical mass balance (CMB) models in the past (e.g. [48, 49]), but because they are produced by many different sources and degrade during atmospheric transport, they cannot be reliably used as source specific tracer compounds (see Chapter 2). Their use for tracing woodsmoke in particular may be very limited, as photolytic degradation of PAHs is enhanced in the presence of methoxyphenols [50].

Levoglucosan

The single most abundant particle-phase compound associated with woodsmoke was levoglucosan (1,6-anhydro-β-D-glucose), comprising 5-16% of the total PM mass (see Table 3.8 below). Only trace amounts were found in the vapour-phase (< 4% w/w). Previous studies have found it to comprise a similar proportion of the particle mass [21, 22]. As woodburning is the only known source of levoglucosan, its abundance and high environmental stability make it an excellent general tracer for biomass combustion [28]. Its resistance to degradation is so great it has even been analysed in sediment cores to trace historical forest fires over the past 7,000 years [29].

Other sugars tentatively identified were 1,4:3,6-dianhydro-β-D-glucose, and possibly an acetate derivative of a sugar-like compound ("115 sugar").

Maltols

Compounds based on maltol (3-hydroxy-2-methyl-4-pyrone, Figure B.1 in Appendix B) were found partitioned between the particle- and vapour- phases depending on the airflow setting. These compounds have not been reported in

previous woodsmoke characterisation studies, but maltol itself has been identified in smoke flavourings for food [51]. They are probably produced from the breakdown of cellulose, and may also be specific tracers for wood burning, although their presence in emissions from other sources and atmospheric stability should be investigated.

3.3.3 Time Variation in Emissions

Changes in burn-rates during the tests were observed, with typical profiles shown in Figure 3.12. These profiles are generally what is expected, with the burn-rates of the open tests initially peaking before steadily decreasing until the end of the tests. The closed tests on the other hand show generally consistent burn-rates over the entire test. The ½-closed tests (not shown) showed a similar profile to the open tests, with a steady decrease over the entire test period.

One test each was conducted with heater models S1 and S2 with open and closed airflow settings in order to gauge the variation in emissions over time. For these tests, the filters and sorbent tubes were changed every 30 minutes, or 20 mins for S2 with an open airflow.

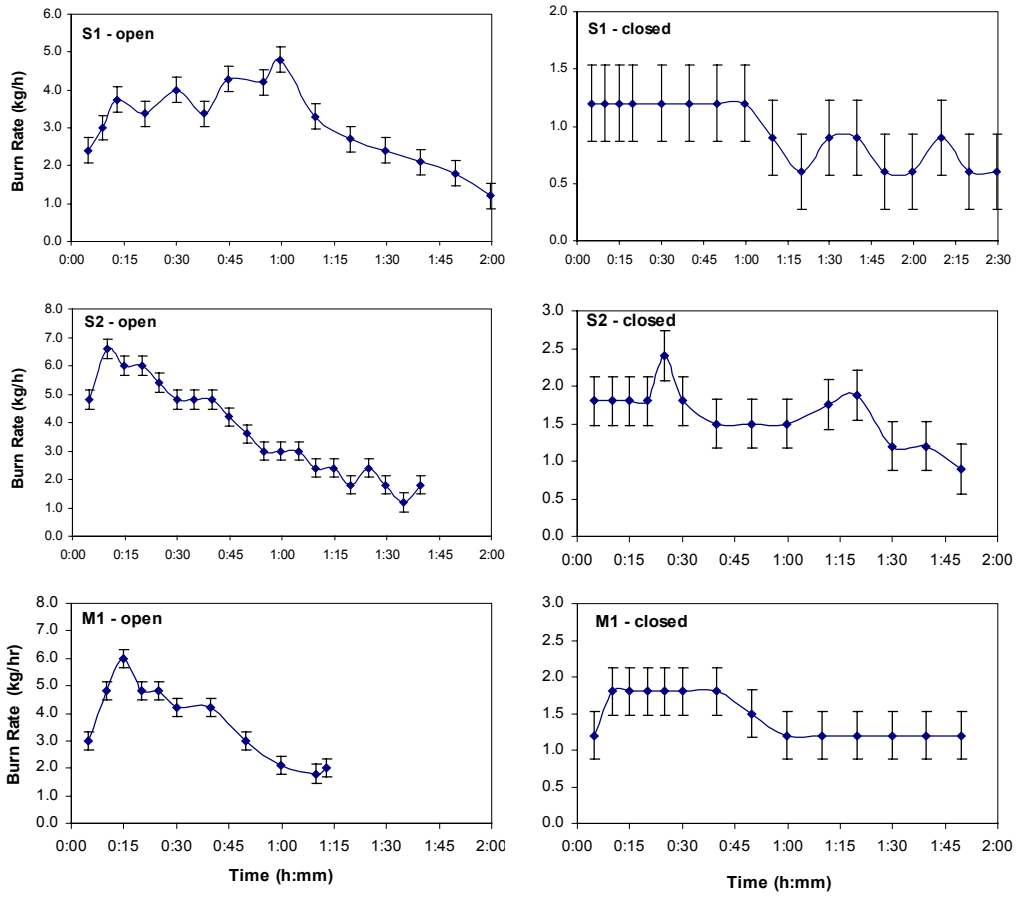

Figure 3.12 Typical time variation in the burn-rate of the three heaters operated with open and closed airflows.

Error bars show the error due to the 0.05 kg resolution of the scales.

It can be seen that the PEFs were considerably lower when the airflow was open than when closed at all periods during the tests (Figure 3.13). The highest emissions were recorded after the fuel was initially loaded; during this phase the wood is dried and many volatile and semi-volatile organics are driven from the wood. The subsequent drop in emissions was due to the reduction in the rate of volatile compound evolution, so that there was sufficient oxygen and it was able to reach the wood surface (primary combustion region).

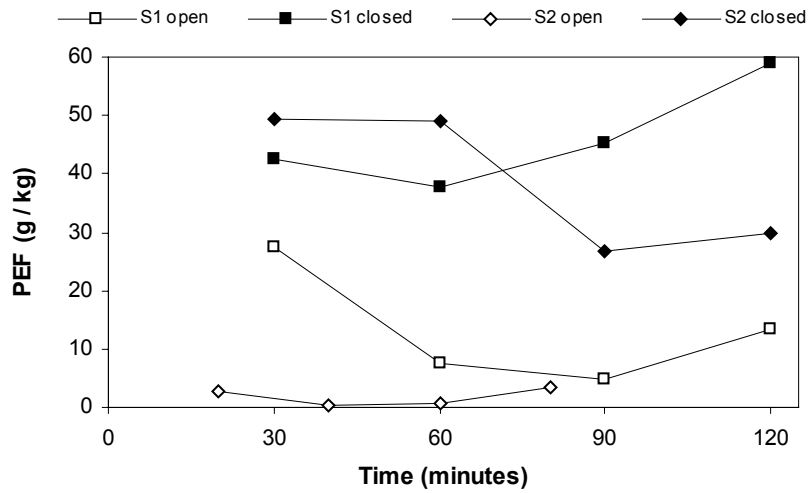

Figure 3.13 Variation in the particle emission factor (PEF) over time from heaters S1 and S2 operated with open and closed airflows.

These results are similar to those reported by Gras *et al.* [8], but are approximately a factor of two higher for the closed tests. They found that after an initial peak in emissions in the first 20-30 minutes, emission rates dropped and remained relatively low for open airflow tests, but climbed again and remained relatively high for the closed airflow tests.

Changes in the emission factors of particle-phase organic compounds over time from heater S1 follow the general trends shown in Figure 3.14. When operated with an open airflow, emission factors decreased throughout the test. When operated with a closed airflow, emissions initially increased before decreasing during the final period. The changes in vapour-phase emission factors tended to show a steady increase throughout the test for both airflow settings (Figure 3.15).

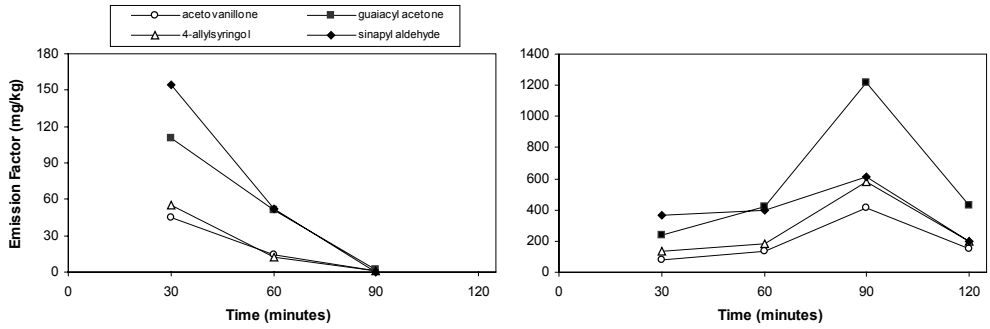

Open **Closed**

Figure 3.14 Time variation in the emission factors of selected particle-phase guaiacols and syringols from heater S1 operated with open and closed airflows.

The open 90-120 minute sample was lost during extraction.

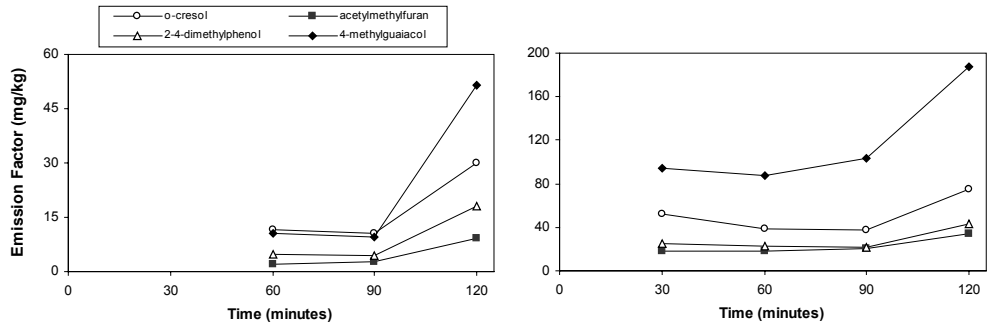

Open **Closed**

Figure 3.15 Time variation in the emission factors of selected vapour-phase compounds from heater S1 operated with open and closed airflows.

The open 0-30 minute sample was lost during extraction.

Unfortunately, due to the combination of short sampling time of each period and the inherently low emission rate for the open time series tests using heater S2, very low vapour- and particle- phase concentrations were found for each test period. As the majority of compounds were not detected at all, these results are not shown.

3.3.4 Organic Emissions Expressed as a Mass Fraction

While it is general practice to report woodheater emissions in terms of the mass of wood burned, the data must be converted to the mass fraction of total PM in order to be used in receptor models.

The mass fraction of the majority of compounds increased with decreasing airflow, in a similar fashion to their respective emission factors. Compounds whose relative proportion of total PM mass varies by at least a factor of two and with little overlap at the one standard deviation level are shown in Figure 3.16. As source apportionment studies generally focus on particulate matter only, results here have been restricted to compounds found predominantly in the particle-phase across all heaters and airflow conditions in order to remove the effect of the dilution-tunnel temperature on partitioning of semi-volatile compounds. There is an obvious trend of increasing proportions of organic compounds as the airflow was closed. The higher temperatures encountered in the open airflow tests appear to destroy a larger proportion of the particle-phase organic compounds. The differences are not as great for heater S1 as for S2 or M1, a similar situation to that seen for the PEF and organic emission factors. So not only do woodheaters operating with an open airflow produce less mass of particles per mass of wood consumed, they also produce less particle-phase organics per gram of emitted particulate matter. These differences could, in theory, be used to identify separate woodburning "sub-sources" ("complete" versus "incomplete" combustion, or "properly" versus "improperly" operated) in CMB source apportionment models.

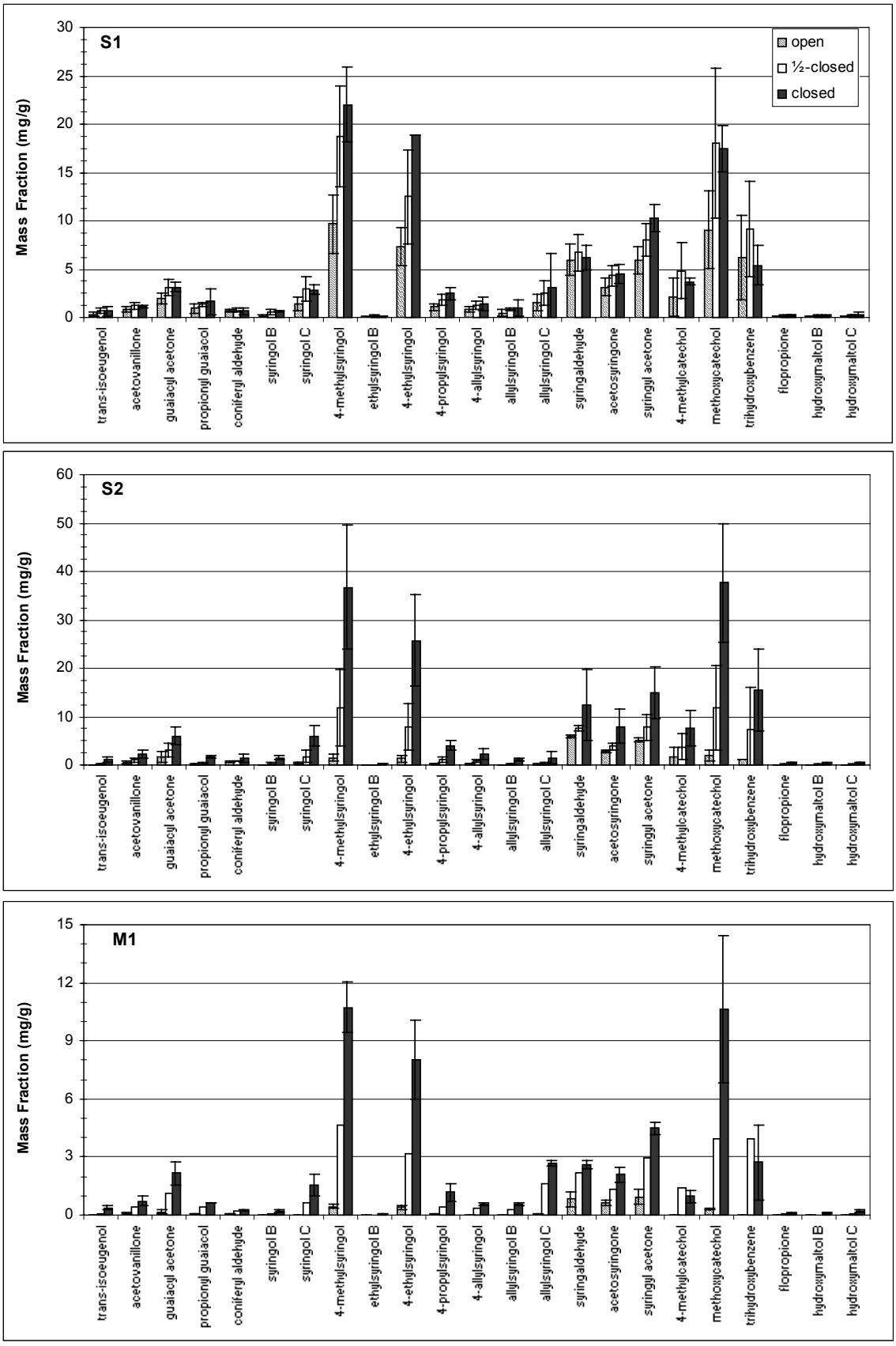

Figure 3.16 Variation in the mass fraction of selected particle-phase organic compounds with airflow setting, mean ± 1σ.

Although the mass fraction of many compounds increased with decreasing airflow, a number of compounds had relatively constant emissions irrespective of the airflow setting. For example, while the emission factors of propionyl syringol and hydroquinone increase greatly with decreasing airflow settings (1.7-19.2 and 12-160 mg/kg wood burned, respectively, for heater S2), their proportions relative to the mass of particles emitted remained reasonably constant (0.41-0.63 and 2.6-5.1 mg/g PM).

Similarly, the mass fraction of levoglucosan did not vary to a great extent with changes in airflow (Table 3.8). Heater S2 consistently produced a higher mass fraction, although the differences are around the one standard deviation level. There is thus a clear need for further testing to gauge the extent of the variation between the heater models. Despite the variations observed, the relative uniformity in levoglucosan emissions could simplify the determination of the biomass contribution to atmospheric pollution to a simple ratio calculation. Schauer *et al.* used a similar principle to determine the woodheater contribution to ambient benzene, ethene and acetylene in Fresno, California [20].

Table 3.8 Emission factor and mass fraction of levoglucosan in woodsmoke, mean ± 1σ.

	Emission Factor (mg/kg wood)			**Mass Fraction (mg/g PM)**		
	S1	**S2**	**M1**	**S1**	**S2**	**M1**
open	738 ± 209	620 ± 320	195 ± 198	52 ± 20	137 ± 50	67 ± 29
½-closed	2026 ± 1017	1533 ± 872	779	65 ± 19	123 ± 31	77
closed	3424 ± 1310	5216 ± 2843	2152 ± 10	95 ± 38	160 ± 91	58 ± 6

Other studies have found that the mass fraction of levoglucosan is relatively constant irrespective of the species of wood burned (98-168 mg/g organic carbon), although softwoods tended to exhibit slightly lower values (36-95 mg/g) [21, 22].

3.3.5 Woodsmoke Tracer Compounds in Launceston Air

3.3.5.1 Ambient concentrations

A total of 20 high-volume PM_{10} and six total-suspended-particle (TSP) samples collected in Launceston were analysed for the organic compounds present in woodsmoke. These samples were collected by DPIWE at Ti-Tree Bend using the apparatus described in Chapters 2.2.1.1 and 4.2.1, and extracted using the same solvent scheme as for the woodheater tests (Chapter 3.2.2.1).

The majority of compounds were not detected in any ambient air samples, and the few compounds that were consistently detected are listed in Table 3.9 (also see Figure 3.17). With the exception of levoglucosan, compounds that were detected had mass fractions very much lower than found in woodsmoke.

Table 3.9 Typical concentration and mass fraction of woodsmoke tracer compounds in Launceston ambient air.

	26 Jan 2003	**03 June 2002**	**19 June 2003**	**18 July 2003**	**19 Aug 2003**	**19 Aug 2003**	**Woodheater smoke**
	PM_{10}	PM_{10}	PM_{10}	PM_{10}	PM_{10}	TSP	S2 open
PM loading ($\mu g/m^3$)	48.4	37.8	56.7	74.5	43.5	41 [a]	na
Concentration (ng/m^3)							
propionyl guaiacol		0.29	1.69				na
syringol			2.97	3.27	2.79	7.42	
4-methylsyringol		0.30	1.18	0.92	0.48	1.21	
4-ethylsyringol			1.65			1.28	
allylsyringol C		1.64	3.73				
syringaldehyde		1.97	3.17	3.37	1.05	67.3	
acetosyringone		3.38	17.0	10.9	6.68	68.1	
syringyl acetone		1.72	3.51	4.65	1.71	95.6	
sinapyl aldehyde		3.42	2.54	9.49		11.0	
levoglucosan	440	5030	5862	7549	3408	4011	
Mass Fraction (mg/g PM)							
propionyl guaiacol		0.01	0.03				0.17 ± 0.09
syringol			0.05	0.04	0.06	0.18	1.37 ± 1.14
4-methylsyringol		0.01	0.02	0.01	0.01	0.03	1.52 ± 0.73
4-ethylsyringol			0.03			0.03	1.27 ± 0.61
allylsyringol C		0.04	0.07				0.23 ± 0.15
syringaldehyde		0.05	0.06	0.06	0.02	1.64	5.89 ± 0.37
acetosyringone		0.09	0.30	0.15	0.15	1.66	2.81 ± 0.19
syringyl acetone		0.05	0.06	0.06	0.04	2.33	5.15 ± 0.43
sinapyl aldehyde		0.09	0.04	0.13		0.27	2.96 ± 0.06
levoglucosan	9.1	133	103	101	78.4	97.8	137 ± 50

[a] TSP loading was estimated from DPIWE TEOM data (hourly averages) during the sampling period.
na: not applicable.

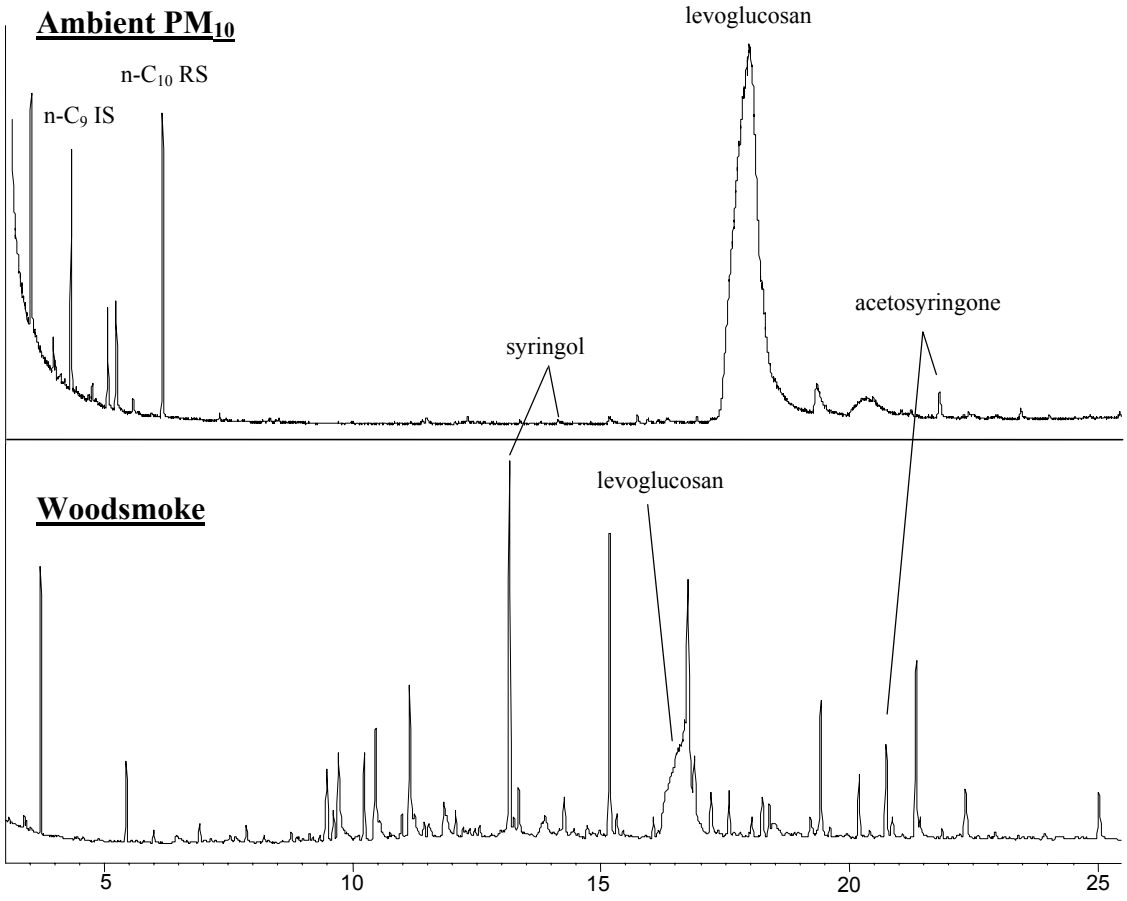

Figure 3.17 Comparison of gas chromatograms of extracts from Launceston PM_{10} (19/6/03) and particle-phase woodsmoke.
Retention times differ due to changes in instrument configuration.

There are three possible stages when losses of organic compounds from the ambient samples could have occurred:

1) atmospheric transport
2) high-volume sampling
3) storage before analysis

Differences between the methoxyphenol composition of woodsmoke and ambient samples collected using a high-volume sampler were also observed by Hawthorne *et al.* [52], though not to the extent seen in this study. They found that while the

vapour-phase compounds (e.g. lower molecular weight guaiacols and syringol) collected using polyurethane foam situated behind the filter were not degraded relative to woodsmoke, the particle-phase higher-molecular weight syringols were found to be degraded. By comparing samples collected during the day and at night, they concluded that photodegradation caused the majority of the observed losses, with the PM somehow enhancing the degradation. PAHs are known to degrade faster in the presence of methoxyphenols [50], which themselves were found to be susceptible to photolytic degradation. There is no reason at present to exclude the possibility of some other class of compounds degrading methoxyphenols in a similar fashion, and this may become apparent in future studies.

Sampling may have caused losses through "blow-off" of already collected particle-phase compounds, as high-volume sampling is known to enhance the partitioning of PAHs into the vapour-phase (Chapter 2.3.1.2). Though this is certainly a problem for the more volatile compounds such as guaiacol and syringol, it cannot explain why levoglucosan is present at similar mass fractions to that found in woodsmoke, while compounds with similar boiling points or which eluted well after levoglucosan from the GC, such as acetosyringone, have much lower mass fractions.

The type of filter material has been shown to play a role in degradation of PAHs (Chapter 2.3.1.2), with glass-fibre filters having greater "activity" than more inert materials such as PTFE. However, as both the woodsmoke and PM_{10} samples were collected using the same filter media, the filter is unlikely to have had a significant effect.

Losses from the TSP samples due to storage are likely to be small, as they were stored in the dark at -18^{o}C; the same storage conditions used for the woodsmoke samples, which showed little degradation up to 12 months in storage. However, the PM_{10} samples were not kept in the dark or the freezer while stored at the DPIWE laboratories (up to 2 years). Comparison of the PM_{10} and TSP samples collected in parallel on 19 August 2003 (Table 3.9) shows that differences in storage conditions accounts for a significant proportion of the losses from the PM_{10} samples. Even so, the mass fractions of the methoxyphenols in the TSP samples are still less than half those in woodsmoke.

Thus, it is likely that the majority of the losses of organic compounds from ambient samples observed in this study occurred during atmospheric transport and storage.

3.3.5.2 Quantifying the woodheater contribution to air pollution in Launceston using levoglucosan

The fact that levoglucosan was not degraded in the ambient samples was due to its high environmental resistance. Other researchers have also found levoglucosan at "expected" concentrations when methoxyphenol concentrations were depleted after atmospheric transport [25, 42]. This again highlights its potential as a stable, consistent tracer for atmospheric woodsmoke emissions.

Therefore, a semi-quantitative determination of the contribution of woodheaters to Launceston ambient air pollution can be made using the average levoglucosan mass fraction. To gauge the average mass fraction across the entire airshed would have required testing a much larger number of heater models, and was beyond the scope

of the present study. The lowest- and highest- case estimates of the levoglucosan mass fraction in woodheater emissions based on this study are about 50 and 200 mg/g (Table 3.8). While this range is far too high to be of any practical use in determining accurate source contributions, it is obvious that the lower limit of the average emissions must be at least the mass fraction of levoglucosan found in ambient PM (approximately 100-120 mg/g, Table 3.10). Linear regression of ambient levoglucosan concentration versus PM_{10} loading gives an estimate of 133 ± 22 mg/g PM averaged over the airshed (Figure 3.18).

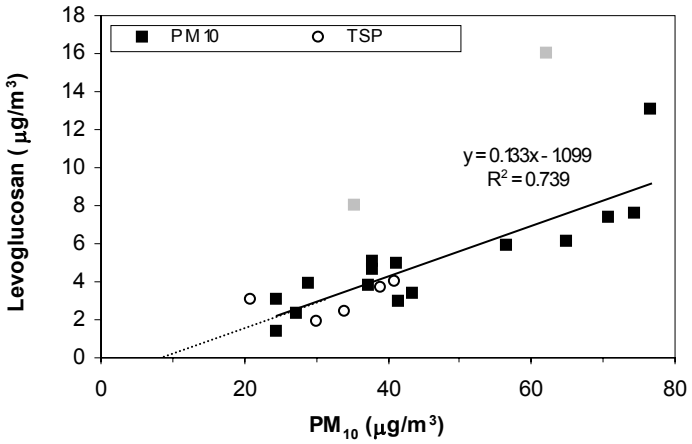

Figure 3.18 Determination of the "average" levoglucosan mass fraction in Launceston woodsmoke during winter by correlation with PM_{10} loading.

Outliers in grey were excluded from the least-squares fit.

An alternative estimate of the average levoglucosan mass fraction was gained from concurrent levoglucosan and radiocarbon (^{14}C) measurements made on thirteen PM_{10} and five TSP samples (see Chapter 4.3). Assuming that the radiocarbon "fraction contemporary" (f_C) was a direct measure of the woodheater contribution, the average mass fraction of levoglucosan in Launceston wintertime aerosols was

107 ± 33 mg/g PM (Table 3.10). This is not significantly different (1σ) to the 133 mg/g estimate from above.

Assuming the average mass fraction of levoglucosan in woodsmoke was 135 mg/g PM, the calculated relative contribution of woodheaters to Launceston ambient PM_{10} in winter was 77 ± 22% (Table 3.10). This compares well with the 95-100% woodsmoke contribution determined using ^{14}C analysis (see Chapter 4). The high cost of ^{14}C analyses has prevented it from being routinely used in atmospheric studies, whereas the relative ease of determination coupled to its tracer-like qualities may make levoglucosan a much cheaper and simpler alternative for quantifying woodsmoke contributions to air pollution.

Extrapolating the least-squares fit in Figure 3.18 to the PM_{10} (x)-axis, a "background" or "non-woodsmoke" input of about 8-10 μg/m^3 PM_{10} is evident. This is consistent with the 5-15 μg/m^3 measured by DPIWE during the summer months (November - February, see Figure 1.3). Wind-blown dust is expected to account for the majority of this, with automobile exhaust and industrial sources also contributing smaller amounts. This value is less than one half of that assumed for dispersion modelling (25 μg/m^3) undertaken in Launceston by Power (Chapter 1.2.3) [53]. Power also stated that further studies were required to quantify the contribution of "other" diffuse sources of PM_{10} in Launceston.

Table 3.10 Estimated contribution of woodheater emissions to PM_{10} and TSP in Launceston using levoglucosan as a woodsmoke tracer (assuming the average mass fraction of levoglucosan in woodsmoke was 135 mg/g PM).

Date	**PM_{10} loading** ($\mu g/m^3$) [a]	**Measured mass fraction levoglucosan** (mg/g PM)	**Estimated woodheater contribution to PM_{10}** (%)	**f_C** [b]	**"Average" levoglucosan mass fraction** (mg/g PM)
13 May 02	29.1	134.9	100	0.871	155
28 May 02	76.6	170.0	126	0.959	177
03 June 02	37.8	133.1	99		
14 June 02	62.2	257.6	191 [c]	0.920	280 [c]
24 July 02	35.5	226.1	167 [c]		
02 Aug 02	41.3	121.0	90	0.869	139
26 May 03	64.9	93.3	69		
19 June 03	56.7	103.4	77	1.008	103
08 July 03	38	122.7	91	1.022	120
09 July 03	70.9	104.0	77		
18 July 03	74.5	101.3	75	0.985	103
19 Aug 03	43.5	78.4	58	0.948	83
19 Aug 03 (TSP)	41	97.8	72	0.951	103
20 Aug 03	37.3	102.1	76	0.998	102
20 Aug 03 (TSP)	39	93.8	69	0.941	100
21 Aug 03	41.6	70.2	52	0.937	75
21 Aug 03 (TSP)	34	72.0	53	0.873	82
07 Sept 03	24.5	123.6	92	1.010	122
07 Sept 03 (TSP)	21	147.6	109	0.994	149
08 Sept 03	27.3	83.9	62	0.943	89
08 Sept 03 (TSP)	30	63.4	47	0.974	65
09 Sept 03	24.5	57.6	43	1.002	57
25 Jan 03	52.3	9.0	7 [c]		
26 Jan 03	48.4	9.1	7 [c]		
04-11 Nov 03 (TSP)	10	15.1	11 [c]		
16 Jan 04	15	0.0	0 [c]		
		Average	77 ± 22		107 ± 33

[a] TSP loading was estimated from DPIWE TEOM data for the sampling period.
[b] "fraction contemporary", see Chapter 4.3.
[c] result not included in average.

Emissions of levoglucosan from industrial combustion of wood products also needs to be addressed, as these sources contribute year-round and the combustion conditions employed may produce very little levoglucosan compared to woodheaters.

Samples collected in summer when Launceston was significantly impacted by bushfire smoke from Victoria (over 500 km to the north across Bass Straight, 25-26 January 2003) show lower than expected mass fractions of levoglucosan. While degradation during the long-range atmospheric transport may have played a part, long-range transport is unlikely to be the major cause of the lower levoglucosan levels in the bushfire smoke because a TSP sample collected during intermittent minor local bushfires also showed reduced levels (04-11 November 2003). It is more likely that the different fuel and combustion conditions encountered in bushfires caused the lower mass fractions observed. Emissions from foliar fuels (i.e. leaves and branches) exhibit much lower mass fractions of levoglucosan than from woodsmoke, at around 28-36 mg/g PM [24], presumably because of the very low cellulose content of leaves. Further work arising from this observation could establish an alternative bushfire marker species to levoglucosan, based on emissions from combustion of foliage.

As expected, levoglucosan was not detected in a summer sample not influenced by bushfire smoke (16 Jan 2004).

3.4 Conclusion

This study has presented emission factors for PM mass and nearly 100 organic compounds in both the vapour- and particle- phases from woodheaters operated with varying airflow settings. This is the first time to the authors knowledge that compounds based on maltol have been reported in woodheater emissions. The particle emission factors for all heater models increased significantly when the airflow setting was progressively closed, exhibiting an inverse relationship to the overall burn-rate. A similar trend was also observed for many of the organic compounds, possibly allowing differentiation between clean burning and "smokey" woodheaters in chemical mass balance models. However, the majority of the identified organic compounds were not detected in ambient samples, presumably because of photolytic degradation and losses during non-ideal storage conditions.

Contrary to the majority of identified organic compounds, the mass fraction of levoglucosan emitted was relatively constant across all airflow settings, but varied between heater models. Estimations of the "average" levoglucosan emission mass fraction in Launceston PM obtained using two different methods were in good agreement (107 ± 33 and 133 ± 22 mg/g PM), and a semi-quantitative estimation of the woodsmoke input to wintertime PM_{10} in Launceston was calculated at between 50-110%. For levoglucosan to be used as a reliable and accurate tracer for woodsmoke, further work must be undertaken to quantify emissions from an expanded range of woodheater models and operating conditions.

This study complements and adds to previous work undertaken using local Australian wood species and heater designs, and confirms that woodheaters are a major source of ambient pollution in Launceston during winter.

3.5 References

1. Sjöström, E. *Wood chemistry. Fundamentals and applications*. 2nd ed. **1993,** San Diego: Academic Press.
2. Tillman, D.A.; Rossi, A.J.; Kitto, W.D. *Wood Combustion: Principles, processes, and economics*. **1981,** New York: Academic Press, Inc.
3. Quraishi, T.A. Emissions from residential wood combustion appliances: A review of their origin, effects, nature, and measurement techniques, Centre for Environmental Studies, University of Tasmania, Hobart, **1984**.
4. Todd, J.J. Wood-smoke handbook: Woodheaters, firewood and operator practice, Environment Australia, **2003**.
5. Todd, J.J.; Gras, J.; Meyer, M.; Weeks, I.; Gillett, R.; Galbally, I.; Carnovale, F.; Joynt, R.; Hinwood, A.; Berko, H.; Brown, S. Technical report no. 4: Review of literature on residential firewood use, wood-smoke and air toxics, Environment Australia, Canberra, www.deh.gov.au/atmosphere, **2002**.
6. Kleeman, M.J.; Schauer, M.J.; Cass, G.R. Size and composition distribution of fine particulate matter emitted from wood burning, meat charbroiling, and cigarettes, *Environ. Sci. Technol.* **1999**, 33(20), 3516-3523.
7. Hueglin, C.H.; Gaegauf, C.H.; Kunzel, S.; Burtscher, H. Characterisation of wood combustion particles: Morphology, mobility, and photoelectric activity, *Environ. Sci. Technol.* **1997**, 31(12), 3439-3447.
8. Gras, J.; Meyer, C.; Weeks, I.; Gillett, R.; Galbally, I.; Todd, J.; Carnovale, F.; Joynt, R.; Hinwood, A.; Berko, H.; Brown, S. Technical report no. 5: Emissions from domestic solid fuel burning appliances, Environment Australia, Canberra, www.deh.gov.au/atmosphere, **2002**.
9. Dockery, D.W.; Pope, C.A.; Xu, X.; Spengler, J.D.; Ware, J.H.; Fay, M.E.; Ferris, B.G.; Speizer, F.E. An association between air pollution and mortality in six U.S. cities, *New Eng. J Med* **1993**, 329(24), 1753-1759.
10. McCrillis, R.C.; Watts, R.R.; Warren, S.H. Effects of operating variables on PAH emissions and mutagenicity of emissions from woodstoves, *J. Air Waste Manage. Assoc.* **1992**, 42(5), 691-694.
11. McDonald, J.D.; Zielinska, B.; Fujita, E.M.; Sagebiel, J.C.; Chow, J.C.; Watson, J.G. Fine particle and gaseous emission rates from residential wood combustion, *Environ. Sci. Technol.* **2000**, 34(11), 2080-2091.
12. Khalil, M.A.K.; Rasmussen, R.A. Tracers of wood smoke, *Atmos. Environ.* **2003**, 37, 1211-1222.
13. Ramdahl, T. Retene - a molecular marker of wood combustion, *Nature* **1983**, 306, 580-582.
14. Simoneit, B.R.T.; Rogge, W.F.; Mazurek, M.A.; Standly, L.J.; Hildemann, L.M.; Cass, G.R. Lignin pyrolysis products, lignins, and resin acids as specific tracers of plant classes in emission from biomass combustion, *Environ. Sci. Technol.* **1993**, 27(12), 2533-2541.
15. Standley, L.J.; Simoneit, B.R.T. Resin diterpenoids as tracers for biomass combustion aerosols, *J. Atmos. Chem.* **1994**, 18(1), 1-15.

16. Benner, B.A.; Wise, S.A.; Currie, L.A.; Klouda, G.A.; Klinedinst, D.B.; Zweidinger, R.B.; Stevens, R.K.; Lewis, C.W. Distinguishing the contributions of residential wood combustion and mobile source emissions using relative concentrations of dimethylphenanthrene isomers, *Environ. Sci. Technol.* **1995**, 29(9), 2382-2389.
17. Hawthorne, S.B.; Miller, D.J.; Barkley, R.M.; Krieger, M.S. Identification of methoxylated phenols as candidate tracers for atmospheric wood smoke pollution, *Environ. Sci. Technol.* **1988**, 22(10), 1191-1196.
18. Hawthorne, S.B.; Krieger, M.S.; Miller, D.J.; Mathiason, M.B. Collection and quantitation of methoxylated phenol tracers for atmospheric pollution from residential wood stoves, *Environ. Sci. Technol.* **1989**, 23(4), 470-475.
19. Rogge, W.F.; Hildemann, L.M.; Mazurek, M.A.; Cass, G.R. Sources of fine organic aerosol. 9. Pine, oak, and synthetic log combustion in residential fireplaces, *Environ. Sci. Technol.* **1998**, 32(1), 12-22.
20. Schauer, J.J.; Kleeman, M.J.; Cass, G.R.; Simoneit, B.R.T. Measurement of emission from air pollution sources. 3. C1-C29 organic compounds from fireplace combustion of wood, *Environ. Sci. Technol.* **2001**, 35(9), 1716-1728.
21. Fine, P.M.; Cass, G.R.; Simoneit, B.R.T. Chemical characterization of fine particle emissions from fireplace combustion of woods grown in the Northeastern United States, *Environ. Sci. Technol.* **2001**, 35(13), 2665-2675.
22. Fine, P.M.; Cass, G.R.; Simoneit, B.R.T. Chemical characterization of fine particle emissions from the fireplace combustion of woods grown in the Southern United States, *Environ. Sci. Technol.* **2002**, 36(7), 1442-1451.
23. Fine, P.M.; Cass, G.R.; Simoneit, B.R.T. Chemical characterization of fine particle emissions from the fireplace combustion of wood types grown in the Midwestern and Western United States, *Environ. Engin. Sci.* **2004**, 21(3), 387-409.
24. Hays, M.D.; Geron, C.D.; Linna, K.J.; Smith, D.; Schauer, J.J. Speciation of gas-phase and fine particle emissions from burning of foliar fuels, *Environ. Sci. Technol.* **2002**, 36(11), 2281-2295.
25. Nolte, C.G.; Schauer, J.J.; Cass, G.R.; Simoneit, B.R.T. Highly polar organic compounds present in wood smoke and in the ambient atmosphere, *Environ. Sci. Technol.* **2001**, 35(10), 1912-1919.
26. Elias, V.O.; Simoneit, B.R.T.; Pereira, A.S.; Cabral, J.A.; Cardoso, J.N. Detection of high molecular weight organic tracers in vegetation smoke samples by high-temperature gas chromatography-mass spectrometry, *Environ. Sci. Technol.* **1999**, 33(14), 2369-2376.
27. Simoneit, B.R.T.; Schauer, J.J.; Nolte, C.G.; Oros, D.R.; Elias, V.O.; Fraser, M.P.; Rogge, W.F.; Cass, G.R. Levoglucosan, a tracer for cellulose in biomass burning and atmospheric particles, *Atmos. Environ.* **1999**, 33, 173-182.
28. Fraser, M.P.; Lakshmanan, K. Using levoglucosan as a molecular marker for the long-range transport of biomass combustion aerosols, *Environ. Sci. Technol.* **2000**, 34(21), 4560-4564.
29. Elias, V.O.; Simoneit, B.R.T.; Cordeiro, R.C.; Turcq, B. Evaluating levoglucosan as an indicator of biomass burning in Carajás, Amazônia: A comparison to the charcoal record, *Geochim. Cosmochim. Acta.* **2001**, 65(2), 267-272.

30. AS/NZS 4013:1999 Domestic solid fuel burning appliances - Methods for determination of flue gas emission, Standards Association of Australia, Sydney, **1999**.
31. Zou, L.Y.; Zhang, W.; Atkiston, S. The characterisation of polycyclic aromatic hydrocarbon emissions from burning of different firewood species in Australia, *Environmental Pollution* **2003**, 124(2), 283-289.
32. Purvis, C.R.; McCrillis, R.C.; Kariher, P.H. Fine particulate matter (PM) and organic speciation of fireplace emissions, *Environ. Sci. Technol.* **2000**, 34(9), 1653-1658.
33. Hildemann, L.M.; Markowski, G.R.; Cass, G.R. Chemical composition of emissions from urban sources of fine organic aerosol, *Environ. Sci. Technol.* **1991**, 25(4), 744-759.
34. AS/NZS 4012:1999 Domestic solid fuel burning appliances - Method for determination of power output and efficiency, Standards Association of Australia, Sydney, **1999**.
35. AS/NZS 4014.1:1999 Domestic solid fuel burning appliances - Test fuels, Part 1: Hardwood, Standards Australia, Sydney, **1999**.
36. AS 4323.1:1995 Stationary source emissions. Method 1: Selection of sampling positions, Standards Australia, Sydney, **1995**.
37. Zdrahal, Z.; Oliveira, J.; Vermeylen, R.; Claeys, M.; Maenhaut, W. Improved method for quantifying levoglucosan and related monosaccharide anhydrides in atmospheric aerosols and application to samples from urban and tropical locations, *Environ. Sci. Technol.* **2002**, 36(4), 747-753.
38. Gras, J.L.; Keywood, M.D.; Ayers, G. Factors controlling winter-time aerosol light scattering in Launceston, Tasmania, *Atmos. Environ.* **2001**, 35, 1881-1889.
39. Hedberg, E.; Kristensson, A.; Ohlsson, M.; Johansson, C.; Johansson, P.-A.; Swietlicki, E.; Vesely, V.; Wideqvist, U.; Westerholm, R. Chemical and physical characterization of emission from birch wood combustion in a wood stove, *Atmos. Environ.* **2002**, 36, 4823-4837.
40. Schauer, J.J.; Kleeman, M.J.; Cass, G.R.; Simoneit, B.R.T. Measurement of emissions from air pollution sources. 5. C1-C32 organic compounds from gasoline-powered motor vehicles, *Environ. Sci. Technol.* **2002**, 36(6), 1169-1180.
41. Rogge, W.F.; Hildemann, L.M.; Mazurek, M.A.; Cass, G.R.; Simoneit, B.R.T. Sources of fine organic aerosol. 5. Natural gas home appliances, *Environ. Sci. Technol.* **1993**, 27(13), 2736-2744.
42. Simoneit, B.R.T.; Elias, V.O. Organic tracers from biomass burning in atmospheric particulate matter over the ocean, *Marine Chem.* **2000**, 69, 310-312.
43. Jenkins, B.M.; Jones, A.D.; Turn, S.Q.; Williams, R.B. Emission factors for polycyclic aromatic hydrocarbons from biomass burning, *Environ. Sci. Technol.* **1996**, 30(8), 2462-2469.
44. Zou, L.Y.; Hooper, M.A. Polycyclic aromatic hydrocarbon emission loads and profiles from burning of locally grown wood species in Victoria, Australia - Some pilot project results, *Clean Air* **2002**, 35(1), 35-38.
45. Khalili, N.R.; Scheff, P.A.; Holson, T.M. PAH source fingerprints for coke ovens, diesel and gasoline engines, highway tunnels, and wood combustion emissions, *Atmos. Environ.* **1995**, 29(4), 533-542.

46. Sharma, R.K.; Hajaligol, M.R. Effect of pyrolysis conditions on the formation of polycyclic aromatic hydrocarbons (PAHs) from polyphenolic compounds, *J. Anal. Appl. Pyrolysis* **2003**, 66(1-2), 123-144.
47. Morawska, L.; Zhang, J. Combustion sources of particles. 1. Health relevance and source signatures, *Chemosphere* **2002**, 49(9), 1045-1058.
48. Li, C.K.; Kamens, R.M. The use of polycyclic aromatic hydrocarbons as source signatures in receptor modeling, *Atmos. Environ.* **1993**, 27A(4), 523-532.
49. Harrison, R.M.; Smith, D.J.T.; Luhana, L. Source apportionment of atmospheric polycyclic aromatic hydrocarbons collected from an urban location in Birmingham, UK., *Environ. Sci. Technol.* **1996**, 30(3), 825-832.
50. McDow, S.R.; Sun, Q.; Vartiainen, M.; Hong, Y.; Yao, Y.; Fister, T.; Yao, R.; Kamens, R.M. Effect of composition and state of organic components on polycyclic aromatic hydrocarbon decay in atmospheric aerosols, *Environ. Sci. Technol.* **1994**, 28(12), 2147-2153.
51. Guillen, M.D.; Manzanos, M.J. Smoke and liquid smoke. Study of an aqueous smoke flavouring from the aromatic plant Thymus vulgaris L, *J. Sci. Food. Agric.* **1999**, 79(10), 1267-1274.
52. Hawthorne, S.B.; Miller, D.J.; Langenfeld, J.J.; Krieger, M.S. PM-10 high-volume collection and quantitation of semi- and nonvolatile phenols, methoxylated phenols, alkanes, and polycyclic hydrocarbons from winter urban air and their relationship to wood smoke emissions, *Environ. Sci. Technol.* **1992**, 26(11), 2251-2262.
53. Power, M. Air pollution dispersion within the Tamar Valley, Ph.D. Thesis, University of Tasmania, Hobart, **2001**.

Chapter 4

Radiocarbon Analysis of Air Pollution in Launceston

Chapter 4

Radiocarbon Analysis of Air Pollution in Launceston

4.1 Introduction

4.1.1 Introduction to Carbon-14

Carbon-14 analysis is best known as a method used to date historical artefacts, with the Shroud of Turin one of the most famous samples analysed [1]. The technique is used routinely around the globe in areas such as archaeology and the Earth Sciences, for example sedimentology and glaciology. Samples are analysed using either traditional β-counting or the more modern technique of accelerator mass spectrometry (AMS), and items up to 60,000 years old can be reliably dated. More recently the method has been applied to discern the origins of atmospheric pollutants.

4.1.1.1 Production and life-cycle

Carbon-14 is a radioactive isotope (hence the name "radiocarbon") formed primarily in the upper atmosphere by the interaction of cosmic rays with ^{14}N, and is rapidly oxidised to $^{14}CO_2$. The cosmogenic production rate is essentially steady, and atmospheric levels of ^{14}C are kept constant through a dynamic equilibrium between formation and decay. The proportion of ^{14}C is very low compared to the other

isotopes of carbon; the stable isotopes ^{12}C and ^{13}C make up about 99% and 1%, respectively, and the $^{14}C/^{12}C$ ratio is approximately 1.5×10^{-12} [2].

$^{14}CO_2$ is taken up by plants during photosynthesis, where it enters the food chain. All living matter therefore has a similar ^{14}C content as the atmosphere. Uptake of ^{14}C ceases when an organism dies, and levels slowly decrease through β-decay to ^{14}N, with a half-life of approximately 5730 years.

4.1.1.2 Variation in atmospheric ^{14}C levels

The amount of ^{14}C in the atmosphere is not constant over time, and small discrepancies between radiocarbon and dendrochronological ages (dating using tree rings) have been observed for the past few thousand years [3]. Calibration curves have been produced that show radiocarbon dates obtained from around 4000 BC are about 900 years too recent, while radiocarbon dates are 100 years too old for items dating around the 1500s. These variations are thought to arise from changes in solar activity and the earth's magnetic field, both of which influence the production rate. These long-term effects have been overshadowed by more recent human activities, however. The escalating use of fossil fuels in the late 19th and early 20th centuries diluted the atmosphere with carbon containing zero ^{14}C; fossil fuels are so old that all of the ^{14}C has decayed. This is termed the "fossil fuel" or "Suess" effect (Figure 4.1). Atmospheric nuclear weapons testing beginning in the 1950s produced massive amounts of ^{14}C through the interaction of neutrons with ^{14}N, in a similar fashion to the natural cosmogenic formation. Atmospheric levels of ^{14}C were nearly double the usual levels in 1964, and this is appropriately called the "bomb-effect". Mixing throughout the biosphere is gradually bringing levels back to pre-bomb

levels, with levels in the Northern Hemisphere in 2002 approximately "1.09 fraction modern" ($f_{M,}$ or 109 percent modern carbon, pMC) [4]. The Southern Hemisphere was not impacted to the same extent due to the smaller number of nuclear tests conducted in this hemisphere and because little cross-equatorial atmospheric mixing occurs [3, 5].

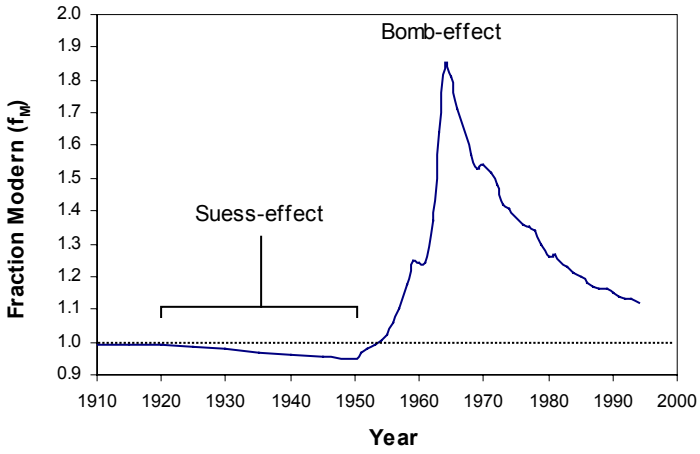

Figure 4.1 Atmospheric ^{14}C levels over the past century in the Northern Hemisphere. Adapted from Currie *et al.* [6].

4.1.2 Principle of Carbon-14 "Dating" of Air Pollution

Particulate matter (PM) and gaseous emissions from combustion sources contain essentially the same isotopic composition as the fuel burned. Thus by measuring the radiocarbon content of atmospheric pollutants it is possible to discriminate "modern" ("contemporary") and "fossil" carbon sources.

Wood and other biomass fuels contain "contemporary" levels of ^{14}C, similar to that found in the atmosphere. The exact levels will depend on the years of growth of the plant, as each tree ring contains levels of ^{14}C indicative of that year of growth only;

once grown, rings cease exchanging carbon with the atmosphere. Subsequent growing periods add further rings with ^{14}C levels indicative of those found in the atmosphere each ensuing year. Thus, a tree growing over several years will contain ^{14}C levels integrated over the years of growth, and if grown during the past 50 years will have ^{14}C levels greater than 100 pMC. The effect of this was demonstrated by Currie *et al.* who presented a table of radiocarbon "concentrations" in trees using the "equal-width ring" model as a function of years of growth and year of harvest [2]. For example, 10 year old trees harvested in 1970 and 1980 would be 162 and 134 pMC, respectively. A more accurate model for predicting the pMC of trees using a growth function for tree volume is given by Lewis *et al.* [7].

In contrast, fossil fuels contain organic materials that are so old that all the ^{14}C has decayed. These sources are sometimes referred to as containing "fossil" or "dead" carbon.

Measuring the ^{14}C content of atmospheric pollutants gives the "percentage modern carbon" (pMC) or "fraction modern carbon" (f_M; other terms commonly used in defining radiocarbon dates are discussed in Chapter 4.2.4). Dividing this value by the current atmospheric ^{14}C levels thus gives the "fraction contemporary carbon" (f_C), which by definition is a direct measure of the biomass contribution. It follows that the "fossil" contribution is $1 - f_C$.

The radiocarbon content of a variety of source types was verified by Hildemann *et al.* after a number of studies found f_M values in ambient PM higher than expected [8]. Not surprisingly, automobile exhaust was less than 6% modern, while meat

cooking, cigarette smoke, and woodsmoke were effectively 100% modern. Sources such as synthetic logs, road dust, tire wear, and brake lining dust contained intermediate amounts of ^{14}C, characteristic of their mixed fossil and contemporary composition.

A number of assumptions are required in order to apply radiocarbon dating to atmospheric pollutants. The technique can obviously only discriminate between two source "types"; contemporary (e.g. residential wood combustion, forest fires, biogenic sources) and fossil (e.g. automobile exhaust, coal and oil fired power stations) carbon sources. As a result, this method is mainly used to verify or complement other source apportionment methods [2, 9, 10]. Despite contemporary carbon having a multitude of potential sources, in many cases the binary system consisting of biomass burning and fossil fuel combustion is a good approximation of a local pollution scenario [9]. This is the case during winter in Launceston, where woodheaters and transport-related fossil fuel combustion are likely to be the main contemporary and fossil carbon sources to atmospheric aerosols, respectively.

4.1.3 Carbon-14 Measurement Methods

4.1.3.1 β-decay counting

The original method for determining the ^{14}C content of samples was by counting the number of β-particles emitted per mass of sample in a given time. "Modern" carbon ($f_M = 1$) decays with approximately 13.6 disintegrations per minute per gram of carbon [11]. Small samples and samples containing very little modern carbon must

consequently be analysed over a period of days or weeks to gain acceptable counting precision. Despite the increased sensitivity of gas proportional counters, which are able to analyse samples containing as little as 10 mg carbon, a large amount of shielding is required to minimise background interferences from natural radioactive sources and cosmic rays [12, 13].

4.1.3.2 Accelerator mass spectrometry

Accelerator mass spectrometry (AMS), developed in the late 1970s, is a relatively new technique for measuring ^{14}C. The greatest advantage with regard to atmospheric samples is its capability of measuring samples as small as 10 μg [14]. As it measures the number of atoms of each isotope and not the number of decay particles, AMS has much greater sensitivity than traditional β-decay counting techniques.

In AMS analysis, samples are usually converted to graphite and pressed into "cathodes" which acts as "targets" for a Cs^+ ion beam (sputter source). This produces negatively charged carbon species which are accelerated towards an injection magnet (Figure 4.2). Here the appropriate mass to charge (m/z) ratios are sequentially selected for the species of interest (^{12}C, ^{13}C, ^{14}C), which are then directed into the main accelerator. Here the negative ions are accelerated towards a positive terminal in the centre of the insulating tank where they are stripped of a few electrons using either a foil or gas stripper. The resulting positive ions (C^{3+}) are then accelerated away from the positive terminal, hence the name "tandem accelerator". The total energy of the particles is now in the order of 4-5 MeV. The particles are then selected for energy, momentum and velocity, and directed along "beam lines"

to Faraday cups capable of detecting the arrival of individual atoms. A detailed description of the components of ANTARES (Australian National Tandem Accelerator for Applied Research), the AMS used at the Australian Nuclear Science and Technology Organisation (ANSTO) is given by Smith *et al.* [15].

The acceleration, electron stripping and beam selection removes interfering species such as $^{12}CH_2$, ^{13}CH, and $^{11}BH_3$, while ^{14}N does not pose a problem because it does not form stable negative ions.

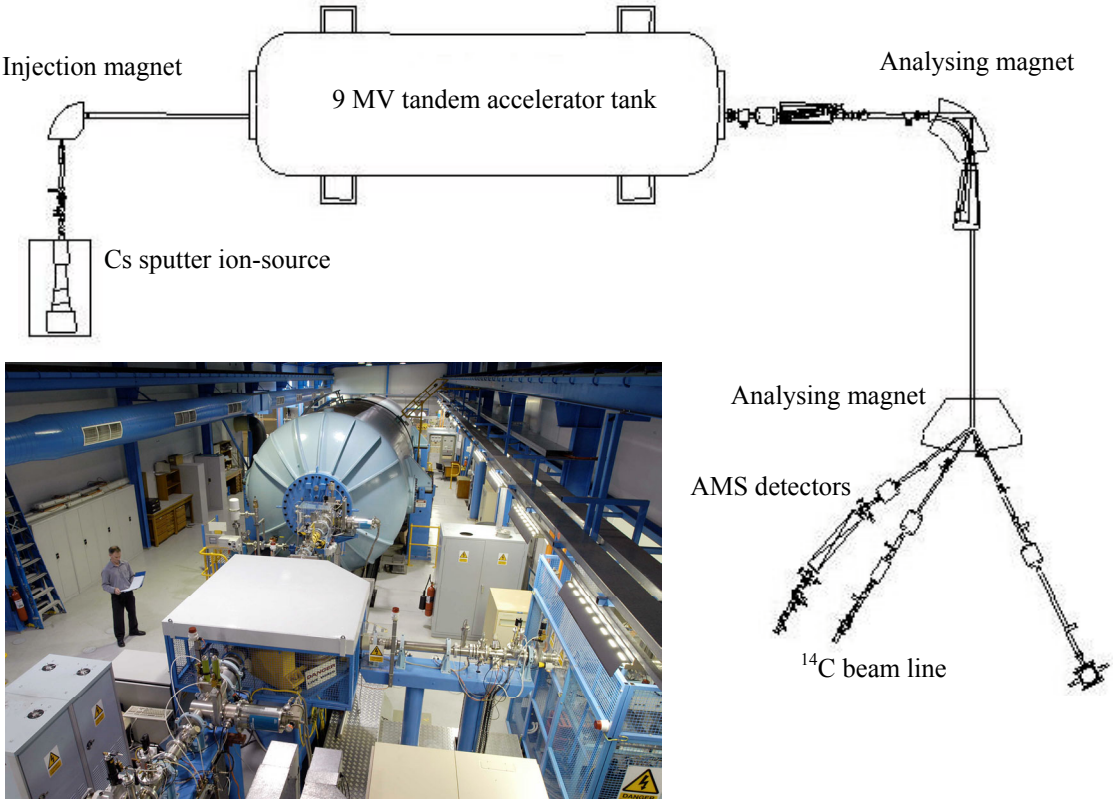

Figure 4.2 ANTARES, the AMS facility at the Australian Nuclear Science and Technology Organisation, Sydney.
Schematic adapted from Lawson *et al.* [16], photo courtesy of ANSTO Environment.

4.1.4 Early Carbon-14 Aerosol Studies

As with any new analytical method, ^{14}C analysis was quickly adapted from its conception in the late 1940s to many new areas, including that of discriminating biomass and fossil carbon sources. The first study to use radiocarbon as a biomass tracer in aerosols was undertaken in 1955, where 3-8 g carbon was collected in Los Angeles and Detroit [17]. Results showed that the sources were primarily fossil, between 12-26 pMC.

Development of low-level counting allowed sample sizes of 5-10 mg C to be analysed, greatly enhancing the potential of the technique. Currie and Klouda used mini-radiocarbon counting methods in conjunction with chemical tracers to determine source strengths in a number of US cities [18]. Not surprisingly, aerosols from urban regions (Los Angeles and Salt Lake City) were found to have a greater impact from fossil sources (23-28 pMC) compared to samples collected from the Utah desert (90 pMC).

A number of reviews on the evolution of radiocarbon dating to discriminate pollution sources have been published. Klouda *et al.* [19] present a background of the method using low-level counting methods, and summarised previously published studies. Currie and co-authors [13, 20] have reviewed the technique from its origins in 1955, through low-level counting in the 1970s, and then in light of the increased sensitivity delivered by accelerator mass spectrometry in the 1980s, and contemplate the current constraints and future direction of the method. Currie and Klouda have indeed been instrumental in developing the technique and are considered world leaders in the area.

4.1.5 Isotopic Heterogeneity of Atmospheric Aerosols - Evolution of the Method

Even from the beginning, it was anticipated that the various components or fractions of atmospheric aerosols would have varying isotopic compositions [18]. For example, the elemental carbon fraction is expected to have a greater influence from diesel emissions than would the polar organic extract, which would be expected to arise largely from biomass burning [6]. Due to the large sample mass required for β-decay counting, early studies only measured the ^{14}C content of the entire sample (or total carbon). With the increased sensitivity delivered firstly by low-level gas counting and then AMS, it became possible to make radiocarbon measurements on an increasingly larger number of chemical and physical fractions.

Selecting the appropriate size fraction of ambient PM may also be important. A comparison of radiocarbon analyses conducted on fine (PM_2) and total-suspended-particles (TSP) in Portland, Oregon, indicated that the fine fraction gave results which were more realistic because that fraction was impacted to a lesser extent by large diameter sources of contemporary carbon such as pollen and vegetative abrasion debris [12].

4.1.5.1 Elemental carbon

Elemental carbon (EC) is possibly the most important fraction of ambient aerosols because of its potential affect on the earth's climate by absorbing and scattering solar radiation. It is formed exclusively during incomplete combustion, and is very inert to degradation in the environment. Elemental carbon is also hard to define

chemically because it is essentially a continuum of condensed carbon compounds, and is usually operationally defined by the chemical or thermal separation method employed. These different types of EC may actually have significantly different chemical properties. As such, it is also known as black-, graphitic-, or soot- carbon.

A recent interlaboratory study investigated various methods for determining EC using the "urban dust" standard reference material, NIST SRM 1649a [6]. The ^{14}C content of EC was determined for each method, and was also measured in other chemical fractions. Results indicated that there was great heterogeneity between the various chemical fractions and between the different EC isolation techniques (Table 4.1). EC separated using thermal oxidation methods gave ^{14}C results similar to those obtained from PAHs (~95% fossil), and it was suggested that these methods were better at isolating a more resilient form of "soot" from combustion sources than the chemical-based methods.

Table 4.1 Interlaboratory comparison of ^{14}C speciation of various chemical fractions of SRM 1649a.

Fraction	**f_M**
Total Carbon	0.51 - 0.61
EC (thermal)	0.04 - 0.07
EC (chemical)	0.15
Polar	0.43
Aromatic	0.17
Aliphatic	0.02
Individual PAHs	0.04 - 0.09

Adapted from Currie *et al.* [6].

The certificate of analysis for SRM 1649a now includes the isotopic speciation shown in Table 4.1 as information values [21].

4.1.5.2 Organic carbon fractions

Solvent extraction followed by column liquid chromatography or normal phase HPLC are the usual methods for separating the various organic fractions for radiocarbon analysis [22, 23].

It is not surprising that the polar organic fraction tends to have a much higher f_M than either the aliphatic or aromatic fractions, indicative of the greater proportion of polar compounds emitted from biomass combustion. It would also be expected that the aliphatic organic compounds would derive mainly from petroleum products. In contrast, however, the low polarity fraction of atmospheric PM in Albuquerque, New Mexico, was found to be largely (60-80%) derived from residential wood combustion [22]. The organic solvents themselves have to be carefully analysed as they have been shown to contribute a large proportion of carbon to the overall blank [23]; the solvent blank contained up to 50% of the mass of the extracted analytes making the dichloromethane extracts of ambient samples and SRM 1649a unfit for analysis.

The increased sensitivity of AMS has now made it possible to measure the ^{14}C content of individual compounds. Polycyclic aromatic hydrocarbons (PAHs) are a class of compounds studied extensively throughout the past 30 years, primarily due to their carcinogenic nature (see Chapter 2). Separation and collection of sufficient mass of individual PAHs from PM and sediments for ^{14}C analysis is now possible using preparative capillary gas chromatography alone [24], or combined with normal phase HPLC to gain better baseline-resolved GC peaks [25]. Analysis of NIST SRM 1649a showed that while there was a large modern input to the total

carbon fraction, the elemental carbon and PAHs were primarily of fossil origin (Table 4.1). Similar trends in f_M values for the total organic, EC and PAH fractions were also seen in a number of sediment SRMs [25]. Radiocarbon analysis of PAHs in sediments around Stockholm, Sweden, showed that 17 ± 9% originated from biomass combustion, similar to an estimate (15.5%) derived from analysis of wood consumption records [26].

The evolution of radiocarbon analysis to PAHs in sediments inevitably led to its use in sediment cores to trace changes in inputs over time. Kanke *et al.* measured the f_M of PAHs in a sediment core taken from the moat surrounding the Imperial Palace, Tokyo [27]. The f_M of PAHs in the three sections of the core unexpectedly increased towards the surface, but without a chronology established no firm conclusions could be given for this trend. It is likely that radiocarbon studies of PAHs in dated sediments with high temporal resolution will be undertaken in the near future.

4.1.5.3 Volatile organic compounds

Volatile organic compounds (VOCs) are an important class of urban air pollutants directly involved with the creation of photochemical smog. Significant inputs of VOCs come from both biogenic (living plants) and anthropogenic (mainly transport-related) sources. Radiocarbon measurements are usually made on volatile organic compounds collected in canisters, as demonstrated by Klouda *et al.* [28]. They found that high blank levels had a considerable effect on the final measurements, and that the corrected f_M was not significantly different from zero. A thorough

review of isotopic analysis (C, H, Cl) applied to atmospheric VOCs has been published recently [29].

4.1.5.4 Ice cores

Historical profiles of atmospheric pollution, climate, and the radiocarbon bomb pulse can be gained by analysing $^{14}CO_2$ trapped in polar ice [30, 31]. The environmental stability and insolubility of EC makes it an ideal long-range pollution tracer in polar regions, and has been used in conjunction with other chemical measurements to identify sources of pollutants in Greenland ice [32].

4.1.6 Isotopic Fractionation and Carbon-13

While the three isotopes of carbon are chemically indistinguishable, kinetic effects can cause appreciable differences in the isotopic abundances in many biological and chemical systems [3]. Plants tend to uptake greater amounts of the lighter isotopes, meaning that ^{13}C is depleted relative to ^{12}C, and ^{14}C is depleted relative to both the stable isotopes. This depletion is termed fractionation, and it is taken into account by measuring the $\delta^{13}C$ value (delta carbon-13) relative to a standard (Vienna Pee Dee Belemnite), and is reported in units of ‰ (per thousand, or commonly referred to as per mil). Most trees and plants (so-called C_3 plants) have a $\delta^{13}C$ value around -25‰ (i.e. they are depleted by 25 parts per thousand relative to the standard) [33]. Grasses and other C_4 plants such as maize and sugar cane have values around -11 to -14‰ [34]. Atmospheric CO_2 has a value of -9‰, marine carbonates are around 0‰, and fossil fuels range in value between -25‰ and -40‰.

Kinetic isotopic fractionation may also occur during combustion processes. Soot obtained from the muffler of a petrol car has been shown to be depleted in ^{13}C relative to the petrol itself [35]. A slight depletion in ^{13}C was also observed in emissions from flaming combustion of oak (-0.7‰) and pine (-0.4‰) when compared to the original fuel [33], while combustion of a paraffin wax resulted in emissions that were enriched (+1.3‰). The authors concluded that ^{13}C itself could discriminate a two-source system. Indeed, $\delta^{13}C$ values have been used to identify sources of atmospheric pollutants [36], although the relatively large variation of values within source categories limits it usefulness. Using $\delta^{13}C$ values alone, automotive sources have been estimated to contribute 65-75% of PAHs in Malaysia, with woodsmoke contributing the remainder [37]. Using both ^{14}C and $\delta^{13}C$ potentially allows 3-source discrimination [13].

4.1.7 Previous Work Undertaken in Australia

Very little work has been undertaken in Australia using radiocarbon to source atmospheric pollutants; only one published study to date has been found [35]. In this study, researchers from the NSW State Pollution Control Commission, Sydney, and the Australian National University, Canberra, used liquid scintillation counting to determine the ^{14}C content of some source types and atmospheric PM from a number of sites across Sydney. Delta-carbon-13 values were also measured. The percent of "non-fossil" carbon varied from 33% in the city centre to 89% in a number of outer suburbs. The large non-fossil input in the suburban areas was attributed to backyard burning, while the much greater fossil input in the city was

expected to arise from automobile exhaust. The majority of ambient samples were slightly enriched in ^{13}C relative to the petroleum and vegetative samples tested.

4.1.8 Outline of Work to be Presented in this Chapter

This chapter will describe methodology for quantifying the woodsmoke contribution to Launceston air pollution by radiocarbon analysis using accelerator mass spectrometry. Samples collected by the Tasmanian Government (DPIWE) using borosilicate filters will be compared to samples collected in parallel using conventional quartz filters to validate the use of borosilicate filters in radiocarbon analyses. The potential impact of sample storage on the isotopic content of the organic carbon fraction will be investigated. Finally, the relative impact of fossil and contemporary carbon sources to Launceston PM_{10} will be presented.

4.2 Experimental

4.2.1 Air Sampling

Air samples were collected using high-volume samplers located at Ti-Tree Bend, Launceston (see Figure 2.3). The Department of Primary Industries, Water and Environment (DPIWE, Tasmanian Government) monitors 24-hour average PM_{10} levels using two high-volume samplers at this site. The samplers operate on alternate calender days (midnight-midnight) running at 70 m^3/hour using borosilicate glass-fibre filters (EPM 2000, Gelman). Samples for analysis were donated by DPIWE after gravimetric determination of the PM_{10} levels. A co-located total-suspended-particle (TSP) sampler was kindly made available for use by DPIWE (Figure 4.3). TSP samples were collected at 68 m^3/hour using quartz-microfibre filters (QM-A, Whatman). A number of summer samples were collected over a period of one week to collect sufficient sample mass because of low PM levels. TSP mass loadings were estimated from tapered-element-oscillating-microbalance (TEOM) PM_{10} data also collected by DPIWE at Ti-Tree Bend. The effect of particle-size was not expected to be significant because a previous study has shown that PM_{10} accounts for approximately 90% of TSP mass in Launceston during winter [38] (see figure 1.4).

Figure 4.3 TSP sampler with quartz filter in place after sampling.

The borosilicate filters were weighed at constant humidity before and after sampling by DPIWE with no other treatment, and stored in plastic snap-lock bags at room temperature. Prior to sampling, the quartz filters were pre-combusted at 600^{o}C for 24 hours to remove any residual carbon, wrapped in pre-combusted aluminium foil, and sealed in snap-lock bags. After sampling they were re-wrapped, sealed, and stored in a freezer at -18^{o}C.

4.2.2 Sample Pre-treatment & AMS Analysis

The size of filter required to give approximately 500 μg of carbon was calculated for each sample based on the PM_{10} loading and the lower limit of the reported organic carbon (OC) and elemental carbon (EC) content of Launceston ambient PM; 50% OC and 4% EC [39]; these estimations were reduced to approximately 35% OC and <1% EC for ambient PM_{10} based on the amount of carbon recovered from sample combustion. Filter areas of 4-6.25 cm^2 and 36 cm^2 were cut from a central region of each filter for the OC and EC tests, respectively.

Samples were treated to remove inorganic carbon (carbonate), which is generally geological in origin, by placing them in a desiccator with approximately 30 mL of concentrated HCl for 24 hours [23]. The acid was replaced with a beaker of NaOH pellets to neutralise the acidic fumes and desiccate the samples. The carbon remaining was termed "organic" carbon, although this also included EC. EC was isolated by thermal oxidation of the more labile organic material at 375^{o}C for 24 hours in a muffle furnace, as operationally defined by Gustafsson *et al.* [40].

The pre-treated samples were cut into thin strips (4-5 mm) and packed into combustion tubes that had been pre-cleaned by baking in a stream of oxygen (Figure 4.4). The tubes were placed under vacuum (<10^{-4} mbar) for 1 hour to remove adsorbed CO_2 and other gases before flame sealing.

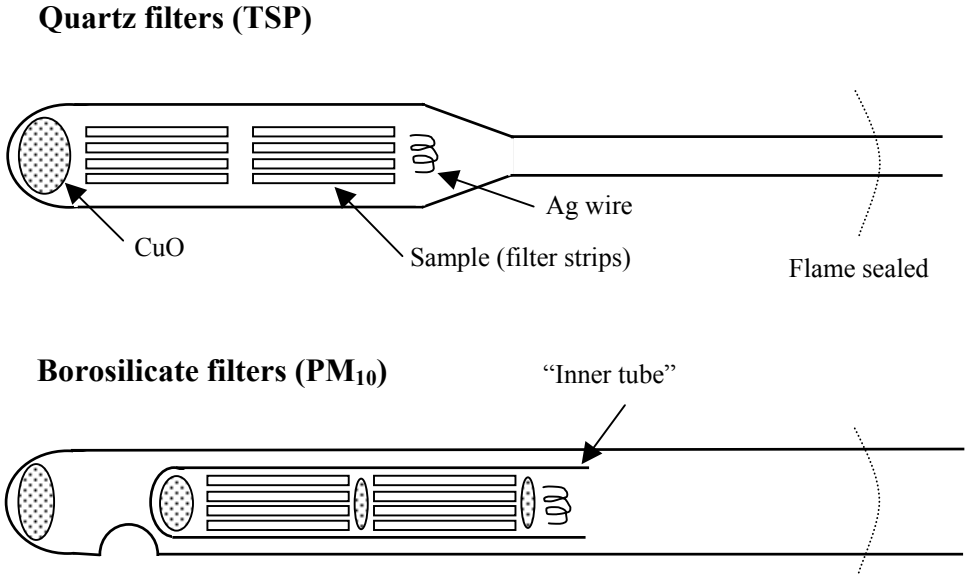

Figure 4.4 Combustion tubes for ^{14}C sample preparation.

Samples were combusted in the presence of CuO and silver wire (to remove sulfur) and the resulting CO_2 reduced to graphite, using the previously documented procedure [14, 16]. Briefly, the evolved CO_2 was collected under vacuum, separated from other combustion products with an ethanol-dry ice cold trap (-78°C), purified using a liquid N_2 cold-finger, and quantified by manometry in a known volume. Uncertainty in the measurement of mass was generally less than 2%. The CO_2 was reduced to graphite at 600°C using zinc with iron catalyst in the presence of excess hydrogen (Figure 4.5). ^{14}C and $\delta^{13}C$ analyses were carried out at the ANTARES facility, ANSTO, Sydney [41]

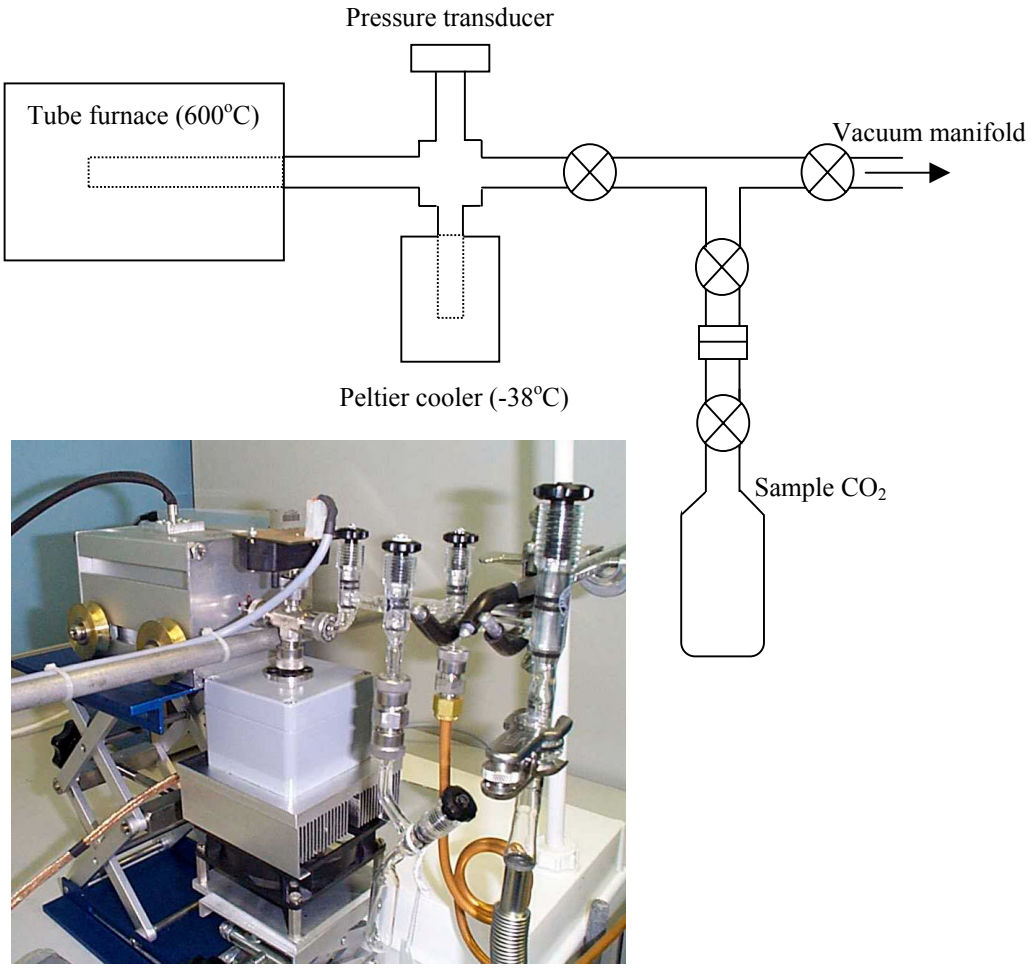

Figure 4.5 Graphitisation unit at ANSTO.
Schematic adapted from Hua *et al.* [14], photo courtesy of ANSTO Environment.

TSP samples (quartz filters) were combusted at 900^{o}C, as per the above procedure. However, the PM_{10} samples required a modified temperature program because of the low melting point of the borosilicate filters (~700^{o}C). The modified temperature program involved heating the sample from room temperature to 680^{o}C over 2 hours, holding at 680^{o}C for 8 hours in an attempt to maximise combustion before the filters melted, and a final ramp to 800^{o}C (held for 2 hours) to maximise combustion of any remaining available carbon. To protect the combustion tube from cracking during cooling (solidifying) of the borosilicate filters, PM_{10} samples were contained in an "inner-tube" (Figure 4.4), and additional CuO added to maximise contact with the filter strips.

4.2.3 Blank Correction

Blank borosilicate and quartz filter samples were processed with each batch of samples to determine the mass and f_M of the carbon blank associated with the filter material (Table 4.2). The blank values for OC were very similar to those determined by other researchers [4, 10].

Table 4.2 Fraction modern carbon and mass of carbon associated with filter blanks, mean ± 1σ.

	n	f_M	Mass carbon (μg)	% of ambient sample mass
Borosilicate				
OC	4	0.659 ± 0.067	74 ± 13	16 ± 6
EC	1	0.676	84	72 ± 3
Quartz				
OC	1	0.425	28 ± 3	7.3 ± 1.6
EC	2	0.443 ± 0.020	24 ± 3	68 ± 31

Full results are shown in Table C.3, Appendix C.

Ambient PM samples were corrected for both the mass and f_M of the appropriate filter blank, according to the following equations:

$$M_{(measured)}f_{M(measured)} = M_{(sample)}f_{M(sample)} + M_{(blank)}f_{M(blank)} \quad (4.1)$$

and $$M_{measured} = M_{sample} + M_{blank} \quad (4.2)$$

where M is the mass of carbon. Substituting Equation 4.2 into Equation 4.1 and rearranging gives [23]:

$$f_{M(corr)} = \frac{f_{M(measured)} - (\phi_{(blank)} \times f_{M(blank)})}{1 - \phi_{(blank)}} \quad (4.3)$$

where $$\phi_{(blank)} = \frac{mass\ blank\ carbon}{mass\ total\ carbon} \quad (4.4)$$

4.2.4 Units for Reporting Radiocarbon Results

There are a number of different ways of reporting radiocarbon results [34]. The radiocarbon activity is generally reported as "percent modern carbon" (pMC)

relative to a standard that contains modern carbon, and is equivalent to the "fraction of modern carbon" (f_M) multiplied by 100. The reference standard for radiocarbon measurements is an oxalic acid, NIST SRM 4990B (known as HOxI), and approximates wood grown in 1890 (Equation 4.5); the factor of 0.95 corrects for the fossil fuel effect in the year the standard was prepared (1950). Other terms such as "radiocarbon age" and "$\delta^{14}C$" are also used in various situations [34].

$$f_M = \frac{(^{14}C/^{12}C)_{sample}}{0.95 \times (^{14}C/^{12}C)_{SRM}} \quad (4.5)$$

As f_M values greater than unity have physical meaning because of the bomb-effect, a further correction can be applied and the result reported as the "fraction contemporary" (f_C):

$$f_C = f_{M(sample)} / f_{M(atmosphere)} \quad (4.6)$$

To determine the fraction of contemporary carbon in Launceston PM, a sample of woodsmoke was analysed and used as a reference for the current f_M. The use of woodsmoke from locally grown wood provides a time integrated f_M during the growing period, and one that is representative of the target species (woodsmoke). A dilution tunnel was used to collect woodsmoke (0.026 g) on a 37 mm diameter (10.8 cm^2) borosilicate filter (see Chapter 3.2.1), which was subsampled for OC (2.7 cm^2) and EC (8.1 cm^2) determinations. The woodsmoke sample had OC and EC contents of approximately 50% and 0.9%, respectively, and the blank corrected f_M of the organic carbon fraction was 1.040 (Table C.1, Appendix C). While the f_M of the EC fraction was slightly higher (1.049), the f_M of the OC fraction was used to correct the results of the OC fraction of the ambient samples.

4.3 Results & Discussion

The overall aim of this section of work was to measure the radiocarbon content of PM_{10} samples collected by DPIWE to quantify the contribution of woodheaters to wintertime air pollution in Launceston. Because these samples were stored under less than ideal conditions at the Government laboratories, there were concerns that losses of more volatile and reactive compounds may have occurred during storage. Consequently, it was proposed that analysis of the inert elemental carbon fraction of the samples would alleviate this problem.

4.3.1 Methodology for Sample Preparation of Aerosols Collected on Borosilicate Filters

Quartz fibre filters are the preferred collection media for aerosols when undertaking radiocarbon analysis. As noted previously, the filters employed by DPIWE for monitoring PM_{10} in Launceston were composed of borosilicate glass fibres, which have a relatively low melting point (~700^{o}C). This presented a problem during combustion at 900^{o}C in that the filters melted, with the possibility that some particles might become trapped in the molten glass and that quantitative combustion may not occur.

Another concern was there may be insufficient oxygen released from the CuO at temperatures below the melting point of the borosilicate. Brandova *et al.* showed that CuO starts releasing $O_{2(g)}$ at around 700^{o}C, with a maximum release rate at 850^{o}C [42]. Although CuO-C solid-solid oxidation occurs at lower temperatures

(300-600^{o}C), it is much slower than the O_2-C gas-solid oxidation at higher temperatures, and because the glass-fibre filters are a "depth" collection media, the solid-solid oxidation is of limited use.

Another problem associated with the molten borosilicate fibres occurred during cooling after combustion, where the molten borosilicate "wet" the sides of the combustion tubes, cracking them as it solidified (Figure 4.6).

Figure 4.6 Cracked 9 mm combustion tubes after combustion of borosilicate filters, compared with 6 mm tube before combustion.

A number of changes were implemented in order to alleviate the problems mentioned above. Firstly, the filters were held in an inner "test tube" contained inside a larger flame-sealed combustion tube (Figure 4.4), protecting the outer tube from cracking during cooling. Secondly, the samples were combusted using the modified temperature program detailed previously (held at 680^{o}C for 8 hours before ramping to 800^{o}C for "final" combustion, Chapter 4.2.2).

To confirm that the modified temperature program yielded complete sample combustion, TSP samples collected on quartz filters were collected in parallel to the PM_{10} samples. The results in Table 4.3 show, within experimental uncertainties, that there is no significant difference between the two combustion programs. Consistency in the mass, f_C and $\delta^{13}C$ of OC replicate analyses was observed for both PM_{10} and TSP samples, with one standard deviation averaging 25 μg C for mass (~6%), 0.014 for f_C (1.4%), and 1.0 for $\delta^{13}C$ (~4%).

Table 4.3 Comparison of sample preparation (combustion) methods; mass and isotopic composition of organic carbon fraction of parallel PM_{10} and TSP samples collected on borosilicate and quartz filters, respectively, mean ± 1σ.

	PM_{10}				TSP			
Sample Date	**n**	**mass C** (μg)	**f_C**	**$\delta^{13}C$** (‰)	**n**	**mass C** (μg)	**f_C**	**$\delta^{13}C$** (‰)
19/8/03	1	466	0.948	-24.3	1	492	0.951	-18.2
20/8/03	3	432 ± 12	0.998 ± 0.025	-24.6 ± 0.5	4	459 ± 29	0.939 ± 0.013	-25.3 ± 1.2
21/8/03	3	419 ± 25	0.937 ± 0.006	-23.9 ± 1.9	4	369 ± 32	0.874 ± 0.012	-25.4 ± 0.3
07/9/03	1	256	1.010	-24.6	1	232	0.994	-25.9
08/9/03	1	236	0.943	-25.4	1	352	0.974	-25.6

Full results are shown in Table C.1, Appendix C.

4.3.2 Carbon Content of Launceston Aerosols

As expected, the mass of OC in the radiocarbon samples (determined by manometry) had a strong linear correlation with PM_{10} loading (Figure 4.7), accounting for approximately 35% of total PM_{10} mass.

Conversely, the corrected EC mass was very low and relatively constant across all PM loadings. Whereas the amount of OC contributed by the blanks was quite small (5-20%), around 70% of the EC mass on both PM_{10} and TSP filters was contributed by the blank (Table 4.2). The high proportion of EC mass contributed by the blank resulted in nonsensical corrected f_C values much greater than unity (see Table C.2, Appendix C).

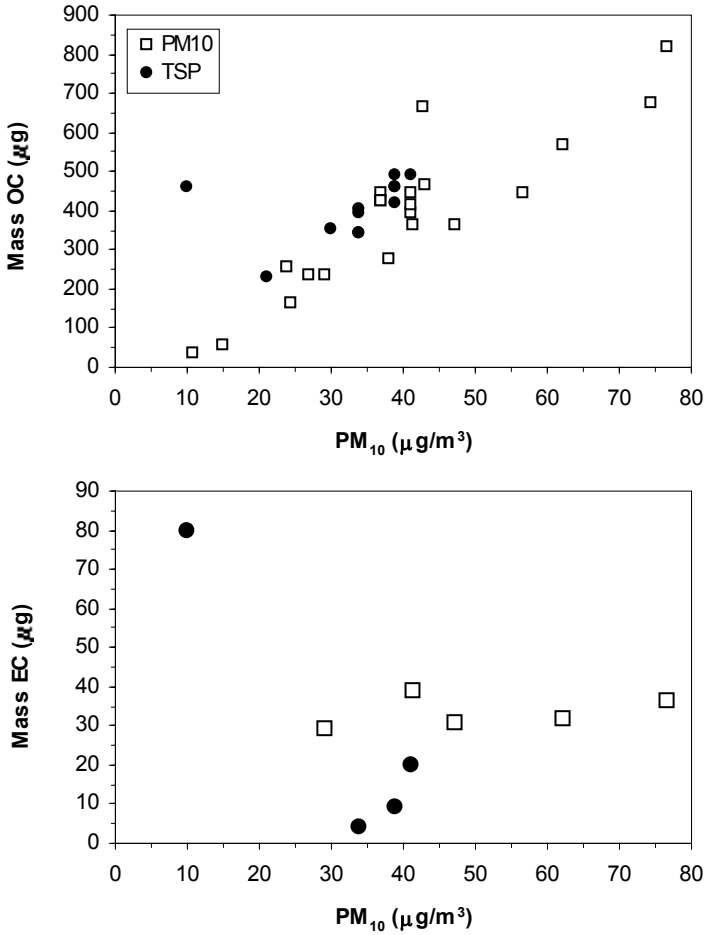

Figure 4.7 Blank-corrected mass of organic and elemental carbon in samples of Launceston PM used for radiocarbon analysis.
Measurement uncertainty is contained within the symbol size.
Filter size: OC 6.25 cm^2, EC 36 cm^2.

Although light absorption studies have previously suggested Launceston ambient PM contains 4-9% EC [38, 39], the thermal oxidation method employed here (24 hours at 375^{o}C [40]) has found that EC comprises <0.5% of Launceston PM. While an interlaboratory radiocarbon study using NIST SRM 1649a "urban dust" found that this method gave the best approximation for combustion derived EC (when compared with PAHs, Table 4.1, Chapter 4.1.5), it yielded the lowest EC to total carbon ratios of the 13 methods tested [6]. Thus it appears that this method of isolation is too severe in areas where fossil fuel combustion sources (diesel in particular) are not considerable sources of EC.

4.3.3 Assessing the Suitability of the Organic Carbon Fraction of Aerosols for Radiocarbon Analysis

As the attempt to utilise EC was not successful, focus of the study shifted to the OC fraction. Specifically, to confirm that PM_{10} filter storage conditions did not adversely alter the isotopic composition of the sample, at least for relatively short-term storage (<1 year). To this end, two TSP samples were "artificially aged" by subjecting them to ultraviolet light for three hours and heating in an oven at 55^{o}C for five days to simulate storage conditions at the Government laboratories. Comparison of the f_C and mass of OC shows less than 5% variation before and after "aging", demonstrating that storage of the PM_{10} filters was unlikely to result in sample loss or variation in the isotopic composition (Table 4.4).

Table 4.4 Results from accelerated "aging" of TSP samples to simulate storage conditions, mean ± 1σ.

Sample	Mass C (μg)	f_C
20/8/03	459 ± 29	0.939 ± 0.013
aged	492	0.939
21/8/03	369 ± 32	0.874 ± 0.012
aged	362	0.905

Full results are shown in Table C.1, Appendix C.

4.3.4 Quantifying the Woodheater Contribution to Air Pollution in Launceston

A total of 15 PM_{10} and 5 TSP samples collected during the winters of 2002 and 2003 at Ti-Tree Bend, Launceston, were analysed for radiocarbon. The $\delta^{13}C$ values were all clustered around –25‰, similar to those found in wood and other biomass sources [34]. The contemporary and fossil organic carbon components of PM_{10} calculated from the radiocarbon results are shown in Figure 4.8 (full results are shown in Table C.1, Appendix C). The contribution of fossil carbon shows little variation with PM_{10} loading and is relatively constant at around 1.0 ± 0.7 μg C/m^3, consistent with transport-related emissions in a small regional city such as Launceston. As the weight percentage of carbon in vehicle exhaust is approximately 60-70% [43], the total PM_{10} mass accounted for by fossil sources is expected to be only slightly above this value (~1.5 ± 1.0 μg/m^3). Conversely, a strong positive relationship exists between contemporary carbon and PM_{10} loading, with around 34% of total PM_{10} mass accounted for by contemporary carbon alone.

An extremely strong correlation was found between the contemporary and total organic carbon fractions of Launceston PM, indicating that about 97-99% of carbonaceous matter emanates from contemporary sources, most likely woodsmoke. These results are consistent with previous studies and provide very strong evidence that woodsmoke dominates automobile exhaust as the principle contributor to air pollution in Launceston during winter.

Additional TSP and PM_{10} samples collected during summer were also analysed for radiocarbon. The summer samples all have high contemporary organic carbon inputs (f_C = 0.925-1.106, Table C.1, Appendix C), however, as levoglucosan (a tracer for woodburning) was not detected in summer samples not impacted by bushfires (see Chapter 3.3.5), woodsmoke was unlikely to be a significant contributor. This implies that contemporary carbon sources other than woodsmoke are important during the warmer months of the year. Possible sources include windblown dust, biomass abrasion products [44, 45], and secondary PM formed from oxidation of volatile organic compounds (VOCs) emitted from vegetation [46]. Hidy *et al.* have designed an experiment to determine the contribution of secondary PM using radiocarbon analyses [47]. The slightly more negative $\delta^{13}C$ values obtained for the summer samples (–27.7‰ and –26.8‰) are also consistent with the $\delta^{13}C$ values of tree leaves (-27‰) compared to wood (-25‰) [34]. The contribution of secondary particles during winter would be expected to be small because of the lower solar intensity and reduced vegetative VOC emissions at the colder temperatures. Windblown dust is also likely be a small contributor during episodes of high PM_{10} in winter because these periods are usually associated with calm atmospheric conditions and very little wind.

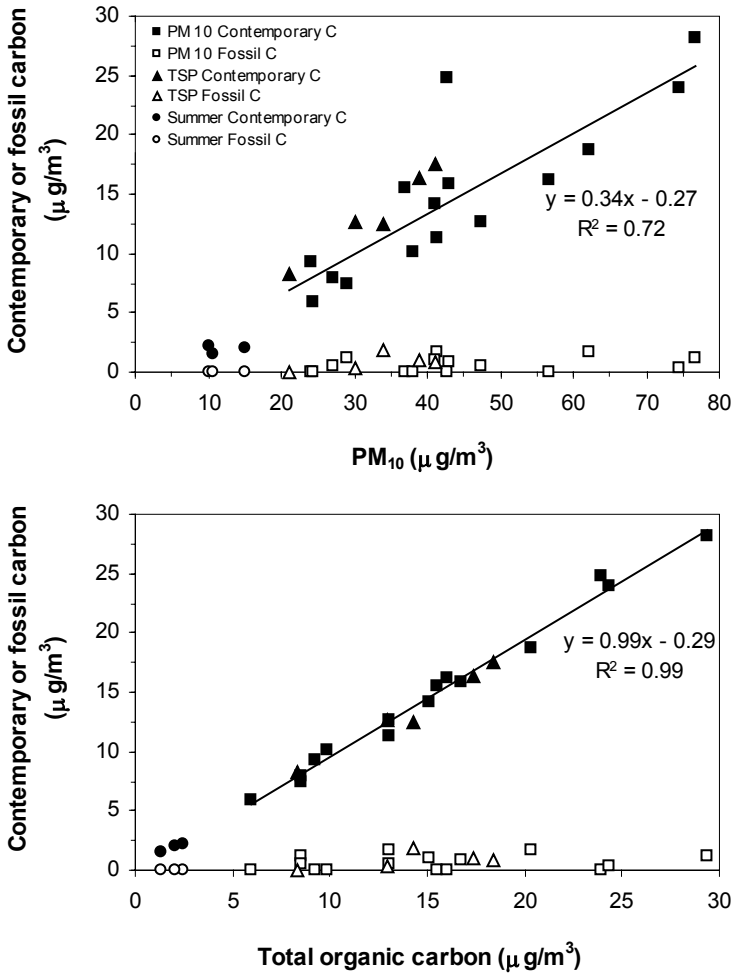

Figure 4.8 Calculated contribution of contemporary and fossil organic carbon to PM_{10} and total organic carbon in Launceston aerosols.

Uncertainty is contained within the symbol size. Regression line calculated for winter PM_{10} samples only.

4.4 Conclusion

This chapter has described the results from radiocarbon analysis of atmospheric aerosols collected in Launceston. It was confirmed that borosilicate filters are a suitable collection medium for radiocarbon analysis, although they require a modified combustion method during AMS sample preparation. The low elemental carbon content of Launceston PM_{10} precluded meaningful results being produced from this fraction, and verification that sample storage did not alter the isotopic composition of the organic carbon fraction was obtained. Input of contemporary carbon, most likely from woodsmoke, was found to increase linearly with PM loading and contributed around 97-99% of carbonaceous matter in Launceston wintertime PM_{10}. On the other hand, fossil carbon contributed a low and relatively constant amount independent of the PM_{10} loading. This study provides further evidence that woodsmoke is the major contributor to wintertime air pollution in Launceston using isotopic (^{14}C) measurements.

4.5 References

1. Damon, P.E.; Donahue, D.J.; Gore, B.H.; Hathaway, A.L.; Jull, A.J.T.; Linick, T.W.; Toolin, P.J.; Bronk, C.R.; Hall, E.T.; Hedges, R.E.M.; Housley, R.; Law, I.A.; Perry, C.; Bonani, G.; Trumbore, S.; Woelfli, W.; Ambers, J.C.; Bowman, S.G.E.; Leese, M.N.; Tite, M.S. Radiocarbon dating of the Shroud of Turin, *Nature* **1989**, 337, 611.
2. Currie, L.A.; Klouda, G.A.; Gerlach, R.W. Radiocarbon: Nature's tracer for carbonaceous pollutants, in *Proceedings of the 1981 International Conference on Residential Solid Fuels: Environmental impacts and solutions*, Cooper, J.A. and Malek, D., Editors. **1982**, Oregon Graduate Center: Beaverton, Oregon. p. 365-385.
3. Bowman, S. *Radiocarbon Dating*. **1990,** London: British Museum Publications.
4. Bench, G.; Herckes, P. Measurement of contemporary and fossil carbon contents of $PM_{2.5}$ aerosols: Results from Turtleback Dome, Yosemite National Park, *Environ. Sci. Technol.* **2004**, 38(8), 2424-2427.
5. Hua, Q.; Barbetti, M.; Jacobsen, G.E.; Zoppi, U.; Lawson, E.M. Bomb radiocarbon in annual tree rings from Thailand and Australia, *Nucl. Instrum. Methods Phys. Res., Sect. B* **2000**, 172, 359-365.
6. Currie, L.A.; Benner, B.A.; Kessler, J.D.; Klinedinst, D.B.; Klouda, G.A.; Marolf, J.V.; Slater, J.F.; Wise, S.A.; Cachier, H.; Hedges, J.I.; Prentice, K.M.; Kirchstetter, T.W.; Novakow, T.; Puxbaum, H.; Schmid, H. A critical evaluation of interlaboratory data on total, elemental, and isotopic carbon in the carbonaceous particle reference material, NIST SRM 1649a, *J. Res. Natl. Inst. Stand. Technol. (*http://www.nist.gov/jres*)* **2002**, 107(3), 279-298.
7. Lewis, C.W.; Klouda, G.A.; Ellenson, W.D. Radiocarbon measurement of the biogenic contribution to summertime PM-2.5 ambient aerosol in Nashville, TN, *Atmos. Environ.* **2004**, 38, 6053-6061.
8. Hildemann, L.M.; Klinedinst, D.B.; Klouda, G.A.; Currie, L.A.; Cass, G.R. Sources of urban contemporary carbon aerosol, *Environ. Sci. Technol.* **1994**, 28(9), 1565-1576.
9. Currie, L.A.; Klouda, G.A.; Schjoldager, J.; Ramdahl, T. The power of ^{14}C measurements combined with chemical characterization for tracing urban aerosol in Norway, *Radiocarbon* **1986**, 28(2A), 673-680.
10. Currie, L.A.; Klouda, G.A.; Klinedinst, D.B.; Sheffield, A.E.; Jull, A.J.T.; Donahue, D.J.; Connolly, M.V. Fossil- and bio-mass combustion: C-14 for source identification, chemical tracer development, and model validation, *Nucl. Instr. Meth. Phys. Res., Sect. B* **1994**, 92, 404-409.
11. Sheffield, A.E.; Currie, L.A.; Klouda, G.A. Trace radiocarbon analysis of environmental samples, *J. Res. National Bureau of Standards* **1988**, 93(3), 289-292.
12. Cooper, J.A.; Currie, L.A.; Klouda, G.A. Assessment of contemporary carbon combustion source contributions to urban air particulate levels using carbon-14 measurement, *Environ. Sci. Technol.* **1981**, 15(9), 1045-1050.

13. Currie, L.A. Evolution and multidisciplinary frontiers of ^{14}C aerosol science, *Radiocarbon* **2000**, 42(1), 115-126.
14. Hua, Q.; Jacobsen, G.E.; Zoppi, U.; Lawson, E.M.; Williams, A.A.; Smith, A.M.; McGann, M.J. Progress in radiocarbon target preparation at the ANTARES AMS centre, *Radiocarbon* **2001**, 43(2A), 275-282.
15. Smith, A.M.; Fink, D.; Hotchkis, M.A.C.; Jacobsen, G.E.; Lawson, E.M.; Shying, M.; Tuniz, C.; Watt, G.C.; Fallon, J.; Ellis, P.J. Equipment and methodology for high precision, high throughput ^{14}C AMS analyses at ANTARES, *Nucl. Instrum. Methods Phys. Res., Sect. B* **1994**, 92, 122-128.
16. Lawson, E.M.; Elliott, G.; Fallon, J.; Fink, D.; Hotchkis, M.A.C.; Hua, Q.; Jacobsen, G.E.; Lee, P.; Smith, A.M.; Tuniz, C.; Zoppi, U. AMS at ANTARES - The first 10 years, *Nucl. Instrum. Methods Phys. Res., Sect. B* **2000**, 172, 95-99.
17. Clayton, G.; Arnold, J.; Patty, F. Determination of sources of particulate atmospheric carbon, *Science* **1955**, 122, 751-753.
18. Currie, L.A.; Klouda, G.A. Mini-radiocarbon measurements, chemical selectivity, and the impact of man on environmental pollution and climate, *Radiocarbon* **1980**, 22(2), 349-362.
19. Klouda, G.A.; Currie, L.A.; Gerlach, R.W.; Continetti, R.E.; Tompkins, G.B. Estimating the impact of atmospheric carbonaceous particulates on urban and rural environments by radiocarbon measurements, *Resid. Wood Coal Combust., Spec. Conf., Proc.* **1982**, 189-206.
20. Currie, L.A.; Klouda, G.A.; Voorhees, K.J. Atmospheric carbon: The importance of accelerator mass spectrometry, *Nucl. Instr. Meth. Phys. Res., Sect. B.* **1984**, 233(2), 371-379.
21. NIST Certificate of Analysis, Standard Reference Material (SRM) 1649a, Urban Dust, National Institute of Standards and Technology, Gaithersburg, MD, **2001**.
22. Sheffield, A.E.; Currie, L.A.; Klouda, G.A.; Donahue, D.J.; Linick, T.W.; Jull, A.J.T. Accelerator mass spectrometric determination of carbon-14 in the low-polarity organic fraction of atmospheric particles, *Anal. Chem.* **1990**, 62(19), 2098-2102.
23. Klinedinst, D.B.; Currie, L.A. Direct quantification of $PM_{2.5}$ fossil and biomass carbon within the Northern Front Range Air Quality Study's domain, *Environ. Sci. Technol.* **1999**, 33(23), 4146-4154.
24. Currie, L.A.; Eglinton, T.I.; Benner, B.A., Jr.; Pearson, A. Radiocarbon "dating" of individual chemical compounds in atmospheric aerosol: First results comparing direct isotopic and multivariate statistical apportionment of specific polycyclic aromatic hydrocarbons, *Nucl. Instrum. Methods Phys. Res., Sect. B* **1997**, 123(1-4), 475-486.
25. Reddy, C.M.; Pearson, A.; Xu, L.; McNichol, A.P.; Benner, B.A., Jr.; Wise, S.A.; Klouda, G.A.; Currie, L.A.; Eglinton, T.I. Radiocarbon as a tool to apportion the sources of polycyclic aromatic hydrocarbons and black carbon in environmental samples, *Environ. Sci. Technol.* **2002**, 36(8), 1774-1782.
26. Mandalakis, M.; Gustafsson, O.; Reddy, C.M.; Xu, L. Radiocarbon apportionment of fossil versus biofuel combustion sources of polycyclic aromatic hydrocarbons in the Stockholm Metropolitan area, *Environ. Sci. Technol.* **2004**, 38(20), 5344-5349.

27. Kanke, H.; Uchida, M.; Okuda, T.; Yoneda, M.; Takada, H.; Y., S.; Morita, M. Compound-specific radiocarbon analysis of polycyclic aromatic hydrocarbons (PAHs) in sediments from an urban reservoir, *Nucl. Instrum. Methods Phys. Res., Sect. B* **2004**, 223-224, 545-554.
28. Klouda, G.A.; Lewis, C.W.; Rasmussen, R.A.; Rhoderick, G.C.; Sams, R.L.; Stevens, R.K.; Currie, L.A.; Donahue, D.J.; Jull, A.J.T.; Seila, R.L. Radiocarbon measurements of atmospheric volatile organic compounds: Quantifying the biogenic contribution, *Environ. Sci. Technol.* **1996**, 30(4), 1098-1105.
29. Goldstein, A.H.; Shaw, S.L. Isotopes of volatile organic compounds: An emerging approach for studying atmospheric budgets and chemistry, *Chem. Rev.* **2003**, 103, 5025-5048.
30. Van de Wal, R.S.W.; Van Roijen, J.J.; Raynaud, D.; Van der Borg, K.; De Jong, A.F.M.; Oerlemans, J.; Lipenkov, V.; Huybrechts, P. From $^{14}C/^{12}C$ measurements towards radiocarbon dating of ice, *Tellus* **1994**, 46B(2), 94-102.
31. Levchenko, V.A.; Etheridge, D.M.; Francey, R.J.; Trudinger, C.; Tuniz, C.; Lawson, E.M.; Smith, A.M.; Jacobsen, G.E.; Hua, Q.; Hotchkis, M.A.C.; Fink, D.; Morgan, V.; Head, J. Measurement of the $^{14}CO_2$ bomb pulse in firn and ice at Law Dome, Antarctica, *Nucl. Instrum. Methods Phys. Res., Sect. B* **1997**, 123(1-4), 290-295.
32. Slater, J.F.; Currie, L.A.; Dibb, J.E.; Benner, B.A. Distinguishing the relative contribution of fossil fuel and biomass combustion aerosols deposited at Summit, Greenland through isotopic and molecular characterization of insoluble carbon, *Atmos. Environ.* **2002**, 36(28), 4463-4477.
33. Currie, L.A.; Klouda, G.A.; Benner, B.A., Jr.; Garrity, K.; Eglinton, T.I. Isotopic and molecular fractionation in combustion; three routes to molecular marker validation, including direct molecular "dating" (GC/AMS), *Atmos. Environ.* **1999**, 33(17), 2789-2806.
34. Stuvier, M.; Polach, H.A. Reporting of ^{14}C data, *Radiocarbon* **1977**, 19(3), 355-363.
35. Court, J.D.; Goldsack, R.J.; Ferrari, L.M.; H.A., P. The use of carbon isotopes in identifying urban air particulate sources, *Clean Air* **1981**, 15, 6-11.
36. Norman, A.L.; Hopper, J.F.; Blanchard, P.; Ernst, D.; Brice, K.; Alexandrou, N.; Klouda, G. The stable carbon isotope composition of atmospheric PAHs, *Atmos. Environ.* **1999**, 33(17), 2807-2814.
37. Okuda, T.; Kumata, H.; Zakaria, M.P.; Naraoka, H.; Ishiwatari, R.; Takada, H. Source identification of Malaysian atmospheric polycyclic aromatic hydrocarbons nearby forest fires using molecular and isotopic compositions, *Atmos. Environ.* **2002**, 36(4), 611-618.
38. Keywood, M.D.; Ayers, G.P.; Gras, J.L.; Gillett, R.W.; Cohen, D.D. Size distribution and sources of aerosol in Launceston, Australia, during winter 1997, *J. Air & Waste Manage. Assoc.* **2000**, 50, 418-427.
39. Ayers, G.P.; Keywood, M.D.; Gras, J.L.; Cohen, D.; Garton, D.; Bailey, G.M. Chemical and physical properties of Australian fine particles: A pilot study, Environment Australia, Canberra, http://www.dar.csiro.au/publications/CSIRO_AFP.pdf, **1999**.

40. Gustafsson, O.; Haghseta, F.; Chan, C.; MacFarlane, J.; Gschwend, P.M. Quantification of the dilute sedimentary soot phase: Implications for PAH speciation and bioavailability, *Environ. Sci. Technol.* **1997**, 31(1), 203-209.
41. Fink, D.; Hotchkis, M.; Hua, Q.; Jacobsen, G.; Smith, A.M.; Zoppi, U.; Child, D.; Mifsud, C.; van der Gaast, H.; Williams, A.; Williams, M. The ANTARES AMS facility as ANSTO, *Nucl. Instrum. Methods Phys. Res., Sect. B* **2004**, 223-224, 109-115.
42. Brandova, D.; Maciejewski, M.; Keller, W.A. The utilisation of thermal analysis to optimise radiocarbon dating procedures, *J. Thermal Analysis and Calorimetry* **1999**, 56, 893-899.
43. Rogge, W.F.; Hidlemann, L.M.; Mazurek, M.A.; Cass, G.R.; Simoneit, B.R.T. Sources of fine organic aerosol. 2. Noncatalyst and catalyst-equipped automobiles and heavy-duty diesel trucks, *Environ. Sci. Technol.* **1993**, 27(4), 636-651.
44. Hildemann, L.M.; Markowski, G.R.; Cass, G.R. Chemical composition of emissions from urban sources of fine organic aerosol, *Environ. Sci. Technol.* **1991**, 25(4), 744-759.
45. Rogge, W.F.; Hildemann, L.M.; Mazurek, M.A.; Cass, G.R.; Simoneit, B.R.T. Sources of fine organic aerosol. 4. Particulate abrasion products from leaf surfaces of urban plants, *Environ. Sci. Technol.* **1993**, 27(13), 2700-2711.
46. Szidat, S.; Jenk, T.M.; Gaggelar, H.W.; Synal, H.-A.; Fisseha, R.; Baltensperger, U.; Kalberer, M.; Samburova, V.; Reimann, S.; Kasper-Giebl, A.; Hajdas, I. Radiocarbon (^{14}C)-deduced biogenic and anthropogenic contributions to organic carbon (OC) of urban aerosols from Zurich, Switzerland, *Atmos. Environ.* **2004**, 38(24), 4035-4044.
47. Hidy, G.M.; Eatough, D.J.; Klouda, G.A. Design scenario for the radioisotopic estimation of the biogenic component of airborne particles, *J. Air & Waste Manage. Assoc.* **2004**, 54, 600-613.

Chapter 5

Conclusions

Chapter 5

Conclusions

This study has used a number of techniques to characterise and quantify the contribution of woodsmoke to wintertime air pollution in Launceston, Tasmania. This included analysis of polycyclic aromatic hydrocarbons (PAHs) in ambient air and estuarine sediments, characterisation of the organic composition of woodheater emissions, and application of tracer species (chemical and isotopic) to apportion sources of ambient pollution.

Pyrogenic sources were found to dominate input of polycyclic aromatic hydrocarbons to ambient air in Launceston and sediments of the Tamar Estuary. Inclusion of a third sourcing ratio (Pyr/BaP) in addition to two traditional ratios (Phen/Anth and FluA/Pyr) suggested that woodsmoke was the most likely source, however, more data is required to validate the use of the Pyr/BaP ratio for sourcing PAHs. Quantification of the inputs was not possible using PAHs alone. An historical reconstruction of PAHs in Tamar Estuary sediment revealed that air quality in Launceston has not changed significantly in the past 70-80 years. A number of historical peaks in sedimentary PAH concentrations could not be rationalised to any specific event, but are likely to have arisen from urbanisation and industrialisation.

Further source discrimination of PAHs could be gained from radiocarbon analysis of individual compounds, which may also clarify the causes for the peaks in sedimentary concentration, although the high cost of sample preparation and analysis is likely to be prohibitive. Improved quantification of the historical impact of woodsmoke pollution could be achieved by measuring levoglucosan levels in a sediment core. While levoglucosan was not detected in the sediment core during this study, conversion to the trimethylsilyl- derivative is expected to make it more amenable for GC-MS analysis. The effect of PAH partitioning onto various components of the low-volume sampling train should be investigated, especially the adsorptive potential of the glass-fibre support pads.

Characterisation of the organic composition of woodheater emissions identified nearly 100 compounds from both the vapour- and particle- phases. This is the first time the effect of airflow setting on the composition of emissions has been investigated in detail. The mass fraction of many woodsmoke specific compounds, such as the methoxyphenols, was found to increase with decreasing airflow, and could possibly be used in chemical mass balance models to discriminate sub-sources of woodburning. However, these compounds were found at much lower concentrations in ambient samples than expected (relative to woodsmoke), and may not be suitable as atmospheric tracers for woodsmoke. Conversely, levoglucosan was identified as a relatively consistent tracer for woodsmoke irrespective of the airflow setting, and was found to be not degraded in ambient samples. Levoglucosan concentrations were used to estimate that woodsmoke contributed on average about 80 ± 20% of wintertime pollution in Launceston. "Non-woodsmoke" or "background" sources contributed around 8-10 $\mu g/m^3$ to Launceston PM_{10}.

Future work characterising emissions from woodheaters could include analysis of inorganic and ionic species, and a larger suite of organic compounds, especially low-molecular weight compounds collected using canisters and highly polar compounds after derivatisation. Particle emission factors have been measured for a large number of woodheater models in Australia, however, no such data is currently available for the composition of emissions.

The atmospheric (and storage) stability of methoxyphenols requires investigation, followed by a re-evaluation of their application as woodsmoke tracer species. In the meantime, these compounds should be used with caution in source apportionment studies. It is likely that levoglucosan will be used increasingly as a specific tracer for woodsmoke, and so the extent of variation in levoglucosan emissions from a greater range of woodheater models, fuel type, and operating conditions should be investigated. Emissions of levoglucosan from industrial operations must also be determined if accurate quantification of woodheater emissions are to be established.

The radiocarbon content of aerosols from Launceston indicated that woodsmoke dominated fossil fuel sources as the major contributor of organic carbon to air pollution during winter, consistent with the results obtained from levoglucosan measurements. While fossil carbon sources contributed a relatively constant 1.0 ± 0.7 μg C/m^3 , contemporary carbon sources exhibited a strong linear relationship with increasing PM_{10} loading. It was found that samples collected on borosilicate filters by DPIWE were suitable for radiocarbon analysis, albeit with a modified sample preparation, and that the organic carbon fraction of aerosols did not undergo significant losses during storage at the Government laboratories.

This study was only able to measure the radiocarbon content of the organic carbon fraction of Launceston ambient aerosols, as the elemental carbon content of filter blanks was too high. However, different methods of isolation may allow this important fraction to be quantified in future studies. Sources of contemporary carbon in summer remain unknown, although the environmental impact of pollution during these times is minimal.

A major recommendation by Power following his investigation of pollution dispersion in Launceston was that non-woodsmoke source strengths needed to be quantified (Chapter 1.2.3). While the National Pollution Inventory (NPI, Table 1.2, Chapter 1.2.2) has attempted to quantify source contributions, to date there has been no independent verification of these values; this study is now in a position to examine these estimates. The NPI estimate of the "road dust" contribution to PM_{10} in Launceston appears quite high (140,000 kg/year) when compared to woodsmoke (340,000 kg/year), although it is expected to be relatively constant year-round, as are the other non-woodburning sources. If it is assumed that woodsmoke is only present for half of the year, then the ratio of woodsmoke to the sum of other contributing sources averaged over the six months of "winter" is approximately three. Taking the "non-woodsmoke" contribution estimated from the levoglucosan results as 10 $\mu g/m^3$, all else being equal, the woodsmoke input will be around 30 $\mu g/m^3$ (Table 5.1). This gives an overall PM_{10} loading (40 $\mu g/m^3$) that is not significantly different to the winter average (~30-35 $\mu g/m^3$). Likewise, vehicle exhaust was estimated by the NPI to make up approximately 20% (41,000 kg/year) of non-woodburning sources of PM_{10}, equating to 2 $\mu g/m^3$. This is not significantly different to the ~1.5 ± 1.0 μg PM_{10}/m^3 (1.0 ± 0.7 μg C/m^3) estimated from the

radiocarbon results. Thus, the relative NPI estimates of PM_{10} source contributions to the Launceston airshed are not unreasonable.

Table 5.1 Comparison of estimated PM_{10} source contributions to the Launceston airshed during winter ($\mu g/m^3$); this study versus the National Pollution Inventory (NPI).

Source	This Study	NPI [b]
Non-woodsmoke	10 [a]	10
Road Dust		*7*
Vehicle exhaust	*1.5 ± 1.0* [c]	*2*
Other sources		*1*
Woodsmoke	31 ± 9 [d]	30

[a] estimated PM_{10} loading in winter when levoglucosan concentration was zero (Chapter 3.3.5.2).
[b] see Table 1.2, based on a non-woodsmoke contribution of 10 $\mu g/m^3$.
[c] calculated from radiocarbon results (Chapter 4.3.4.4).
[d] 77 ± 22% woodsmoke contribution to a 40 $\mu g/m^3$ PM_{10} episode (Chapter 3.3.5.2).

This study has provided further evidence that woodsmoke is the major contributor to wintertime air pollution in Launceston using various chemical and isotopic measurements. It has indicated that air quality has changed relatively little over the past century despite large increases in population, although a definitive historic source reconciliation could not be obtained. Chemical (levoglucosan) and isotopic (^{14}C) measurements were consistent in their estimation of the contribution of woodsmoke to current air pollution.

Monitoring of the chemical composition of winter air pollution in Launceston would ideally continue or be undertaken regularly in the future, and could be used to

evaluate the effectiveness of woodheater pollution abatement strategies. Monitoring of PAHs, for instance, may become a requirement of a future National Environment Protection Measure (NEPM).

Appendices

Appendix A – Polycyclic Aromatic Hydrocarbons

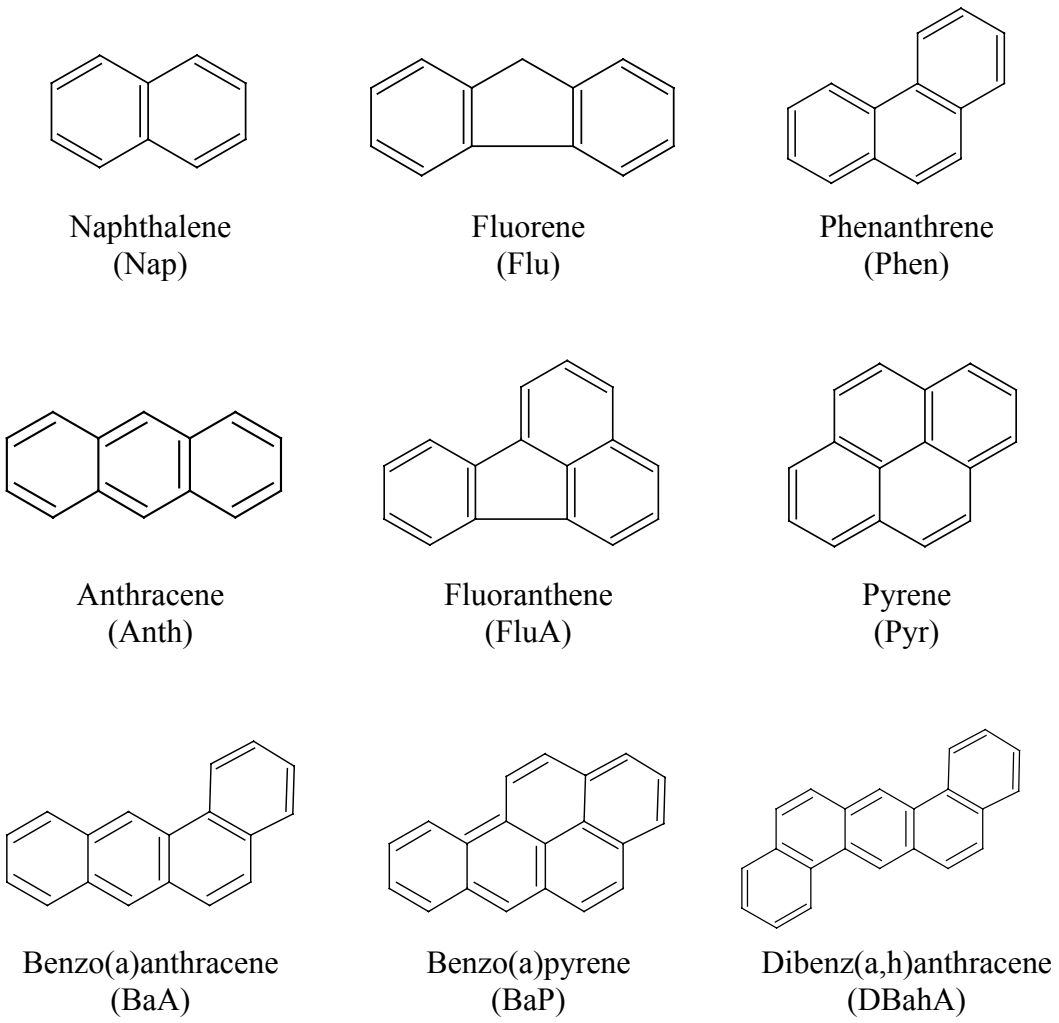

Figure A.1 Structure of PAHs investigated in this study.

Table A.1 Concentration of PAHs in IAEA-383 standard reference material and extraction efficiency determined in this study.

Compound	**Reference concentration** (ng/g)	**Reference 95% confidence interval** (ng/g)	**Mean wet SRM concentration** (ng/g)	**Mean extraction efficiency** (%)
Naphthalene	96	52 - 110	19.1	19.9
Fluorene	27	24 - 34	16.0	59.4
Phenanthrene	160	140 - 190	100.4	62.7
Anthracene	30	25 - 34	17.6	58.5
Fluoranthene	290	260 - 350	206.0	71.0
Pyrene	280	210 - 350	233.0	83.2
Benzo(a)anthracene	105	83 - 130	69.8	66.4
Benzo(a)pyrene	120	77 - 140	90.9	75.7
Dibenz(ah)anthracene [a]	20	18 - 41	10.0	49.9

[a] information value only.

See Carvalho *et al.* for more information on this SRM:

Carvalho, F.P., Villeneuve, J.-P., Cattini, C. Determination of organochlorine compounds, petroleum hydrocarbons, and sterols in a sediment sample, IAEA-383. Results of an intercomparison exercise, *Inter. J. Environ. Anal. Chem.* **1999**, 75(4): p.315-329.

HPLC Analysis

Fluorescence detection of PAHs allows excellent selectivity to be combined with high sensitivity when compared to UV-visual detection. As such, fluorescence detection was used exclusively for quantification purposes. Figure A.2 shows typical fluorescence chromatograms for a standard solution, sediment extract, and method blank.

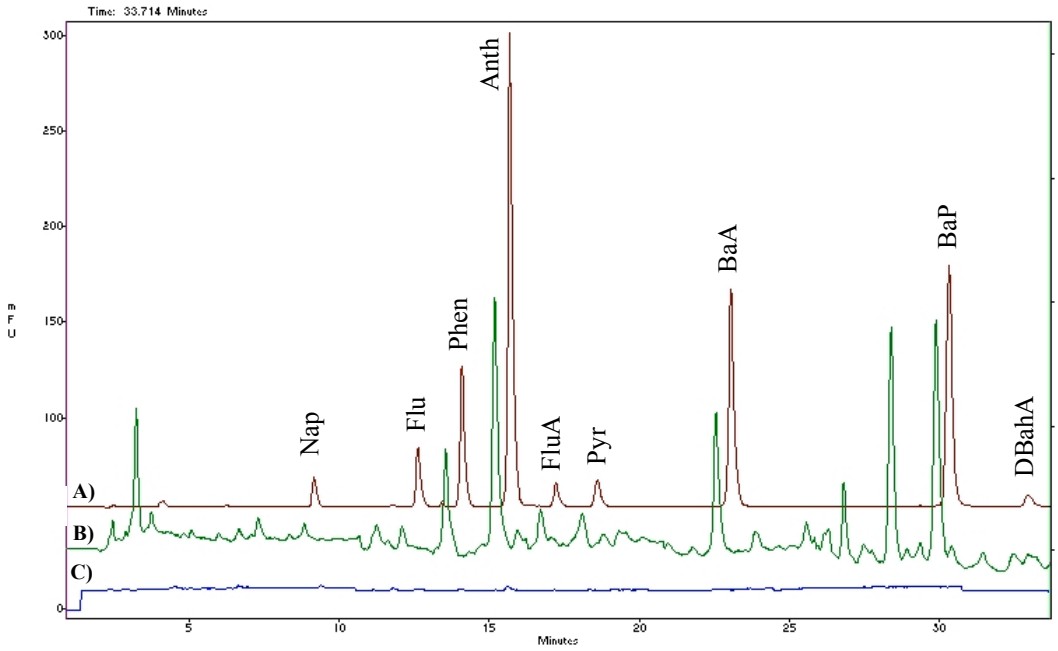

Figure A.2 HPLC chromatograms with fluorescence detection.
A) authentic standards, B) sediment extract, C) method blank.

Scanning the fluorescence excitation- and emission- spectra of the chromatographic peaks also aided in confirming peak identity (Figure A.3). Naphthalene did not produce meaningful spectra at the low concentrations found in sediment and is not shown. It appears that the Flu peak had a co-eluting contaminant, but this was most likely screened out with selection of the 310 nm emission band.

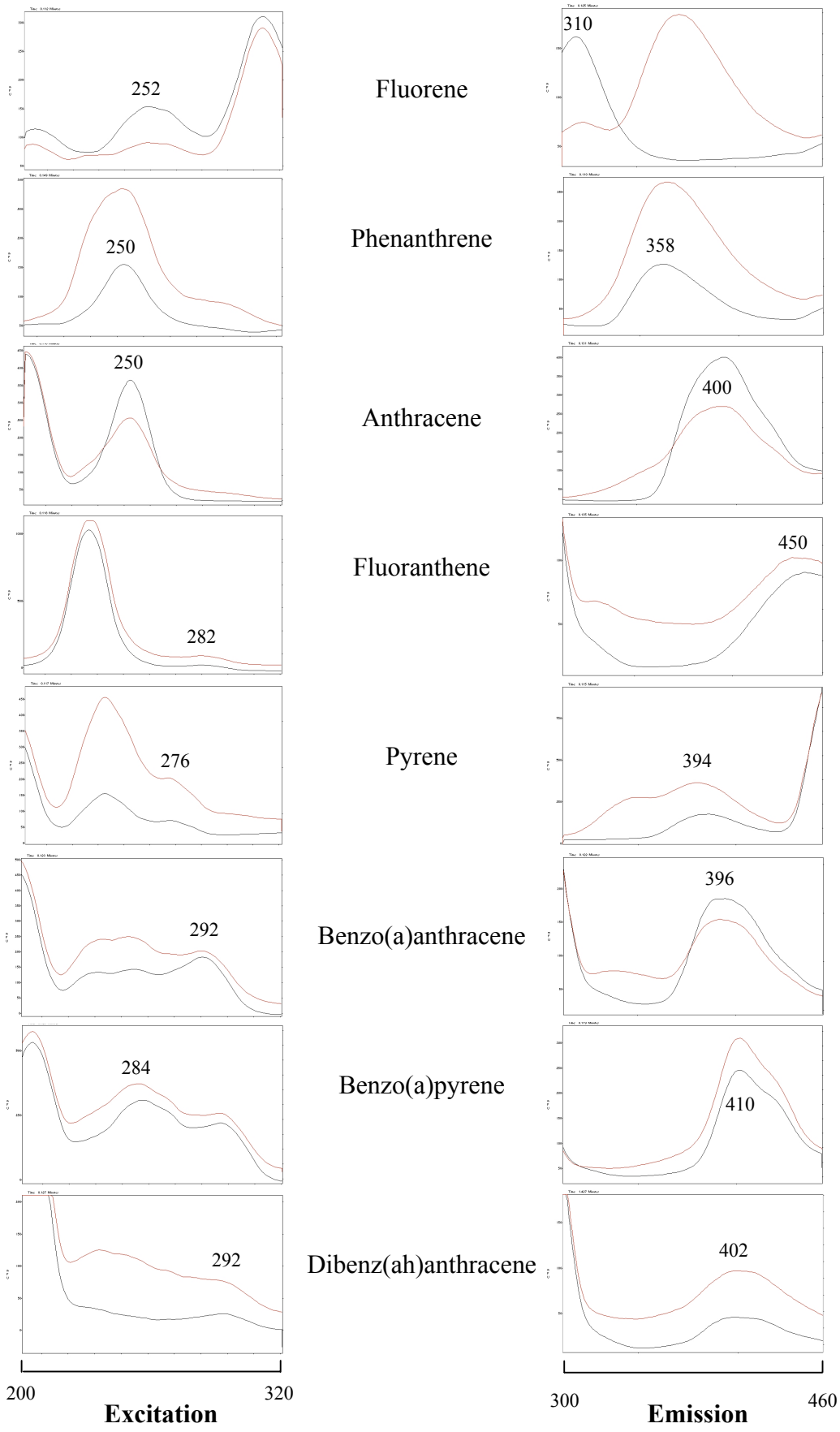

Figure A.3 Fluorescence excitation and emission spectra of target PAHs.
Solid line: authentic standard, dashed line: sediment extract, wavelength in nm.

Table A.2 Concentration of PAHs in low-volume samples collected in Launceston (ng/m^3).

Samples are designated by the site (E: Elphin, C: City) and the date, ordered chronologically. The sampling conditions describe the total volume sampled and sampling flow rate. The components of the sampling system are: PTFE: PTFE filter, GFF: glass-fibre filter, O100: front section of ORBO sorbent tube (100 mg XAD-2), O50: back section of sorbent tube (50 mg XAD-2), O100+50: both beds of XAD-2 combined before extraction, cassette: plastic sampling cassette housing the filter, support pad: glass-fibre support pad for PTFE filters, glass tube: tube housing XAD-2 resin. na: not analysed, d: below detection limit.

		Nap	Flu	Phen	Anth	FluA	Pyr	BaA	BaP
E 07/5/01									
1.372 m^3	PTFE					7.8		2.1	3.5
2.0 L/min	O100	301	6.7		3.7				
	O50	32.9							
E 20/5/01									
1.040 m^3	PTFE		0.6	2.9	0.6			2.5	5.2
2.0 L/min	O100	487	13.9		3.7				
	O50	50.6							
	cassette	1.9	0.2	0.4	0.2	0.1		0.2	0.3
	glass tube	2.9			0.3				
E 17/6/01									
1.310 m^3	PTFE			4.9	1.3	d	d	6.1	8.4
2.0 L/min	O100	607	16.7	14.1	6.8				
	O50	93.7							
	glass tube	1.8			0.3				
E 17/7/01									
1.372 m^3	PTFE			0.8	0.3			0.8	0.9
2.0 L/min	O100								
	O50	5.6							
E 22/7/01									
2.696 m^3	PTFE			0.6	0.2	5.7	1.2	1.5	2.1
2.0 L/min	O100	301	2.8	3.4	4.2				
	O50	46.7							
E 26/7/01									
1.294 m^3	GFF			0.6	0.1	0.8	1.5	2.0	3.1
2.0 L/min	O100	331	2.6	3.3	5.0	3.2	1.8		
	O50	80.1							
E 29/7/01									
1.346 m^3	GFF			0.4	0.1	0.6	1.1	1.4	2.3
2.0 L/min	O100	294	2.0	2.7	4.0	2.3			
	O50	77.3							
C 02/8/01									
1.206 m^3	PTFE			2.5	0.6	5.0	d	1.4	2.5
2.0 L/min	O100	257	2.9	2.0	1.3				
	O50	42.1							

Table A.2 continued

		Nap	Flu	Phen	Anth	FluA	Pyr	BaA	BaP
E 06/8/01									
1.200 m^3	PTFE			1.8	0.4	4.0		1.2	1.6
2.0 L/min	O100	153	3.2	4.8	2.0				
	O50	40.7							
	cassette	1.2		0.7	0.1	0.3			
E 04/9/01									
2.036 m^3	PTFE		d	d	d	4.1		0.7	1.1
2.0 L/min	O100	94.5	4.7	6.7	1.1	0.4			
	O50	27.7	d	d	d				
	cassette	0.3	d	d	d				
E 04/9/01									
2.324 m^3	GFF			d	d		d	d	
2.0 L/min	O100	84.3	4.5	6.6	1.1	0.4			
	O50	28.3	0.2	0.3	d				
	cassette	0.3	d	d	d				
C 06/3/02									
2.712 m^3	PTFE	0.1	d	0.2	0.1	d	0.6	0.3	0.2
2.3 L/min	O100	96.2	4.3	4.4	1.0	0.5	0.3		
	O50	39.5	0.5	0.2	0.1				
C 14/3/02									
2.443 m^3	PTFE	0.1	0.0	d	d		0.3	0.1	d
2.3 L/min	O100	76.4	3.8	4.5	0.9	0.5	0.3		
	O50	37.6	0.5	0.3	0.1				
C 30/4/02									
2.645 m^3	PTFE			d	0.2	0.7	1.3	1.0	2.0
2.3 L/min	O100	251	11.7	14.2	3.3	1.4	0.7		
	O50	98.2	1.0	0.5	0.2				
E 21/5/02									
2.304 m^3	PTFE			1.2	0.3	1.1	0.9	0.7	0.9
2.3 L/min	O100+50	229	6.6	6.4	1.1				
C 28/5/02									
3.043 m^3	GFF				0.1	1.8	1.3	1.8	1.9
2.3 L/min	O100+50	381	14.7	15.3	2.8	0.5	0.2		
E 29/5/02									
0.908 m^3	PTFE			2.4	0.8	5.4	2.0	2.5	2.9
2.0 L/min	O100+50	605	13.2	6.1	1.4				
E 29/5/02									
2.353 m^3	GFF			0.7	0.1	1.5	1.1	1.4	1.5
2.3 L/min	O100+50	419	15.3	13.9	2.3	d			
E 01/7/02									
2.157 m^3	PTFE			1.3	0.3	2.3	1.0	1.2	1.5
2.3 L/min	O100+50	350	8.8	7.3	1.6	0.2	0.1		
E 01/7/02									
2.148 m^3	GFF			0.7	0.1	0.8	0.7	1.0	1.1
2.3 L/min	O100+50	332	8.1	6.1	1.4	0.1	0.1		

Table A.2 continued

		Nap	Flu	Phen	Anth	FluA	Pyr	BaA	BaP
E 17/7/02									
2.514 m^3	PTFE			0.5	0.1	0.5	0.5	0.6	0.8
2.3 L/min	O100+50	232	5.9	20.1	1.0	0.3	0.1		
E 21/7/02									
2.100 m^3	GFF			0.4	0.1	0.6	0.5	0.5	0.7
2.3 L/min	O100+50	238	7.0	14.8	0.9	0.1			
E 30/7/02									
2.854 m^3	PTFE		0.2	0.4	0.2	1.2	0.7	1.9	2.1
2.0 L/min	O100+50	269	7.2	7.7	2.2	0.8	0.3		
E 30/7/02									
2.854 m^3	GFF		0.1	0.3	0.1	0.8	0.6	1.6	1.8
2.0 L/min	O100+50	264	6.0	7.1	2.1	1.9	0.9		
E 04/8/02									
2.286 m^3	PTFE		0.2	0.6	0.2	d	0.9	2.3	2.4
2.3 L/min	O100+50	297	6.0	6.8	2.1	0.4	0.2		
E 14/8/02									
2.020 m^3	GFF		0.1	0.5	0.1	2.4	2.0	2.3	2.6
2.0 L/min	O100+50	272	5.2	5.2	2.2	1.9	0.7		
E 14/8/02									
2.020 m^3	PTFE		0.2	0.7	0.4	2.5	2.0	2.6	3.2
2.0 L/min	O100+50	262	4.9	4.1	1.6				
E 15/8/02									
2.013 m^3	GFF		0.2	0.6	0.2	1.9	1.7	2.2	2.7
2.3 L/min	O100+50	249	4.7	4.0	1.9	1.8	0.8		
E 15/8/02									
2.013 m^3	PTFE		0.2	0.7	0.4	2.0	1.3	2.1	2.6
2.3 L/min	O100+50	270	4.9	4.2	1.8				
E 24/8/02									
3.236 m^3	PTFE a		0.1	0.2	d	0.4	0.2	0.8	1.0
2.3 L/min	O100+50	148	3.4	3.2	0.8	0.4	0.1		
E 24/8/02									
3.236 m^3	PTFE b		0.1	0.1	d	0.3	0.2	1.4	1.8
2.3 L/min	O100+50	138	3.5	3.7	1.0	0.4	0.1		
E 25/8/02									
2.842 m^3	PTFE a		0.1	0.2	0.1	0.5	0.4	0.9	2.0
2.0 L/min	O100+50	168	3.3	4.0	0.6	0.3	0.05		
E 25/8/02									
2.842 m^3	PTFE b		0.1	0.3	0.1	0.5	0.5	1.2	1.7
2.0 L/min	O100+50	168	3.5	3.3	0.7	0.3	0.1		
E 12/9/02									
2.875 m^3	PTFE	1.2	0.2	0.6	0.1	1.0	0.4	0.7	0.8
2.5 L/min	O100+50	139	6.0	10.2	1.2	0.4	0.1		

Table A.2 continued

		Nap	Flu	Phen	Anth	FluA	Pyr	BaA	BaP
E 26/1/03									
3.151 m^3	PTFE	1.0	0.1	0.5	0.1	d			
2.3 L/min	O100+50	61.7	3.2	5.0	0.2	0.4	0.4		
E 04/3/03									
3.737 m^3	PTFE	0.9	0.1	0.5	0.1	d			0.3
2.3 L/min	O100+50	43.1	1.5	3.9	0.1	0.2	0.3	0.1	d
C 25/3/03									
4.050 m^3	PTFE	1.0	0.1	0.5	0.1	0.1	0.3	0.1	0.3
2.3 L/min	O100+50	151	4.4	5.9	1.0	0.7	1.0	0.2	0.1
E 26/3/03									
3.305 m^3	PTFE	1.5	0.1	0.4	0.1	d		0.1	0.2
2.3 L/min	O100+50	90.2	4.5	6.9	0.8	0.4	0.1		
E 27/5/03									
8.825 m^3	PTFE	0.5	0.1	0.5	d	0.1	0.1	0.5	0.9
2.3 L/min	O100+50	na							
E 27/5/03									
8.825 m^3	GFF	0.4	0.1	0.2	d	d	d	0.1	0.1
2.3 L/min	O100+50	na							
E 02/7/03									
6.589 m^3	PTFE b	0.7	0.1	0.8	0.1	0.6	0.6	1.6	1.7
2.3 L/min	O100	183	7.4	14.6	2.6	0.6	0.7		
	O50	50.8	0.6	0.7	0.1				
	support pad	0.7	0.2	1.2	0.3	2.6	2.1	0.2	
E 02/7/03									
6.589 m^3	PTFE a	0.7	0.1	0.9	0.2	0.8	0.7	1.4	1.5
2.3 L/min	O100	158	6.6	10.7	2.2	0.3	0.3		
	O50	53.7	0.6	0.7	0.1				
	support pad	0.7	0.2	1.1	0.2	2.1	1.8	0.1	
E 17/7/03									
7.966 m^3	PTFE	0.6	0.1	0.6	0.1	1.3	0.3	1.4	1.7
2.0 L/min	O100+50	na							
E 30/7/03									
5.690 m^3	PTFE	0.5	0.1	0.7	0.1	0.2	0.3	0.3	0.4
2.0 L/min	O100+50	61.9	2.2	2.8	0.3	0.2	0.2		
E 30/7/03									
5.690 m^3	GFF	0.6	0.1	0.6	0.1	0.4	0.6	1.3	1.1
2.0 L/min	O100+50	268	10.8	15.3	3.0	1.7	1.8		
E 18/8/03									
5.750 m^3	PTFE	0.3		1.1	0.1	0.2	0.3	1.4	2.0
2.0 L/min	O100+50	208	6.3	9.3	1.3	0.3	0.5		
	support pad			1.2		1.8	2.1	0.2	
E 18/8/03									
5.750 m^3	GFF	0.6	0.1	0.5	0.1	0.4	0.4	0.7	0.8
2.0 L/min	O100+50	217	6.8	10.4	2.0	1.6	1.6		

Table A.2 continued

		Nap	Flu	Phen	Anth	FluA	Pyr	BaA	BaP
E 25/2/04									
5.028 m^3	PTFE	0.6	0.4	0.8	0.1		0.5	0.2	0.2
2.0 L/min	support pad	0.8	0.5	0.8	0.2	1.0	1.8		
	cassette	0.9	0.2	1.0	0.1				
	O100+50	221	4.9	4.4	0.7	1.2	0.6		
	glass tube	1.1	1.2	0.6	0.1				
E 01/3/04									
3.900 m^3	PTFE	0.5	0.4	0.8	0.1		0.8	0.1	0.3
2.0 L/min	support pad	0.6	0.6	0.9	0.2	0.7	1.4		
	cassette	1.4	0.1	1.2	0.2				
	O100+50	228	4.2	5.0	1.1	1.3	1.1		
	glass tube	1.0	1.8	0.6	0.1				
E 10/3/04									
4.924 m^3	PTFE	0.5	0.2	1.0	0.2	0.5	0.5	0.3	0.8
2.0 L/min	support pad	1.7	0.7	1.4	0.3	1.2	1.2		
	cassette	1.4	0.3	1.1	0.1				
	O100+50	311	8.8	5.4	0.7	0.7	0.4		
	glass tube	1.0	1.3	0.5	0.1				

Table A.3 Concentration of PAHs in Launceston air collected using high-volume PM_{10} samplers (ng/m^3).

	PM_{10}	Nap	Flu	Phen	Anth	FluA	Pyr	BaA	BaP
Winter	($\mu g/m^3$)								
13/5/2002	29.1				0.01	0.01		0.05	0.08
15/5/2002	47.5				0.01	0.02		0.08	0.18
25/5/2002	32.1		0.01		0.01	0.03	0.03	0.30	0.47
28/5/2002	76.6		0.01	0.15	0.01	0.09	0.11	0.29	1.31
31/5/2002	72.5		0.01		0.01	0.03		0.25	0.39
14/6/2002	62.2				0.01	0.02		0.19	0.31
24/7/2002	35.5				0.01	0.02	0.02	0.06	0.10
25/7/2002	47.3		0.01		0.01	0.02		0.05	0.07
02/8/2002	41.3				0.01	0.02		0.07	0.13
19/6/2003	56.7		0.01	0.03	0.01	0.04	0.02	0.20	0.68
24/6/2003	73.4		0.01	0.22	0.01		0.08	0.18	0.94
08/7/2003	38.0		0.01	0.07	0.01	0.02	0.02	0.05	0.21
09/7/2003	70.9			0.13	0.01	0.05	0.11	0.41	1.05
18/7/2003	74.5		0.02	0.21	0.01	0.06	0.06	0.22	0.98
19/8/2003	43.5			0.14	0.02		0.21	0.07	0.42
21/8/2003	41.6			0.06	0.01	0.02	0.01	0.05	0.37
09/9/2003	24.5					0.02	0.03	0.02	0.04
Summer									
25/1/2003	52.3	0.07	0.01	0.01	0.01	0.01	0.01	0.01	0.02
26/1/2003	48.4	0.06	0.01	0.01	0.01	0.01		0.01	0.01
03/12/2003	10.7	0.01		0.01					
16/1/2004	15.0			0.01			0.07	0.00	0.01

Appendix B – Woodsmoke Characterisation

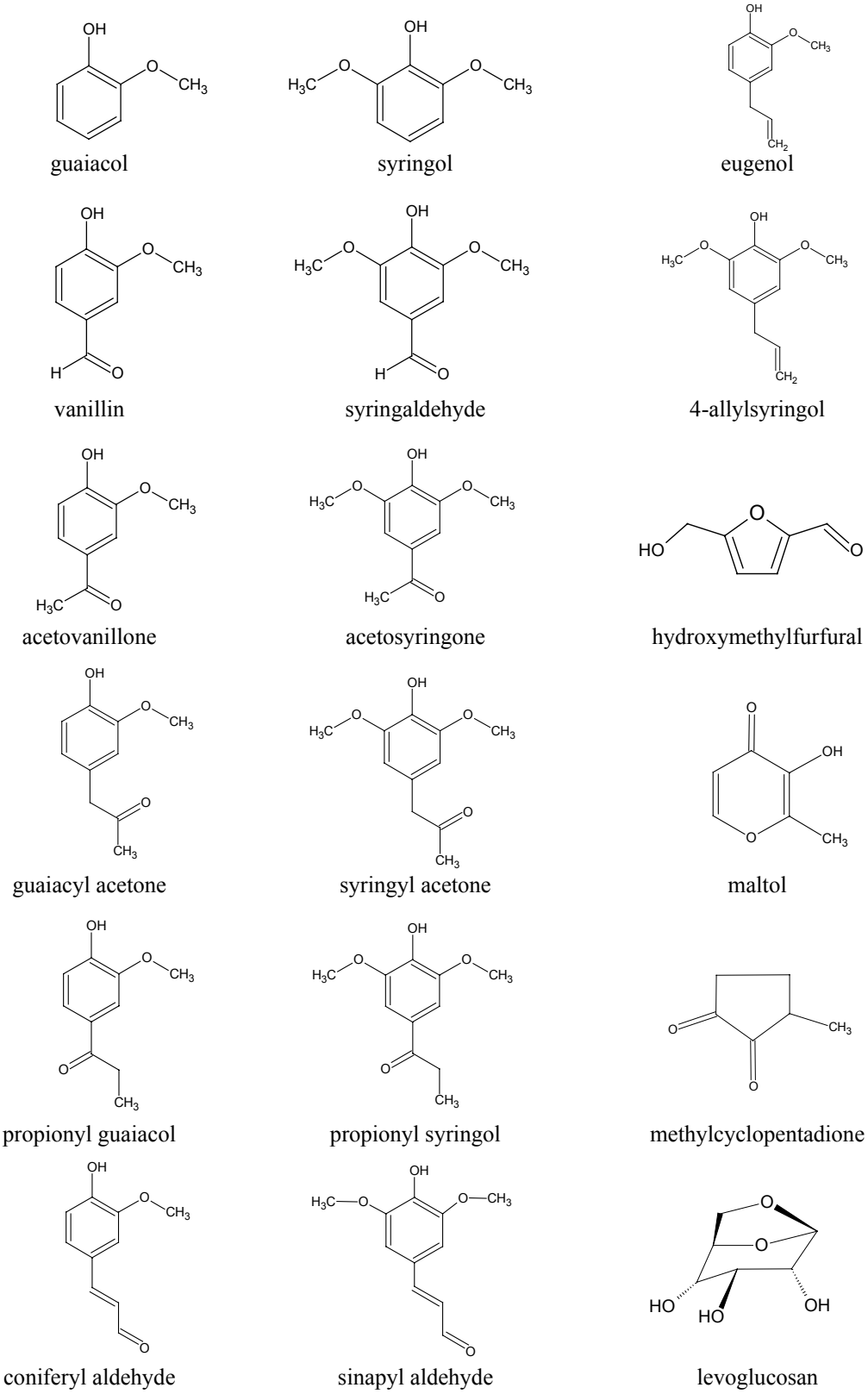

Figure B.1 Chemical structure of selected organic compounds identified in woodsmoke.

Dilution Tunnel Flow Calculations

The dilution tunnel flow-rate was calculated using the following equation given in the product data sheet:

$$v = F_p * 1096.2 * 0.00508 * \sqrt{\left(\frac{P_v\, C}{D}\right)\left(\frac{T}{298}\right)} \qquad \text{(B.1)}$$

where:

ν	=	flow velocity (m/s)
F_p	=	cross-sectional flow calibration factor (0.9465)
1096.2	=	manufacturers pitot tube multiplying constant
0.00508	=	conversion from feet/min to m/s
P_ν	=	velocity pressure ("H_2O)
C	=	pitot tube flow coefficient (0.84, given)
D	=	air density (0.075 pounds/feet^3)
T	=	flue-gas temperature (K)

The volumetric flow was calculated using:

$$Q = \nu * A \qquad \text{(2)}$$

where:

Q	=	volumetric flow rate (m^3/s)
ν	=	flow velocity (m/s)
A	=	duct cross-sectional area (0.01767 m^2)

Table B.1 Summary of woodheater emissions tests.

Airflow Setting	Filter No.	Sampling Time (mins)	Mass Wood Burned (kg, dry)	Average Burn Rate (dry kg/hr)	PEW (g)	PEF (g/kg, dry)	PER (g/hr)
S1							
open	7	73	3.36	2.77	74.4	22.1	61.1
open	6+5	90	5.78	3.88	93.7	16.2	62.5
open	3+4	83	3.49	2.50	59.9	17.1	43.3
closed	1+2	90	0.99	0.66	24.2	24.4	16.1
closed	9+10	110	1.21	0.66	46.4	38.5	25.3
open	12	67	3.45	3.09	23.7	6.9	21.2
½-closed	13	90	2.89	1.92	57.8	20.0	38.6
closed	14	90	0.69	0.46	23.4	34.0	15.6
½-closed	16+17	19	0.56	1.77	- [a]	-	-
½-closed	18+19	121	1.68	0.84	55.0	32.7	27.3
½-closed	20+21	120	1.42	0.72	48.5	34.1	24.2
open	22+23	120	3.79	1.90	62.9	16.6	31.5
open	24+25	120	4.40	2.20	58.5	13.3	29.3
½-closed	26	34	1.34	2.36	- [a]	-	-
closed	27	150	1.98	0.84	48.1	24.2	19.2
open	28-31	120	5.17	2.59	69.2	13.4	34.6
½-closed	32+33	103	3.58	2.09	141.8	39.6	82.6
closed	34-37	120	1.94	0.97	90.7	46.7	45.3
S2							
open	38	75	4.61	3.69	17.9	3.9	13.4
½-closed	39	75	2.59	2.03	26.0	10.2	20.8
closed	40	150	2.50	1.00	121.1	48.4	48.4
open	41	72	4.40	3.42	21.7	4.9	16.9
½-closed	43	120	4.01	2.01	84.9	21.2	42.5
½-closed	42	110	4.40	2.40	32.1	7.3	17.5
open	44+45	68	5.22	4.60	14.2	2.7	12.5
closed	46+47	100	2.46	1.47	89.0	37.4	53.4
closed	48+49	170	3.45	1.22	96.4	27.9	34.0
open	50-53	100	5.35	3.18	10.1	1.9	6.1
open	54	100	4.48	2.69	3.9	0.9	2.4
closed	55	120	4.31	2.16	105.7	24.5	52.8
open → closed	56+57	120	4.01	2.04	60.5	15.1	30.2
closed	58-61	120	2.54	1.28	101.8	40.0	50.9
M1							
open	62	52	2.63	3.03	11.1	4.2	3.9
closed	63	170	3.19	1.13	126.5	39.6	44.6
open	66+67	73	3.66	3.01	5.5	1.5	4.5
open	65	80	3.54	2.66	6.7	1.9	5.0
closed	68+69	150	2.46	0.98	84.6	34.4	33.9
½-closed	70+71	117	3.97	2.03	40.0	10.1	20.5

[a] test was deemed invalid because of problems with the sampling pump.

WOODHEATER EMISSIONS TEST

Date: 28/11/02

Heater Model: Saxon – old (S1)
Air Flow Conditions: ½-closed Sample Probe Diameter: 3.18 mm

Startup Time: 8:40 Sampling Started: 9:20 Stopped: 11:03 ∴ Elapsed: 103
Ambient Temperature: 19 °C Filter: GFF #32 + 33
Sampling Train: 2 x GFF + ORBO + cold finger + silica gel

	Time *(hh:mm)*	**Elapsed** *(mins)*	**Tunnel Temp** *(°C)*	**Tunnel Pitot Pressure** *("H_2O)*	**Sampling Flow** *(L/min)*	**Mass** *(kg)*	**Mass added** *(kg)*
1	9:15	-	-	-		4.55	4.55
2	9:20	5	50	0.085	2.50	4.15	
3	9:25	10	35	0.084	2.50	3.90	
4	9:30	15	34	0.084	2.50	3.65	
5	9:35	20	33	0.085	2.50	3.40	
6	9:40	25	34	0.084	2.50	3.15	
7	9:50	30	34	0.085	2.50	2.70	
8	10:00	40	36	0.086	2.50	2.25	
9	10:10	50	38	0.085	2.50	1.85	
10	10:20	60	36	0.084	2.50	1.45	

Observations / Comments:

3 logs (1.20 + 1.55 + 1.80 = 4.55 kg) added to 1.20 kg coals (= 26.4% of test load), and 0.40 kg pre-burned (= 8.8%).

Door left open 3 mins, closed for 2 mins with air open, then air ½-closed and sampling started.

Door opened at 10:08 and 10:42 to rearrange logs (< 10 seconds).

Continued Over: (Y) / N Page 1 of 4

Figure B.2 Example of woodheater test observations form.

Figure B.2 continued

	Time *(hh:mm)*	**Elapsed** *(mins)*	**Tunnel Temp** *(^oC)*	**Tunnel Pitot Pressure** *("H_2O)*	**Sampling Flow** *(L/min)*	**Mass** *(kg)*	**Mass added** *(kg)*
11	10:30	70	35	0.083	2.50	1.10	
12	10:40	80	36	0.084	2.50	0.80	
13	10:50	90	41	0.084	2.50	0.35	
14	11:00	100	39	0.083	2.50	0.10	
15	11:03	103	38	0.084	2.50	0.00	(4.15)
16							
17							
18							
19							
20							
21							
22							
23							
24							
25							
26							
27							
28							
29							
30							
31							
32							
33							
34							
35							

Continued Over: (Y) / N

Figure B.2 continued

Total Dilution Tunnel Volume (V_d): 574.5 m^3 (during sampling period)

Sample

Flow: 2.50 L/min = 0.0025 m^3/min (weighted average)

Sampling Area: 7.92×10^{-6} (1/8" = 3.18mm)

Total Sampled Volume (V_s) = $Q_s t_s$

= (0.0025 m^3/min) X (103 min)

= Total Sampled Volume (V_s): 0.258 m^3

Volume Ratio = V_d / V_s = 574.5 / 0.258 = V_d / V_s = 2231.0

Filter	**# 32**	**# 33**
m_i =	0.09014 g	0.09020 g
m_f =	0.15268 g	0.09124 g
m_{pm} =	0.06254 g	0.00104 g

= 1.6 % of total mass on backup filter

Wood

m_{wood} consumed during sampling

= 4.15 kg (wet) /

= 3.58 kg (dry)

Emission Factors

Particle Emission Weight (PEW) = m_{pm} * (V_d/V_s) = 0.06358 * 2231.0 = 141.84 g

Particle Emission Factor (PEF) = PEW / m_{wood} = 141.84 / 3.58 = **39.6 g/kg**

Particle Emission Rate (PER) = PEW / t_s = 141.84 / (103 / 60) = 82.6 g/hr

Continued Over: Y / (N)

Page 3 of 4

Figure B.2 continued

Additional Observations / Comments:

none.

Continued Over: Y / (N)

Figure B.3 Total-ion-current chromatogram of woodheater particle-phase extract (IS, internal standard; RS, recovery standard).

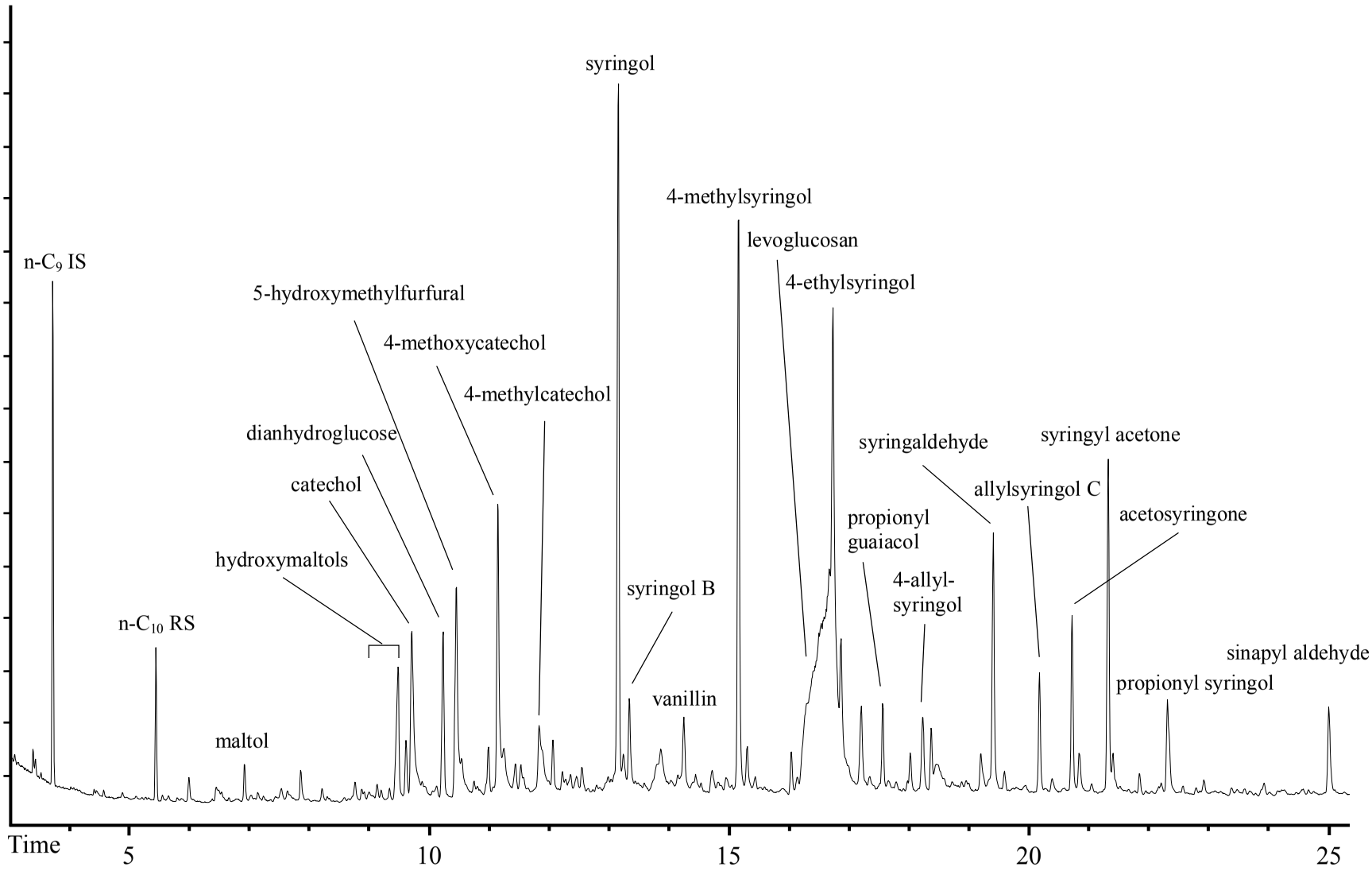
n-C9 IS
n-C10 RS
maltol
hydroxymaltols
catechol
dianhydroglucose
5-hydroxymethylfurfural
4-methoxycatechol
4-methylcatechol
syringol
syringol B
vanillin
4-methylsyringol
levoglucosan
4-ethylsyringol
propionyl guaiacol
4-allyl-syringol
syringaldehyde
allylsyringol C
syringyl acetone
acetosyringone
propionyl syringol
sinapyl aldehyde
Time
5
10
15
20
25

Appendix C – Radiocarbon Results

Table C.1 Summary of radiocarbon results for the organic carbon fraction of Launceston ambient aerosols.

Sample [a]	Laboratory code	PM_{10} loading ($\mu g/m^3$) [b]	Corrected C mass (μg)	$\delta^{13}C$ (‰)	f_C	1σ [d]
PM_{10} 13/5/02	OZG624	29.1	152	- [c]	0.871	0.004
PM_{10} 28/5/02	OZG626	76.6	522	-	0.959	0.004
PM_{10} 14/6/02	OZG628	62.2	362	-	0.920	0.004
PM_{10} 25/7/02	OZG630	47.3	232	-	0.966	0.004
PM_{10} 02/8/02	OZG634	41.3	232	-	0.869	0.004
PM_{10} 25/5/03	OZH190	42.7	665	-25.2	1.035	0.004
PM_{10} 19/6/03	OZH191	56.7	445	-	1.008	0.006
PM_{10} 08/7/03	OZH192	38.0	275	-25.1	1.022	0.004
PM_{10} 18/7/03	OZH193	74.5	675	-24.8	0.985	0.004
PM_{10} 19/8/03	OZG982	43.5	466	-24.3	0.948	0.004
TSP 19/8/03	OZG969	41	492	-18.2	0.951	0.006
PM_{10} 20/8/03	OZG983	37.3	446	-24.4	1.021	0.004
	OZG984		426	-24.3	0.972	0.005
	OZG985		426	-25.2	1.002	0.004
TSP 20/8/03	OZG970	39	462	-24.4	0.925	0.004
	OZG971		462	-27.0	0.951	0.005
	OZG971-2		422	-24.8	0.932	0.004
	OZG972		492	-25.0	0.948	0.004
artificially 'aged'	OZG978		492	-22.9	0.939	0.005
PM_{10} 21/8/03	OZG986	41.6	396	-24.9	0.937	0.004
	OZG987		416	-25.1	0.931	0.004
	OZG988		446	-21.7	0.943	0.008
TSP 21/8/03	OZG973	34	402	-25.3	0.881	0.004
	OZG974		392	-25.4	0.882	0.004
	OZG974-2		342	-25.0	0.877	0.004
	OZG975		342	-25.7	0.857	0.004
artificially 'aged'	OZG979		362	-24.1	0.905	0.004
PM_{10} 07/9/03	OZG989	24.5	256	-24.6	1.010	0.005
TSP 07/9/03	OZG976	21	232	-25.9	0.994	0.005
PM_{10} 08/9/03	OZG990	27.3	236	-25.4	0.943	0.005
TSP 08/9/03	OZG977	30	352	-25.6	0.974	0.005
PM_{10} 09/9/03	OZH194	24.5	165	-24.9	1.002	0.006
TSP 04-11/11/03	OZH189	10	462	-25.9	0.925	0.004
PM_{10} 03/12/03	OZH195	10.7	38	-27.7	1.106	0.005
PM_{10} 16/1/04	OZH196	15.0	58	-26.8	0.980	0.004
Woodsmoke					f_M (corrected)	
Organic carbon	OZG636	-	3271	-	1.040	0.004
Elemental carbon	OZG637	-	64	-	1.049	0.006

[a] sample refers to the size fraction and filter type (PM_{10} on borosilicate filter, TSP on quartz filter), and the date(s) of collection.

[b] TSP loading was estimated from co-located DPIWE PM_{10} tapered element oscillating microbalance (TEOM) data during the sampling period.

[c] a $\delta^{13}C$ value of –25‰ was assumed when the value was not measured or when there was insufficient sample mass remaining after AMS analysis.

[d] error due to AMS counting statistics.

Table C.2 Summary of radiocarbon results for the elemental carbon fraction of Launceston ambient aerosols.

Sample [a]	Laboratory code	PM_{10} loading ($\mu g/m^3$)[b]	Corrected C mass (μg)	$\delta^{13}C$ (‰)	f_M (measured)	f_C	1σ [d]
PM_{10} 13/5/02	OZG625	29.1	29	- [c]	0.860	1.960	0.096
PM_{10} 28/5/02	OZG627	76.6	37	-	1.084	1.950	0.011
PM_{10} 14/6/02	OZG629	62.2	32	-	1.079	2.065	0.012
PM_{10} 25/7/02	OZG631	47.3	31	-	1.001	1.824	0.010
PM_{10} 02/8/02	OZG635	41.3	39	-	0.975	1.562	0.008
TSP 19/8/03	OZH184	41	20	-	0.834	1.268	0.015
TSP 20/8/03	OZH185	39	9.5	-	0.826	1.749	0.021
TSP 21/8/03	OZH186	34	3.9	-	0.902	3.671	0.048
TSP 07/9/03	OZH187	21	-1.0	-	0.815	-	-
TSP 04/11/11/03	OZH188	11	80	-22.7	0.865	0.956	0.007

Table footnotes are presented in Table C.1

Table C.3 Summary of radiocarbon results for filter media blanks.

	Laboratory code	Carbon mass (μg)	$\delta^{13}C$ (‰)	f_M (measured)	1σ [d]
Borosilicate					
OC	OZG632	57.9	- [c]	0.741	0.006
	OZG980	67.5	-	0.646	0.007
	OZG981	61.3	-	0.672	0.005
	OZH197	75.0	-	0.578	0.006
EC	OZG633	84.4	-	0.676	0.006
Quartz					
OC	OZG967	26.0	-	-	-
	OZG968	30.8	-	0.425	0.007
EC	OZH182	22.5	-	0.457	0.008
	OZH183	26.4	-	0.429	0.007

Table footnotes are presented in Table C.1